

# **Molecular mechanisms controlling SH2 domain-containing inositol 5'phosphatase (SHIP) function in B cells**

by

**Samantha Dawn Pauls**

A thesis submitted to the Faculty of Graduate Studies of  
The University of Manitoba  
in partial fulfillment of the requirements for the degree of

**DOCTOR OF PHILOSOPHY**

Department of Biochemistry and Medical Genetics  
University of Manitoba  
Winnipeg

Copyright © 2016 by Samantha Dawn Pauls

# TABLE OF CONTENTS

Table of Contents .....	ii
Thesis Abstract.....	v
Acknowledgement .....	vii
List of Figures .....	ix
List of Tables .....	xii
List of Copywrited materials for which permission was obtained .....	xiii
Abbreviations.....	xiv
CHAPTER 1: GENERAL INTRODUCTION .....	1
1.1    Discovery of B cells .....	1
1.2    The benefits of B cells: immune response to pathogens .....	3
1.3    The hazard of B cells: role in inflammatory and autoimmune conditions .....	5
1.4    B cell development.....	7
1.5    Immune receptor signaling basics: ITAM versus ITIM.....	11
1.6    Signalling through the B cell receptor.....	12
1.6.1    Signal initiation.....	12
1.6.2    PLC $\gamma$ pathway.....	19
1.6.3    MAPK pathways.....	20
1.6.4    PI3K pathway.....	21
1.6.5    BCR signal modulation by co-receptors .....	28
1.6.6    Abnormal BCR signaling and disease .....	30
1.7    SH2 domain-containing inositol 5'phosphatase (SHIP) .....	32
1.7.1    Discovery of SHIPc .....	32
1.7.2    SHIP knock-out models .....	32
1.7.3    Structure and function.....	33
1.7.4    Regulation of SHIP protein levels .....	41
1.7.5    SHIP in autoimmune and inflammatory disorders.....	42
1.8    The actin cytoskeleton and B cell signaling.....	44
1.8.1    Signal initiation.....	44
1.8.2    Branched actin filament formation .....	46
1.8.3    PI3K signaling and actin.....	48
1.9    Thesis overview.....	49
1.9.1    Study Rationale.....	49

1.9.2	General hypothesis.....	50
1.9.3	Objectives .....	50
CHAPTER 2: DEFINING THE INTERACTION NETWORK OF SHIP.....		52
2.1	Specific Introduction.....	52
2.2	Materials and Methods.....	54
2.2.1	Cell lines and reagents .....	54
2.2.2	Co-immunoprecipitation, western blotting and multiple reaction monitoring .....	55
2.2.3	Bioinformatics prediction tools.....	56
2.2.4	Recombinant proteins .....	56
2.2.5	Biacore screening.....	56
2.2.6	Biacore steady-state affinity analysis.....	59
2.3	Results .....	59
2.3.1	Evidence for an interaction between Bam32 and SHIP in B cells.....	59
2.3.2	Identification of potential SHIP interaction partners using prediction tools .....	62
2.3.3	Identification of SHIP interaction partners by a Biacore screening assay.....	66
2.3.4	Biacore affinity analysis of SHIP-FcγRIIB and SHIP-Nck interactions .....	70
2.4	Discussion .....	71
CHAPTER 3: A NOVEL PHOSPHORYLATION SITE IN SHIP INDUCES BINDING TO NCK AND REGULATES ACTIN DYNAMICS IN B CELLS .....		75
3.1	Specific Introduction.....	75
3.2	Materials and Methods.....	78
3.2.1	Cell culture and reagents.....	78
3.2.2	Plasmids and transfections.....	78
3.2.3	Generation of stable cell lines.....	79
3.2.4	GST pull-downs .....	79
3.2.5	FRAP assay for actin turnover .....	80
3.2.6	Membrane recruitment assay .....	80
3.2.7	Intracellular staining .....	81
3.2.8	Spreading assay.....	81
3.2.9	Statistical Analysis.....	82
3.3	Results .....	82
3.3.1	SHIP interacts with the cytoskeletal adaptor protein Nck .....	82
3.3.2	SHIP inhibits actin turnover by a mechanism seemingly dependent on Tyr944....	84
3.3.3	Effect of SHIP-EGFP on actin turnover is overcome by co-overexpression of Nck	87

3.3.4	SHIP membrane recruitment and enzymatic activity are not diminished by Y944F mutation .....	87
3.3.5	Overexpression of SHIP-EGFP has no measurable effect on cell spreading in a transient transfection system.....	89
3.3.6	Cell viability after transfection is variable and vector-dependent .....	90
3.4	Discussion .....	92
CHAPTER 4: CONTROLLING THE INTRACELLULAR LOCALIZATION DYNAMICS OF SHIP .....		97
4.1	Specific Introduction .....	97
4.2	Materials and Methods.....	99
4.2.1	Cell culture and reagents.....	99
4.2.2	Plasmids and transfections.....	99
4.2.3	Membrane recruitment experiments .....	100
4.2.4	Statistical Analysis.....	101
4.2.5	FRAP experiments .....	102
4.2.6	Co-immunoprecipitation experiments .....	102
4.2.7	Antibodies and staining.....	103
4.2.8	Lentivirus-mediated shRNA silencing.....	103
4.3	Results .....	104
4.3.1	SHIP is recruited to the plasma membrane after BCR stimulation with and without FcγRIIB co-engagement .....	104
4.3.2	Mobility of SHIP-EGFP is altered by stimulation.....	110
4.3.3	Dependence of SHIP membrane recruitment on protein interaction motifs.....	111
4.3.4	Dependence of SHIP membrane recruitment on upstream kinases .....	113
4.3.5	Syk activity is required for phosphorylation and association of SHIP with Shc ..	116
4.3.6	A lower stimulation threshold is required for SHIP membrane recruitment compared to SHIP phosphorylation .....	119
4.3.7	Reducing Shc1 expression has no measurable impact on SHIP membrane recruitment .....	120
4.4	Discussion .....	122
CHAPTER 5: GENERAL DISCUSSION .....		127
5.1	Summary of findings.....	127
5.2	Impact and implications .....	129
5.3	Limitations and future research directions .....	132
REFERENCES .....		137

## THESIS ABSTRACT

B lymphocytes are an important type of immune cell that contributes to pathogen clearance, classically by secretion of specific immunoglobulins, or antibodies. When dysregulated, these cells contribute significantly to diseases such as autoimmunity, allergy and B cell cancers. Here we examine an important regulatory circuit that involves the lipid phosphatase SH2 domain containing inositol 5'-phosphatase (SHIP), a key regulator of the phosphoinositol 3-kinase (PI3K) signaling pathway. SHIP was first described as the major effector of inhibitory IgG receptor FcγRIIB, which downregulates B cell antigen receptor (BCR) signaling pathways when co-engaged. However, it is also known to inhibit signaling downstream of several other receptors, both activating and inhibitory. Here we examine the regulation and function of SHIP in B cells, focusing on the inter-related influences of binding partners, tyrosine phosphorylation and localization dynamics.

First, we identify potential interaction partners of SHIP using prediction tools and assess binding to selected candidate proteins *in vitro*. Several novel interactions are identified and mapped to either the SH2 domain or one of the four identified tyrosine phosphorylation sites in the C-terminus of SHIP. The two most robust interactions measured in a screening assay were further characterized with respect to dissociation constant. These were: a novel interaction between SHIP phospho-Tyr944 and the SH2 domain of cytoskeletal adaptor protein Nck, and a known interaction between the SH2 domain of SHIP and FcγRIIB phospho-Y292.

Next, we perform the first examination of SHIP Tyr944, focusing on its interaction with Nck and its effects on the B cell cytoskeleton. We provide evidence that it contributes to interaction with

Nck after BCR engagement. Furthermore, we demonstrate that overexpression of SHIP-EGFP in Ramos B cells is associated with reduced actin dynamics. This effect is lost with mutation of Tyr944 to phenylalanine or by co-overexpression of Nck. The Y944F mutation causes no apparent defect in enzymatic activity or membrane recruitment of SHIP, therefore we propose that loss of interaction with Nck is responsible for disruption of inhibitory function.

Finally, we perform the first detailed examination of the mechanisms controlling SHIP localization in human B cells stimulated through the BCR with and without co-engagement of Fc $\gamma$ RIIB. We discover that SHIP is recruited to the plasma membrane equally in both stimulation contexts, however Fc $\gamma$ RIIB co-ligation results in reduced mobility of SHIP molecules at the cell periphery. We identify the SH2 domain of SHIP as well as the kinase activity of Syk as critical for recruitment under both stimulation conditions, while BCR ligation alone further requires the C-terminus of SHIP. Syk activity was also indispensable for stimulation-induced phosphorylation of both SHIP and its known binding partner Shc1, as well as for an interaction to form between them.

Together, these results provide significant and exploitable insight into the molecular control of a clinically important regulator of B cell responses. Enhancing our understanding of the regulation of SHIP will lead to a greater understanding of how B cell activation is controlled overall and how we might intervene therapeutically in patients whose B cells are responding inappropriately to self-tissues.

## **ACKNOWLEDGEMENTS**

I am indebted to my outstanding advisor, Dr. Aaron Marshall, for his guidance and support throughout my doctoral training. Through his exceptional mentorship, I have been given all the tools I could ask for moving forward. He has provided an inspirational example of a true scientist, working fervently to understand ourselves and our world.

I would like to extend my gratitude to the members of my advisory committee: Dr. Abdel Soussi-Gounni, Dr. John Wilkins and Dr. Mojgan Rastegar. Through thoughtful discussions and challenging critiques, they played an important role in refining both my thesis work and my scientific mindset. I am grateful also to my external examiner, Dr Pauline Johnson.

A big thank you goes out to past and present members of the Marshall lab. Thanks especially to my “lab mom” Sen Hou who, along with my enthusiastic co-op student mentee Arnab Ray, contributed directly to the work described in this thesis. Thanks also to Xun Wu, Ahmed Ali, Nipun Jayachandran, Hongzhao Li, Ivan Landego, Kennedy Makondo and my dearest friend Sandrine Lafarge for truly enriching my experience. I am deeply grateful for the support of two departments at the University of Manitoba - my official Department of Biochemistry and Medical Genetics and my adoptive Department of Immunology. Being part of both has broadened my training and provided me with numerous influential role models. I am also grateful to the funding agencies that have made my research and training possible, including the Canadian Institutes of Health Research, Research Manitoba, the Children’s Hospital Research Institute of Manitoba and the University of Manitoba.

Finally, I am thankful for the grace of God in all aspects of life and for the love and support of my family and close friends, especially my devoted husband Adam Pauls and my biggest little fan Alicia Pauls. I dedicate this thesis to her.



## LIST OF FIGURES

<i>Figure 1-1. Overview of B2 cell development including the major subsets and their primary tissue residency.</i> .....	10
<i>Figure 1-2. Models of BCR signal initiation.</i> .....	17
<i>Figure 1-3. Overview of BCR signaling (105).</i> .....	18
<i>Figure 1-4. Overview of PI3K signaling in lymphocytes.</i> .....	22
<i>Figure 1-5. BCR signal modulation by co-receptors.</i> .....	30
<i>Figure 1-6. Domain structure of SHIP.</i> .....	34
<i>Figure 1-7. Phosphatase-independent adaptor functions described for SHIP.</i> .....	40
<i>Figure 1-8. Key signals involved in branched actin nucleation.</i> .....	47
<i>Figure 2-1. SHIP interaction partners with defined binding sites.</i> .....	53
<i>Figure 2-2. SHIP does not detectably co-immunoprecipitate with Bam32-myc, Lyn, Hck, or SHIP2.</i> .....	60
<i>Figure 2-3. Amino acid sequence of Bam32</i> .....	61
<i>Figure 2-4. Potential SHIP interaction partners identified in a Biacore screening experiment.</i> .....	68
<i>Figure 2-5. Steady-state affinity analysis of selected interactions.</i> .....	70
<i>Figure 3-1. Endogenous SHIP binds recombinant Nck-GST.</i> .....	83
<i>Figure 3-2. Interaction between SHIP and Nck is stimulation-dependent and supported by Tyr 944.</i> .....	84
<i>Figure 3-3. SHIP inhibits actin turnover rate in a Tyr944-dependent manner.</i> .....	86
<i>Figure 3-4. Co-overexpression of Nck abrogates the inhibitory effect of SHIP-EGFP on actin turnover.</i> .....	87

<b>Figure 3-5.</b> Mutation of Tyrosine 944 to phenylalanine does not impair membrane recruitment of SHIP or its PIP <sub>2</sub> -hydrolyzing function.....	89
<b>Figure 3-6.</b> Overexpression of SHIP-EGFP has no measurable effect on Ramos cell spreading. .....	90
<b>Figure 3-7.</b> Cell viability is negatively affected by transient transfection with SHIP and Y944F constructs. ....	91
<b>Figure 3-8.</b> Model demonstrating how binding of SHIP to Nck via Y944 could inhibit F-actin dynamics. ....	95
<b>Figure 4-1.</b> Defining an experimental system to test the influence of FcγRIIB on BCR-induced recruitment of SHIP. ....	105
<b>Figure 4-2.</b> SHIP-EGFP is recruited to the plasma membrane with BCR ligation alone or with FcγRIIB co-ligation.....	106
<b>Figure 4-3.</b> Kinetics of SHIP-EGFP membrane recruitment in live cells.....	107
<b>Figure 4-4.</b> Endogenous SHIP is recruited to the plasma membrane after BCR ligation with or without FcγRIIB co-ligation.....	109
<b>Figure 4-5.</b> Fluorescence recovery after photobleaching analysis of SHIP-EGFP. ....	111
<b>Figure 4-6.</b> Structural requirements for SHIP-EGFP membrane recruitment. ....	113
<b>Figure 4-7.</b> Signaling requirements for SHIP-EGFP membrane recruitment. ....	115
<b>Figure 4-8.</b> Syk inhibition prevents membrane recruitment of endogenous SHIP.....	116
<b>Figure 4-9.</b> Syk inhibition prevents SHIP phosphorylation and association with Shc1. ....	118
<b>Figure 4-10.</b> Low dose anti-BCR stimulation is sufficient for SHIP membrane recruitment but not phosphorylation. ....	119
<b>Figure 4-11.</b> Knockdown of Shc1 has no measurable effect on SHIP membrane recruitment. .	121

**Figure 4-12. Visualizing BCR-mediated SHIP recruitment.** ..... 125

## LIST OF TABLES

Table 2-1. Phosphopeptides derived from candidate proteins .....	58
Table 2-2. Multiple reaction monitoring to identify Bam32-Myc in co-IP samples. ....	62
Table 2-3. SHIP interaction partners predicted by Scansite3. ....	64
Table 2-4. Phospho-SHIP interaction partners predicted by SMALI .....	66
Table 2-5. Interaction partners of SHIP identified by Biacore screening assay .....	69

# **LIST OF COPYRIGHTED MATERIALS FOR WHICH PERMISSION WAS OBTAINED**

Figure 1-2. Overview of BCR signaling (p. 17)

(Reprinted with permission from *Molecular Immunology*, Volume 41:599-613 © 2004 by Elsevier)

Chapter 4. Figures 4-1 to 4-9 and accompanying text

(Reprinted in modified form with permission from *The Journal of Immunology*, vol. 197, pp. 1587-1596, Copyright 2016 by The American Association of Immunologists, Inc. )

## ABBREVIATIONS

APC	Antigen presentation cell
APC	Allophycocyanin
Arp2/3	Actin-related protein 2/3
Bam32	B-lymphocyte adaptor molecule of 32 kDa
BCAP	B-cell PI3K adaptor protein
BCR	B cell receptor
BiFC	Bimolecular fluorescence complementation
BLNK	B cell linker
Btk	Bruton tyrosine kinase
CD	Cluster of differentiation
Cdc42	Cell division control protein 42
CIA	Collagen-induced arthritis
CLL	Chronic lymphocytic leukemia
Co-IP	Co-immunoprecipitation
CSR	Class switch recombination
DAG	Diacylglycerol
DAP12	DNAX-activating protein of 12 kD
DLBCL	Diffuse large B-cell lymphoma
DNA	Deoxyribonucleic acid
Dok	Downstream of tyrosine kinase
DTT	Dithiothreitol
EGFP	Enhanced green fluorescent protein
ER	Endoplasmic reticulum
ERK1/2	Extracellular signal-regulated kinase 1/2
ERM	Ezrin/Radixin/Moesin
FACS	Fluorescence activated cell sorting
F-actin	Filamentous actin
FBS	Fetal bovine serum
Fc $\gamma$ R	Fc gamma receptor
Fc $\epsilon$ R	Fc epsilon receptor
FDC	Follicular dendritic cell
FITC	Fluorescein isothiocyanate
FRAP	Fluorescence recovery after photobleaching
FRET	Förster resonance energy transfer
G-actin	Globular actin
GC	Germinal center
GEF	Guanine nucleotide exchange factor
GM-CSF	Granulocyte macrophage colony stimulating factor
GPCR	G-protein-coupled receptors
GRAP	Grb2-related adaptor protein
GRB2	Growth factor receptor bound protein 2
GST	Glutathione-S-transferase
GTPase	Guanosine triphosphatase
HBS	HEPES buffered saline

HBS-EP	HBS –Ethylenediaminetetraacetic acid-surfactant P20
H-chain	Ig heavy chain
Hck	Hematopoietic cell kinase
HPLC	High performance liquid chromatography
HRP	Horseradish peroxidase
i/n/cSH2	Interstitial/N-terminal/C-terminal SH2 domain
Ig	Immunoglobulin
IKK	I $\kappa$ B kinase
IL	Interleukin
INPP4	Inositol polyphosphate-4-phosphatase
IP	Immunoprecipitation
IP <sub>3</sub>	Inositol(1,4,5)-trisphosphate
IP <sub>3</sub> Rs	IP <sub>3</sub> receptors
ITAM	Immunoreceptor tyrosine-based activation motif
ITIM	Immunoreceptor tyrosine-based inhibitory motif
JNK	c-Jun N-terminal kinase
K <sub>D</sub>	Dissociation constant
L-chain	Light chain
Lyn	Lck/Yes novel tyrosine kinase
MAPKs	Mitogen-activated protein kinases
MEK1/2	MAPK/ERK kinase
Met	Methionine
MFI	Mean fluorescence intensity
MHC	Major histocompatibility complex
MIgG	Mouse IgG
miRNA	Micro-RNA
MS	Multiple sclerosis
MZ	Marginal zone
Nck	Non-catalytic region of tyrosine kinase adaptor protein 1
NFAT	Nuclear factor of activated T cells
NOD	Non obese diabetic
NP40	Nondiet P-40
NP <sub>x</sub> Y	Asperagine-proline-x-tyrosine (where x is any amino acid)
p-	Phospho-
PBS	Phosphate buffered saline
PDGFR	Platelet-derived growth factor receptor
PFA	Paraformaldehyde
PH	Pleckstrin homology
PH-R	Pleckstrin homology-related
PI	Posphatidylinositol
PI(3)P	Phosphatidylinositol-3-phosphate
PI(3,4)P <sub>2</sub>	Phosphatidylinositol-3,4-biphosphate
PI(3,4,5)P <sub>3</sub>	Phosphatidylinositol-3,4,5-tris-phosphate
PI(4,5)P <sub>2</sub>	Phosphatidylinositol 4,5-bisphosphate
PI3Ks	Phosphoinositide 3-kinases
PKA/B/C	Protein kinase A/B/C
PLA	Proximity ligation assay
PLC	Phospholipase C

PTB	Protein tyrosine binding
PTEN	Phosphatase and tensin homologue
PTK	Protein tyrosine kinase
PV	Pervanadate
Q	Quadripole
RA	Rheumatoid arthritis
Rac	Ras-related C3 botulinum toxin substrate 1
Rap1	Ras-related protein 1
Ras	Rat sarcoma
RasGRP1	Ras guanyl nucleotide releasing protein 1
RFP	Red fluorescent protein
RIgG	Rabbit IgG
RNA	Ribonucleic acid
ROI	Region of interest
RPMI	Roswell Park Memorial Institute (Medium)
SDS-PAGE	Sodium dodecyl sulphate polyacrylamide gel electrophoresis
Ser (S)	Serine
SH2	Src homology 2
SH3	Src homology 3
Shc1	Src homology domain containing transforming protein 1
SHIP/SHIP1	SH2 domain containing inositol 5'phosphatase 1
SHIP2	SH2 domain containing inositol 5'phosphatase 2
SHP	SH2 domain containing phosphatase
SLE	Systemic Lupus Erythematosus
SLP-76	SH2 domain containing leukocyte protein of 76 kDa
SMALI	Small matrix assisted ligand identification
SRM	Selective reaction monitoring
Syk	Spleen tyrosine kinase
TAPP	Tandem pleckstrin homology domain protein
TFA	Trifluoroacetic acid
Thr (T)	Threonine
T1D	Type 1 Diabetes
Tyr (Y)	Tyrosine
WASP	Wiskott-Aldrich syndrome protein
WAVE	WASP-family verprolin-homologous protein
WT	Wild-type



# 1 CHAPTER 1: GENERAL INTRODUCTION

## 1.1 Discovery of B cells

B cells are a critical immune cell subset. They contribute to adaptive immunity by producing secreted antibody and by supporting the function of other immune cells. B cells are distinguished by the expression of membrane-embedded antibody, also called immunoglobulin (Ig), on their surface. This antibody forms part of the B cell antigen receptor (BCR). A given antibody has the ability to bind a specific region (epitope) of a specific antigen, where an antigen is simply any substance that can be recognized by the immune system to potentially evoke a response (1).

This definition of a B cell rests on the back of decades of theoretical and experimental observations. In 1947, Astrid Fagraeus published a study implicating plasma cells (not yet understood at that time to be B lymphocytes) as the cells responsible for antibody production (2). This was based on the observation that secondary injection of antigen into rabbit spleen leads to a local increase in (histologically defined) plasma cells in the red pulp, concurrent with an increase in antibody. Furthermore, when spleen tissue was cultured *in vitro*, the red pulp isolates were able to produce antibody to a much greater extent than lymph follicle isolates. Niels Jerne proposed what was known as the “natural selection theory” of antibody formation in 1955 (3). He suggested that millions of antibody specificities are naturally present in the naïve state and antigen exposure somehow promotes the synthesis of specific antibody when an appropriate cell phagocytoses the antibody-antigen complex. David Talmage took it a step further and proposed

that natural antibodies are actually receptors on a cell surface, thus antigen selects cells for replication based on surface expression of the correct receptor (4).

The actual concept of clonality and clonal selection was proposed soon after when the famed Sir Macfarlane Burnet elegantly theorized that each lymphocyte that is produced bears a unique antigen receptor consisting of just one natural antibody (5, 6). Theoretically, this concept explained several experimental observations of the time, such as how antigen exposure (immunization) can select specific cells for proliferation and differentiation into plasma cells, how antibody concentration increases exponentially as this selection occurs and how the cells producing antigen-specific antibody are the ones to rapidly respond after a secondary immunization. Furthermore, if antigen is encountered too early in development, the clonal line is killed rather than selected for. This mechanistically explained natural and experimental self-tolerance phenomena described previously in several systems. It also provided a rational account of autoimmunity, proposed to arise by occasional failings in the tolerogenic system, i.e. “clonal escape” (5, 7).

Before long, Sir Gustav Nossal published the first direct experimental evidence supporting Burnet’s theory (8). Nossal perfected a technique to isolate a single lymph node cell from an immunized rat by suspending it in a microdroplet on a slide. When he introduced a small number of flagellated salmonella of the specific strain used for immunization, anti-flagella antibodies were formed within a subset of droplets and would immobilize the bacteria on the slide. Importantly, a given droplet only yielded one antibody specificity, even after exposure to

different strains of the bacteria (8). Burnet's thought experiments were now backed by laboratory experiments.

Throughout the next decade, especially the mid-1960s to early 1970s, the B lymphocyte was finally formally identified and characterized as the clonal, antibody-producing cell of the immune system. In chickens, cells isolated from the bursa of Fabricius were found to be the antibody producers (9). In mice, cells transplanted from bone marrow but not thymus played this role (10). The first report identifying surface immunoglobulin expression as a marker of B cells was published in 1969 (11). The development of immunophenotyping methods, first established to classify leukemia patients based on surface marker expression (12), also facilitated the characterization of normal B cells and, over the years, has enabled scientists to identify and functionally characterize the multiple subsets of B cells that we know today.

## **1.2 The benefits of B cells: immune response to pathogens**

B cells are critical to humoral immune responses (that is, production of antibodies) and also support the function of other immune cells such as T cells, macrophages, and dendritic cells, by presenting antigen, providing cell-cell contact and producing cytokines (1). B cell-deficient mice are more susceptible to a wide variety of pathogens, including viral (13) or bacterial (14) gastrointestinal infections, bacterial infection in the lung (15) and parasitic infection (16).

Both cell surface and secreted antibodies are central to B cell function. Naïve B cells express antibody on their surface as part of the B cell receptor (BCR) complex. Antigen binding by the BCR is the first crucial step in the classic B cell activation sequence and thus provides the basis

for clonal selection. BCR signaling alone is sufficient to maintain survival in some B cell subsets (17, 18), initiate gene transcription (19) and mount a humoral response to certain multivalent antigens (20, 21). Extensive clonal expansion and production of high affinity antibody requires further support from T cells that are specific for the same antigen although not necessarily the same epitope (22, 23). To obtain this help, B cells internalize the BCR-antigen complex, process it, and present it on their surface bound to Class II Major Histocompatibility Complex (MHCII). This process is termed antigen presentation. Together with interaction of other surface protein pairs (notably CD40 and CD80/CD86 on the B cell with CD40L and CD28 on the T cell, respectively) and localized production of cytokines, this supports clonal expansion of the antigen-specific B cell and differentiation into plasma and memory cells (23-25). Depending on co-stimulation and the cytokine milieu, B cells may change the isotype of antibody they express on their surface and secrete (26, 27).

The most effective place for B and T cells to come together to coordinate an immune response is in germinal centres, specialized regions of secondary lymphoid tissues such as in the spleen, lymph nodes and peyers patches (28, 29). Here, B cells are exposed to antigen on the surface of specialized mesenchymal-derived cells called Follicular dendritic cells (FDCs), interact closely with T cells, proliferate extensively, and ultimately differentiate (29). Clonally expanded B cells undergo somatic hypermutation in the antigen-binding region of their immunoglobulin genes. Mutations that result in higher affinity antibodies out-compete the rest for T cell help, thus this “affinity maturation” refines the humoral response over time (30).

Secreted antigen-specific antibodies are the effective, multifunctional weapons of humoral immunity. They can neutralize toxins and extracellular viruses (IgG and IgA isotypes), coat or “opsonize” pathogens to target them for phagocytosis and/or killing, activate complement pathways (IgM and IgG isotypes) and induce degranulation of mast cells and eosinophils (IgE isotype) (23, 31, 32). B cell effector functions in addition to antibody production are also important. For example, T cell expansion often fails in the absence of B cell priming (33, 34), especially in response to low-dose antigen exposure (35). This reflects a requirement for B cells as effective antigen presenting cells (36) and as essential initiators of germinal centre formation. Germinal centers benefit T cells by supporting T cell activities such as proliferation and cytokine production (37). Additionally, B cells secrete a wide array of cytokines that can act on diverse target cells. They can influence T-cell differentiation (38, 39), modulate the function of dendritic cells (40) and neutrophils (41) and regulate wound healing (1, 42).

### **1.3 The hazard of B cells: role in inflammatory and autoimmune conditions**

Due to their innate potential to inflict damage to their targets, multiple redundant mechanisms exist to prevent B cells from mounting a response to self-antigens, that is, to induce tolerance. Central tolerance mechanisms are at play during B cell development to edit (43) or remove (44) self-reactive precursors while clones that escape are controlled in the periphery by ignorance (45, 46) or anergy (47), a state of active unresponsiveness maintained by inhibitory signaling. Occasionally, these mechanisms fail and autoimmunity develops. Most autoimmune diseases are complex and involve multiple immune cell types, however several studies have clearly identified a key role for B cells in diseases such as Systemic Lupus Erythematosus (SLE), Rheumatoid Arthritis (RA), Type I Diabetes (T1D) (48) and, more recently, multiple sclerosis (49). The B

cells in these patients are abnormal. For example, analysis of blood from SLE patients revealed that their B cells are hyperactive (50) and increased in number during active phases of the disease (51).

B cell depletion therapy has demonstrated efficacy to varying degrees for all of these disorders (52-55). Their central role as major pathogenic contributors has also been carefully studied in animal models. Upon depletion of B cells, mouse strains susceptible to SLE (56), collagen-induced arthritis (CIA) (57, 58) and T1D (59, 60) are protected. Indeed, careful examination of several mouse strains that spontaneously develop SLE-like disease has revealed impairment in negative selection of B cells (61) or abnormally high activation of the phosphatidylinositol 3-kinase (PI3K) signaling pathway that is central to B cell development and function (62-64). Further, passive transfer of antibodies from SLE (65) or CIA (66) mice or from patients with rheumatoid arthritis (66) induces symptoms in otherwise healthy animals.

Autoantibodies and the resulting pathogenic activation of complement pathways are responsible for much of the tissue damage seen in these autoimmune diseases, notably anti-DNA antibodies in SLE (65) and anti-collagen antibodies in arthritis (67), at least in animal models. However, B cells also contribute significantly in other ways (48). This was elegantly demonstrated by genetic modification of an SLE susceptible mouse, creating a strain in which B cells cannot secrete soluble antibody but otherwise develop normally. These mice still developed nephritis (68). Another study identified a synergistic contribution of the antibody secreting function and the antigen presentation function of B cells in autoimmune arthritis (69). Here, mild arthritic symptoms were induced by transfer of arthritic serum into SCID mice or by adoptive transfer of

T cells primed by autoreactive B cells. Concurrent transfer of both resulted in severe arthritis (69). Another group demonstrated the importance of B cell antigen presentation in the non-obese diabetic (NOD) model of T1D. Here, a B cell specific deletion of MHC class II prevented B cells from presenting antigen and resulted in protection from disease development (70). Finally, in a human study, a subset of GM-CSF-producing B cells found to be increased in patients with multiple sclerosis was demonstrated to enhance myeloid cell pro-inflammatory responses in a manner dependent on cytokine production. B cell depletion in these patients led to reduced inflammatory cytokine production by macrophage that was reversible by adding back supernatants from the GM-CSF-producing B cell subset (49). Given the importance of antibody generation, antigen presentation, cytokine production and other B cell effector functions for the clearance of pathogens and given the damage these same functions can cause when targeted inappropriately, there is a need to understand the intricate balance between signals that result in B cell activation and those that result in inhibition. Such insight can inform us of how that balance becomes dysregulated in human disease and how it can be restored.

#### **1.4 B cell development**

Hematopoietic stem cells develop in the fetal liver and seed the bone marrow to provide a continuous source of newly derived immune cells throughout a mammal's lifetime (71). In adults, B cell development is restricted to the bone marrow, although other tissues contribute in the fetus and newborn (72). Lineage commitment begins at the common lymphocyte progenitor stage, which has the potential to give rise to B cells, T cells and Natural Killer cells (73-75). The stages of B cell development have been defined and refined by countless genetic studies in mice and extensive immunophenotyping in humans (76). Indeed details pertaining to the definition of

each stage and the discrepancies between mice and humans are still being debated, however a basic model has been developed and is largely agreed upon (*Figure 1-1*). The three main stages of B cell development in the bone marrow, pro-B, pre-B and immature B cells are dictated by transcription factor expression (77) and are defined by the genetic rearrangements that take place at each stage (76). These genetic rearrangements, along with somatic hypermutation and class switch recombination that occur in mature B cells, are used to create the immense diversity of immunoglobulins (also known as antibodies) required to recognize any conceivable antigen. Immunoglobulin heavy chains (H locus) are generated from combinatorial rearrangement of variable (V), diversity (D) and joining (J) gene segments, while immunoglobulin light chains (L locus) are generated from V and J segments (78). Several alternative segments are available for each and diversity is further amplified by the imprecise joining of segments, thus the number of possible combinations producing a complete Ig of heavy plus light chain is staggering (76, 79).

The first relatively well-defined stage is the pro-B cell stage (80, 81). Here, H-chain D and J segments are rearranged, followed by joining of a V region to DJ. Successfully recombined  $VDJ_H$  unites with a surrogate light chain (82) and  $Ig-\alpha/\beta$  to form a pre-BCR complex on the cell surface (83). If functional, signaling through the pre-BCR leads to the shutting down of H-chain rearrangement (84) and the initiation of L-chain rearrangement, marking the beginning of the pre-B cell stage. In this stage, V and J segments are joined for one the two L-chain alleles, known as  $\kappa$  and  $\lambda$  (85). In the next stage, immature B cells now express  $\kappa$  or  $\lambda$  L-chain along with H-chain, forming surface IgM, allowing survival and exit from the bone marrow. In mice, two transitional stages of immature B cells are characterized, T1 and T2 (86). By chance, many of the newly formed immature B cell clones are self-reactive. When these cells encounter self-



antigen in the bone marrow, developmental progression is blocked and instead the receptors are edited through continued genetic recombination (43, 87).

Immature B cells develop into mature B2 cells (marginal zone or follicular) through the T1 and T2 stages. During fetal development, immature B cells can also develop into B1 B cells, which populate the peritoneal and pleural cavities. Follicular B cells are the classic subtype that give rise to germinal centre responses and differentiate into either antibody-secreting plasma cells or long-lived memory B cells. Marginal zone (MZ) and B1 B cells are innate-like B cell subsets that produce “natural” antibody at homeostasis and can respond to T-independent antigens to produce adaptive antibody (1).

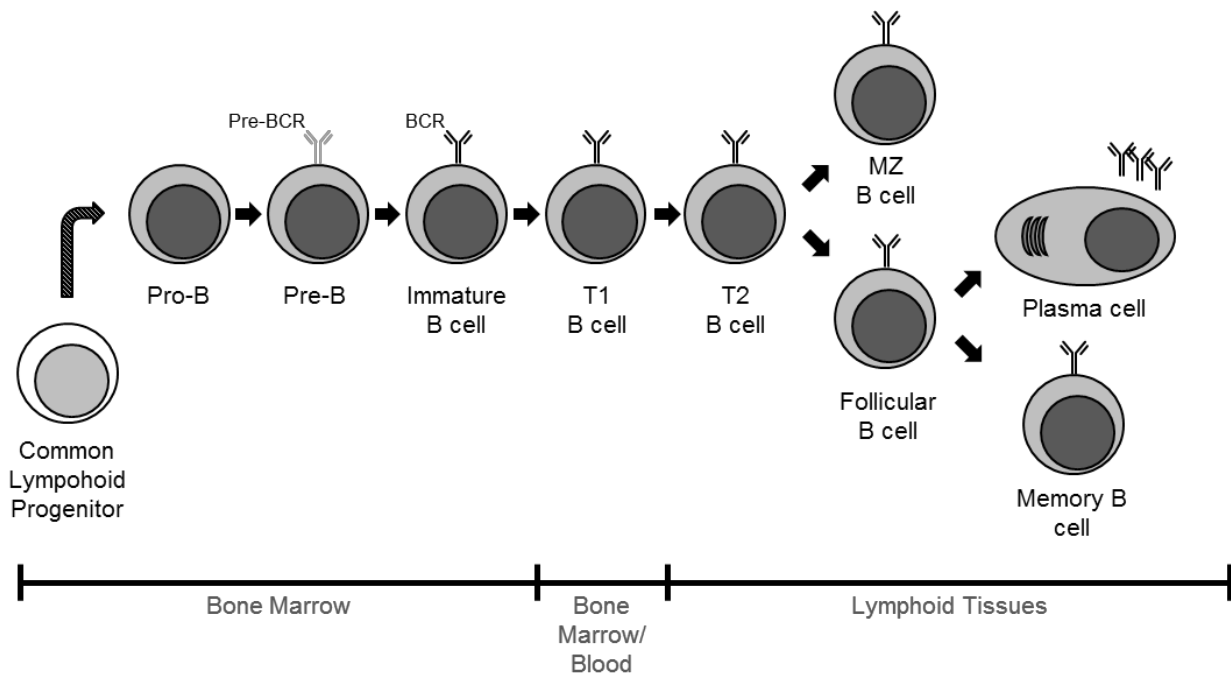


**Figure 1-1. Overview of B2 cell development including the major subsets and their primary tissue residency.**

*The common lymphoid progenitor gives rise to the B cell lineage, including subsets found in the bone marrow progressing from pro-B through pre-B to the immature B cell stage. Immature B cells progress through transitional stages 1 and 2 (T1 and T2), into mature lymphoid tissue resident subsets: marginal zone (MZ) B cells or follicular B cells. Follicular B cells are the subset that partake in classical germinal centre responses and can develop into antibody-secreting plasma cells or memory B cells.*

Throughout the developmental process, checkpoints are in place to reduce the incidence of either non-functional or autoreactive B cell clones. Positive selection checkpoints ensure function. At the pre-B cell stage, genetic rearrangements that result in a functional pre-BCR complex produce a receptor that transmits low-level signals that ensure survival of that clone. In the absence of this positive selection signal, cells will die (83, 88). Positive selection is also important during germinal center responses, as B cell clones generating weaker BCR signals fail to outcompete other clones for T cell help (89). Negative selection checkpoints safeguard auto-reactivity at the immature B cell stage. If a BCR is formed that interacts strongly enough with self-antigen, BCR

signaling will lead to either re-expression of receptor editing genes or to cell death (43, 87). In the absence of this negative selection signal, cells will live and continue through the developmental process.

## **1.5 Immune receptor signaling basics: ITAM versus ITIM**

Immune cells express receptors on their surface that respond to a wide variety of stimuli. Many of these receptors are tyrosine kinase or tyrosine kinase-associated receptors that become phosphorylated in their cytoplasmic tails upon ligation. The sequence context of these residues determines the type of effectors that are recruited and thus the type of signaling pathways that are initiated. Activating receptors contain Immunoreceptor tyrosine-based activation motifs (ITAMs) with consensus sequence YxxL/I(x<sub>6-8</sub>)YxxL/I (90, 91), where x is any amino acid. Generally, binding of tyrosine kinases to ITAM sequences initiate “positive” signaling pathways (92). Inhibitory receptors contain Immunoreceptor tyrosine-based inhibitory motifs (ITIMs) with consensus sequence I/V/L/SxYxxL/V (93, 94). These receptors become phosphorylated when they are co-ligated to activating receptors and thus are accessible to ITAM-associated kinase (93). Generally binding of protein or lipid phosphatases to ITIM sequences initiate “negative” signaling pathways (92). Well-known ITAM-bearing receptors include the BCR, the T cell receptor (TCR), the high affinity receptor for IgE (FcεRI), killer cell activatory receptors (KARs), and activating IgG receptors such as FcγRIIA and FcγRIII. Well-known ITIM-bearing receptors include the inhibitory receptor for IgG (FcγRIIB), CD22, killer cell inhibitory receptors (KIRs) and gp49B. Although these classifications have been useful in establishing our basic understanding of how immune cells balance both positive and negative inputs from their environment, several deviations from the standard model have been described. Inhibitory

phosphatases have been reported to bind ITAMs (95, 96), the binding of phosphatases to ITIMs can play a positive regulatory role (97) and ITIM sequences can be found coded within ITAMs, allowing for potential binding of either kinases or phosphatases depending on the number of phosphorylation events (98). The number of known exceptions is growing, thus it is important to view the ITAM-ITIM dogma as a guide for hypothesis generation without making biased assumptions in the absence of experimental evidence.

## **1.6 Signalling through the B cell receptor**

The BCR is an ITAM-bearing activating receptor that is of critical importance for B cell development and function. It is comprised of a membrane-embedded immunoglobulin (mIg), (99, 100) and a heterodimer of Ig $\alpha$ /Ig $\beta$  (101). The mIg can be of IgG, IgM, IgD, IgE, or IgA subtype and the association with Ig $\alpha$ /Ig $\beta$  is at a 1:1 ratio, at least for IgM (102). Antigen binding triggers a spatial reorganization of the BCRs, inducing an interaction with kinases Lyn and Syk. Lyn is thought to be principally responsible for subsequent phosphorylation of the two ITAM tyrosine residues in Ig $\alpha$  and Ig $\beta$  tails at early stages, although Syk plays this role in some contexts (103). Doubly phosphorylated Ig $\alpha$ / $\beta$  ITAMs provide binding sites for Syk, thereby initiating its activation (104). Lyn and Syk each phosphorylate a variety of target proteins, initiating multiple independent and overlapping signaling cascades that ultimately result in activation of the B cell (105).

### **1.6.1 Signal initiation**

Exactly how antigen binding to mIgM initiates a spatial reorganization of BCRs and how this initiates signaling has been a topic of hot debate. The first hypothesis to garner wide support is the crosslinking model (*Figure 1-2A*), which suggests that BCRs exist as monomers within

the plasma membrane of a resting cell and are induced to form signaling-competent oligomers when multivalent antigen physically joins them (106). It is proposed that this accumulation of BCRs in specific membrane subdomains allows access to signal initiating kinases Lyn and Syk (107). The early observation that divalent  $F_{(ab')_2}$  but not monovalent  $F_{ab}$  anti-BCR antibodies induces signaling backed this theory (108), as did early studies demonstrating that monovalent antigens make poor vaccines (20). More recently, Förster resonance energy transfer (FRET) experiments also seemed to provide support for the crosslinking model (102).  $Ig\alpha$  molecules were tagged with a mixture of FRET donor cyan fluorescent protein and FRET acceptor yellow fluorescent protein. The authors observed a low FRET efficiency in resting cells, suggesting that individual BCR molecules do not associate with each other at rest and are instead monomeric (102). However, careful assessment of the technique in other systems later cautioned against over-interpretation of negative FRET data since several factors are at play such as relative abundance of the tags and their orientation (109).

The next iteration of BCR signal initiation model is known as the conformation-induced oligomerization model (110). It proposes that binding of membrane-bound antigen to BCR exerts a torsion force that exposes an oligomerization interface in the membrane-proximal domain of mIg, the  $C\mu 4$  domain. Oligomerization then leads to the merging of BCRs into “microclusters” within specialized “raft-like” lipid domains that allow association of the BCR signaling chains with raft-resident Lyn (110). The idea was first conceived upon the observation that monovalent antigen failed to induce BCR signaling in solution but succeeded when embedded in a lipid bilayer. Further study was made possible by advancements in total internal reflection fluorescence microscopy and post-processing calculations that allowed for

single particle tracking of fluorescently labelled BCRs (111). Here a small fraction of the BCRs are labelled and the cells are spread on an antigen-coated lipid bilayer to simulate the encounter of cell surface antigen. As the cells spread, BCRs converge into microclusters and their lateral diffusion rate slows until the receptors are immobilized, coincident with the initiation of signal transduction (112). The authors demonstrated that BCRs mutated in either the C $\mu$ 4 domain or the N-terminal region of the transmembrane domain did not immobilize in response to monovalent antigen, and were never fully phosphorylated. Further, if all mIg domains except C $\mu$ V and the transmembrane domain are deleted, spontaneous microcluster formation occurs in the absence of antigen and BCRs become immobilized within the microclusters (110), hinting that these regions might be involved in oligomerization. Thus the “conformation-induced oligomerization” model was born. According to this model, binding of membrane-bound monovalent antigen to BCRs exerts unique physical forces that are not exerted upon binding of soluble antigen. These forces induce a change in conformation or orientation of the extracellular domain, exposing a “clustering interface” in the C $\mu$ 4 domain, leading to oligomerization of BCRs. Oligomerization presumably perturbs the lipid environment within the cluster and leads to opening of the cytoplasmic domains and initiation of signal transduction (113).

The conformation-induced oligomerization model for BCR signal initiation was built almost exclusively on single particle tracking of labelled BCRs. Recognizing certain technical issues associated with this approach led others to investigate further using complementary methods, the results of which led to a complete reversal of previous thinking (by some) and the origin of the dissociation activation model (114). This model proposes the presence of small

oligomeric BCR clusters (or nanoclusters) at rest which dissociate upon ligation, releasing steric constraint and exposing Ig $\alpha$ /Ig $\beta$  ITAMs to the early kinases for signal initiation and reorganization into larger but loosely associated microclusters (114). The experiment driving the formulation of this hypothesis was a bimolecular fluorescence complementation (BiFC) assay where cells expressed Ig $\alpha$  molecules fused to half domains of YFP and CFP (115). These tag fragments are non-fluorescent unless two differentially tagged Ig $\alpha$  molecules are in close proximity, in which case the half domains join and a fluorescent signal is detected. The authors observed a fluorescent signal at rest, suggesting the presence of BCR oligomers prior to receptor ligation. Since the joining of half-domains is irreversible, this experimental system is not suitable to measuring the ligand-induced dissociation of BCR oligomers proposed by the model.

The same group addressed this issue with the development of a specialized proximity ligation assay (PLA) which used Fab fragment of anti-Ig antibodies directly conjugated to specialized DNA fragments, to label the intracellular region of the BCR (116). When two labelled targets are in extremely close proximity (10-20nm), the DNA fragments ligate and are amplified, enabling detection with a fluorescent DNA probe. The authors demonstrated an initially detectable signal at rest that was significantly reduced upon BCR ligation. Further, they demonstrated that interaction of Syk with doubly phosphorylated ITAMs was required for the opening of BCR oligomers (116).

How can this new model be reconciled with previous experiments seemingly endorsing the former models? According to the advocates of the dissociation activation model, the

observation that  $F_{(ab')_2}$  but not  $F_{ab}$  anti-BCR antibodies induces signaling is explained by the ability of the larger, divalent  $F_{(ab')_2}$  fragment to bind two different mIgM molecules and aid in their physical separation (114). Moreover, they suggest that the single particle tracking data initially proposed to support the conformation induced oligomerization model can be interpreted in an alternative way. Even though individual BCRs are fluorescently tagged in this assay, they must account for a very small fraction of the total BCR molecules in the cell to allow for tracking of single molecules. Since BCR complexes measure around 10nm and the optical diffraction limit is around 250nm, this assay cannot distinguish single, monomeric BCR molecules from those participating in an oligomeric complex with other untagged BCRs (114). As a result of newly developed complementary techniques as well as re-interpretation of older experiments, many experts now support the dissociation activation model of BCR signal initiation.



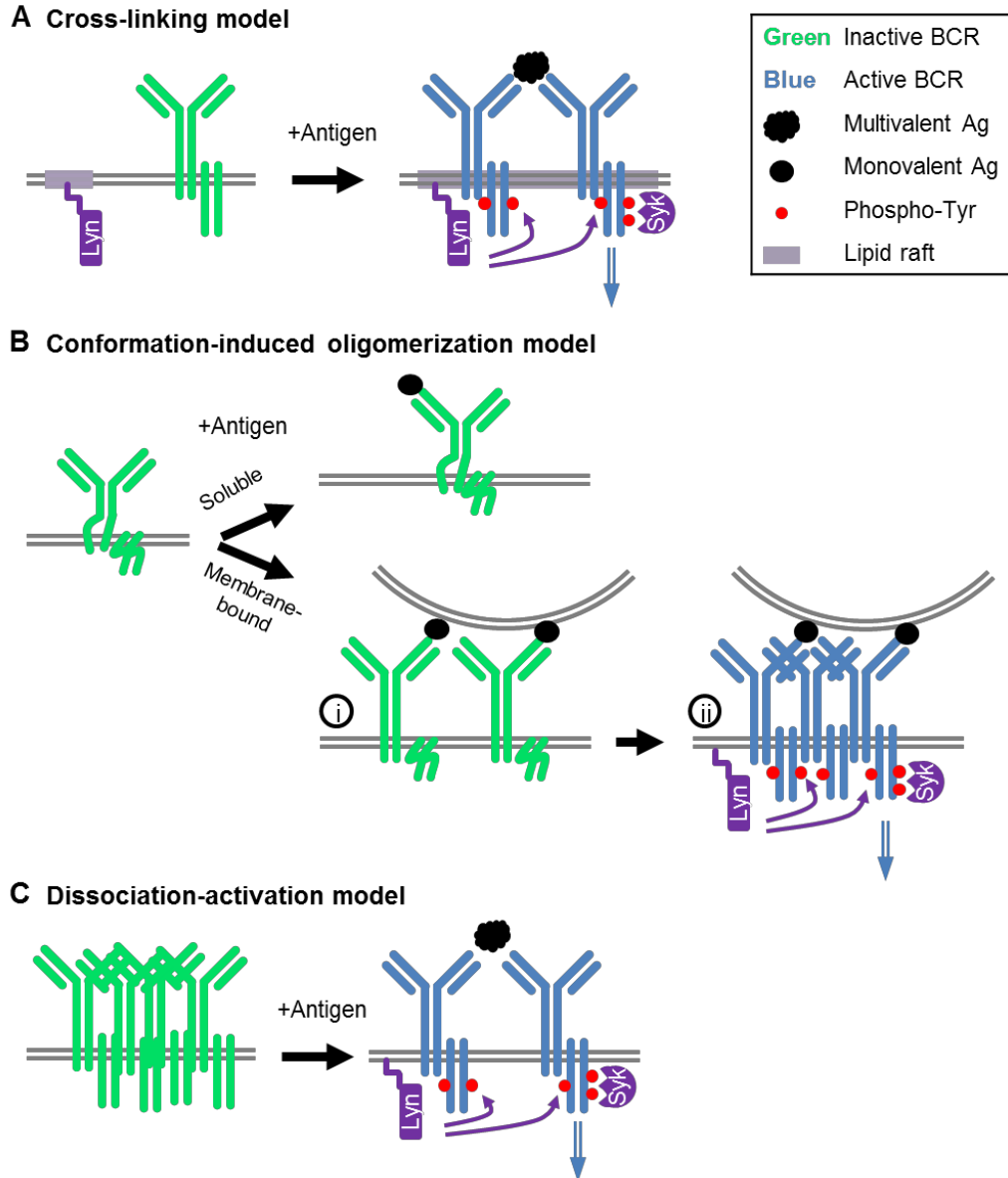


**Figure 1-2. Models of BCR signal initiation.**

(A) *Cross-linking model. BCRs exist as monomers at rest. When multiple BCRs bind to different sites on the same multivalent antigen, they coalesce together into lipid rafts, where resident kinases initiate signaling.*

(B) *Conformation-induced oligomerization model. BCRs exist as monomers in a closed conformation at rest. Upon ligation with membrane-bound (but not soluble) monovalent antigen, mechanical forces favor an extended conformation in the extracellular domain (i). This exposes a clustering interface, leading to oligomerization and subsequent opening of the cytoplasmic domain to initiate signaling (ii).*

(C) *Dissociation-activation model. BCRs exist as auto-inhibited oligomers at rest. Upon ligation with multivalent antigen, the receptors become spatially separated, allowing kinases to access the cytoplasmic domains to initiate signaling.*

All of the above models attempt to describe how the signaling chains of the BCR become accessible to and phosphorylated by Lyn and Syk kinases. Once these kinases come into play, they initiate several signaling pathways that contribute to B cell survival, proliferation and effector functions. The main downstream players are phospholipase C $\gamma$  (PLC $\gamma$ ), mitogen-activated protein kinases (MAPKs), and phosphoinositol 3-kinase (PI3K, **Figure 1-3**) (105).

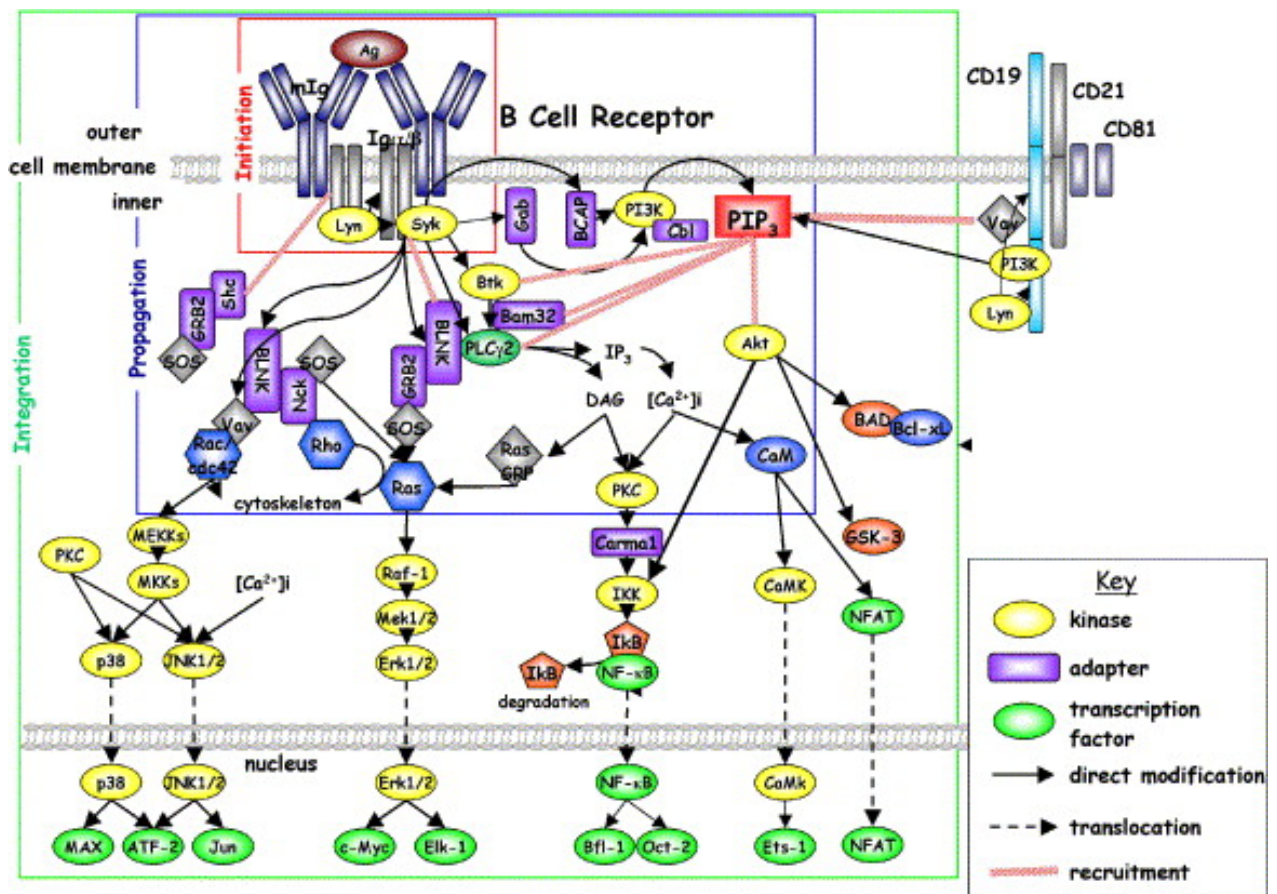


**Figure 1-3. Overview of BCR signaling (105).**

When B cell receptor ligation occurs, early signaling kinases Lyn and Syk become activated and phosphorylate multiple targets, including other protein kinases such as Btk as well as adaptor molecules such as BLNK and BCAP. These facilitate the organization of signaling complexes and initiation of key pathways including the PI3K pathway, the NF $\kappa$ B pathway, and the MAP kinase pathways. These culminate in activation of transcription factors and ultimately changes to the gene expression profile of the cell.

### 1.6.2 PLC $\gamma$ pathway

B cells express the lipid-cleaving enzyme phospholipase C $\gamma$ 2 (PLC $\gamma$ 2) (117). PLC $\gamma$ 2 is recruited to the BCR when the scaffolding protein B cell linker (BLNK or SLP-65) associates with Ig- $\alpha$  pY204 (118, 119) and is phosphorylated on several tyrosine residues by Syk (120). PLC $\gamma$ 2 interacts with BLNK via its SH2 domain (120) and with plasma membrane lipid PI(3,4,5)P<sub>3</sub> (to be discussed later) via its PH domain (121). PLC $\gamma$ 2 is then phosphorylated by Syk (122). Optimal enzymatic activation requires further phosphorylation by PI3K-dependent kinase Btk (123, 124). PLC $\gamma$ 2 then cleaves the plasma membrane lipid PI(4,5)P<sub>2</sub> to produce inositol triphosphate (IP<sub>3</sub>) plus diacyl-glycerol (DAG). IP<sub>3</sub> is the ligand for certain Ca<sup>2+</sup> channels in the endoplasmic reticulum; ligation induces opening and release of Ca<sup>2+</sup> ions into the cytoplasm (125, 126). Depletion of intracellular stores then induces opening of plasma membrane store operated channels, known as Calcium release activated calcium (CRAC) channels, leading to influx of extracellular Ca<sup>2+</sup> (127, 128). This sets the stage for activation of two major transcription factors: NF-AT and NF $\kappa$ B. The activation of these factors can be accomplished and regulated by several means, however only the classical pathways will be discussed here. NF-AT activation occurs when Ca<sup>2+</sup>-bound calmodulin binds to calcineurin and activates its phosphatase activity (129, 130). Calcineurin dephosphorylates NF-AT, triggering its translocation into the nucleus (131) where it activates transcription of target genes including IRF4 (130). NF $\kappa$ B activation is initiated when protein kinase C is activated by DAG plus Ca<sup>2+</sup>. PKC promotes phosphorylation of Inhibitor of NF $\kappa$ B Kinase  $\alpha$  (I $\kappa$ B kinase $\alpha$  or IKK $\alpha$ ), which then phosphorylates I $\kappa$ B, causing it to be degraded and thus release its inhibitory effect on NF $\kappa$ B (132). This frees the transcription factor to enter into the nucleus

where it activates target genes, including those encoding cytokines, chemokines, cell survival proteins and more (133).

### **1.6.3 MAPK pathways**

Activation of MAPKs in B cells largely occurs downstream of small G proteins Ras (for ERK1/2 MAPK) and Rac (for JNK and p38 MAPKs). These small G-proteins are themselves activated by Guanine nucleotide exchange factors (GEFs). GEFs promote dissociation of GDP from the G protein, freeing the binding pocket for interaction with GTP, which is found in higher relative abundance in the cytoplasm (134). The MAPKs ERK, JNK and p38 are all activated downstream of the BCR (134).

In BCR-stimulated B cells, the Ras-GEF Son of Sevenless (SOS) is recruited to the B cell signalosome either by interaction with Grb2 and Shc (135, 136) or Grb2 and BLNK (137). Alternatively, another Ras-GEF called Ras guanyl nucleotide releasing protein 1 (RasGRP1) is phosphorylated by protein kinase C  $\beta$  (PKC $\beta$ ) downstream of PLC $\gamma$ 2 activation. This phosphorylation event promotes the GEF activity of RasGRP1 (138, 139). Once acted upon by these GEFs, Ras-GTP activates the Raf proteins (Raf-1 and BRAF), which then phosphorylate and activate MEK1/2, which then phosphorylate ERK1/2, which dimerize, enter the nucleus, and modulate the activity of transcription factors that control cell proliferation and differentiation (140).

In BCR-stimulated B cells, the Rac-GEF Vav is also recruited to the B cell signalosome by way of binding to BLNK (120, 141). Vav promotes Rac activation by way of GDP-GTP exchange and PKC (activated by PLC $\gamma$  signaling) co-operatively promotes Rac activation

presumably by phosphorylation (137). Rac-GTP then activates the MAPK pathways leading to phosphorylation of the other two family members, p38 and JNK (137).

#### **1.6.4 PI3K pathway**

The importance of the PI3K signaling pathway has been demonstrated through numerous studies confirming that it is central to B cell development (142, 143), survival (144) and activation (145, 146). Upon BCR ligation, the lipid second messenger phosphoinositol-3,4,5-trisphosphate (PI(3,4,5)P<sub>3</sub> or PIP<sub>3</sub>) rapidly accumulates in the plasma membrane (147). It is generated from the plasma membrane precursor phosphoinositol-4,5-bisphosphate (PI(4,5)P<sub>2</sub>) by the activity of Class I PI3Ks (148) (*Figure 1-4*). PIP<sub>3</sub> interacts with specific pleckstrin homology (PH) domain-containing binding partners to relay signals downstream (149). PIP<sub>3</sub> can be dephosphorylated at position D5 by inositol 5-phosphatases SHIP1 and SHIP2, producing PI(3,4)P<sub>2</sub> (150) (*Figure 1-4*). This lipid can also bind certain PH-domain containing proteins, some overlapping and some distinct (151). PTEN removes the D-3 phosphate group, therefore inhibiting the formation of both PIP<sub>3</sub> and PI(3,4)P<sub>2</sub>. INPP4 converts PI(3,4)P<sub>2</sub> to inert lipid PI(3)P (152, 153) (*Figure 1-4*).

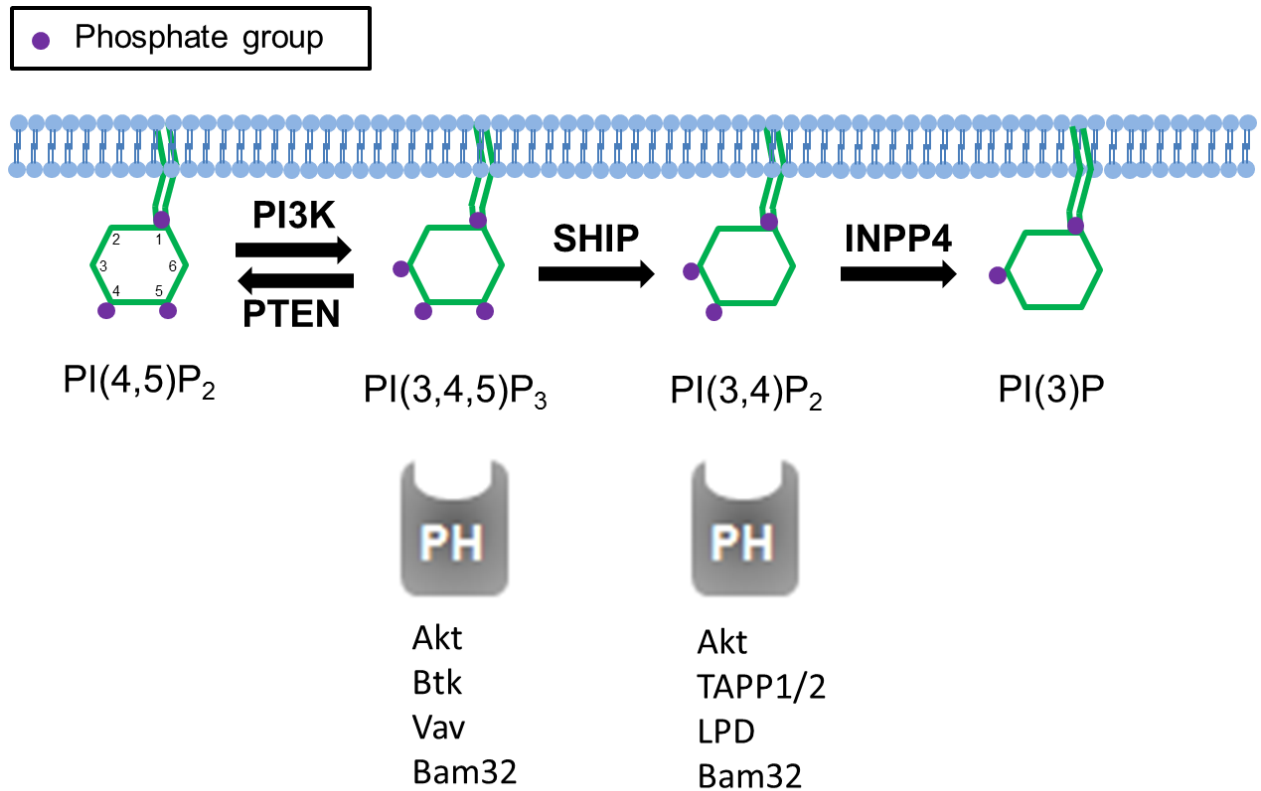


**Figure 1-4. Overview of PI3K signaling in lymphocytes.**

The primary substrate of PI3K in B cells is the membrane lipid PI(4,5)P<sub>2</sub>, which acquires a phosphate group to yield PI(3,4,5)P<sub>3</sub>. PI(3,4,5)P<sub>3</sub> can be bound by specific PH domain-containing proteins. Lipid phosphatases PTEN and SHIP dephosphorylate the phosphate groups at position 3 and position 5 on the inositol ring, respectively. PI(3,4)P<sub>2</sub> produced by SHIP can be bound by an independent yet overlapping set of PH domain-containing proteins and can be further dephosphorylated by INPP4.

**1.6.4.1 PI3K isoforms**

All PI3K isoforms are inositol D3 kinases, however the three different classes have unique regulation and substrate specificities. Class I enzymes catalyze the conversion of PI(3,4)P<sub>2</sub> to PIP<sub>3</sub> and PI4P to PI(3,4)P<sub>2</sub>, with the former being the dominant reaction induced by BCR signaling. Class II and III enzymes convert PI to PI(3)P while class II also produces PI(3,4)P<sub>3</sub> from PI4P. The roles of Class II and III PI3Ks have not been characterized in lymphocytes. Class I on the other hand are known to be central regulators of BCR signaling (148, 154).

Class I PI3Ks exist as heterodimers of a regulatory subunit (p85 subfamily: p85 $\alpha$ / $\beta$ , p55 $\alpha$ / $\gamma$ , p50 $\alpha$  or p101) and a catalytic subunit (p110 $\alpha$ ,  $\beta$ ,  $\delta$  or  $\gamma$ ) and are further subdivided into Class IA and Class IB. Class IA members include PI3K $\alpha$ , PI3K $\beta$  and PI3K $\delta$ , named based on the identity of their p110 catalytic subunit. These are classically described to be activated downstream of tyrosine kinase receptors or tyrosine kinase-linked receptors (155), however recently the  $\beta$  isoform was also demonstrated to be activated by GPCRs through direct binding to G $\beta\gamma$  subunits (156). p110 $\alpha$  and  $\beta$  isoforms are ubiquitously expressed while the p110 $\delta$  is restricted mainly to the hematopoietic compartment. Class IB has only one member: PI3K $\gamma$ , a hematopoietic-restricted, GPCR-activated enzyme (154, 157).

There has been much interest in the isoform-specific requirements for PI3K in B cell development, maintenance and function (Reviewed in (158)). With respect to B cell development in the mouse, loss of p110 $\delta$  leads to a B cell maturation defect whereas double knock of both p110 $\delta$  and p110 $\alpha$  completely blocks development at the pre-B cell stage (159). This likely reflects a requirement for these PI3K isoforms in pre-BCR signaling as well as signaling through the IL-7 receptor. Combined deletion of p110 $\delta$  and p110 $\gamma$  has a more profound effect compared to deletion of p110 $\delta$  alone (160), however the role of p110 $\gamma$  is more likely B-cell extrinsic, impacting T cell development and activation which may influence B cell development indirectly (161). Deletion of p110 $\beta$  has no measurable effect on B cell development or function in the studies performed to date (159).

With respect to B cell maintenance, continuous low level signaling through the BCR, called tonic signaling, is required for the long term survival of mature B cells (17, 162) and this relies on PI3K signaling (163). Loss of either p110 $\alpha$  or p110 $\delta$  activity in the mouse leads to a dose-dependent loss of follicular B cells, with p110 $\delta$  having a more profound effect (159). MZ B cells are thought to require more robust PI3K signaling in order to be maintained, achieved by BCR ligation with self-antigens. p110 $\delta$  but not p110 $\alpha$  is required for maintenance of these cells (159). Thus, the roles of the  $\alpha$  and  $\delta$  isoforms appear to be redundant in the context of tonic signaling while the  $\delta$  isoform is specifically required for antigen-triggered responses (159). This idea was re-enforced by studies specifically examining the effects of p110 $\delta$  inactivation or deletion on mature B cell functions. For example, p110 $\delta$  catalytic activity was required for T cell-dependent antibody responses (146), antigen presentation to T cells (164), and B cell spreading (165), a process that precedes antigen uptake for presentation. B cell adhesion and migration also rely on p110 $\delta$  (166). Furthermore, reduced Akt activation resulting from p110 $\delta$  inactivation resulted in enhanced activation-induced cytosine deaminase (AID) expression and was correlated with increased antibody class switch to the IgE isotype (167, 168).

#### ***1.6.4.2 Recruitment and activation of Class I PI3Ks***

The regulatory subunit serves both to inhibit activity at rest and to trigger activity in response to receptor ligation. For Class IA PI3K, the interstitial SH2 domain (iSH2) of the regulatory subunit interacts strongly with p110. At rest, the N-terminal (nSH2) and C-terminal (cSH2) SH2 domains also interact weakly with p110 to promote an inhibitory conformation (169). This inhibitory conformation is released when nSH2 and/or cSH2 binds to phospho-peptide motifs (170-172) such as the Y-x-x-M sequence found in CD19



(142) and BCAP (142, 173, 174) or to non-canonical Tyr-based motifs in R-Ras2 (175) and Syk (176). Binding to CD19 and BCAP are thought to be the principal recruitment mechanisms in BCR-stimulated B cells (142). Recent evidence suggests the adaptor protein Nck binds to Ig- $\alpha$  to bridge BCAP to the BCR (177). Additional mechanisms have been described to further enhance catalytic activity in some contexts, specifically binding to anionic lipids (178) and to Ras (179, 180) and Rac (181) family GTPases. PI3K $\beta$  is unique in that it can be synergistically activated by binding both phosphotyrosine residues via its regulatory subunit and binding to the G $\beta\gamma$  subunit of activated GPCRs via its catalytic subunit p110 $\beta$  (182, 183).

For class IB PI3K, the regulatory subunit p101 binds membrane bound G $\beta\gamma$  from activated GPCRs to recruit catalytic subunit p110 $\gamma$  to the plasma membrane. G $\beta\gamma$  then allosterically activates p110 $\gamma$  enzymatic activity (184). Unlike the Class IA PI3Ks, p110 $\gamma$  may sometimes function as a monomer, independent of its regulatory subunit (185). In this context membrane recruitment may be facilitated by binding to anionic phospholipids (186) or other membrane-associated proteins such as Ras (187, 188).

### ***1.6.4.3 Major PI3K effectors***

#### ***1.6.4.3.1 Akt***

One of the best described effectors of PI3K signaling downstream of BCR ligation (189, 190) is the pro-survival serine/threonine kinase Akt, also known as protein kinase B (PKB) (191). Overexpression of Akt in chicken DT40 B cells inhibits BCR-induced apoptosis (190). Akt binds both PIP<sub>3</sub> and PI(3,4)P<sub>2</sub> via its N-terminal PH domain (192,

193), inducing its recruitment to the cell periphery (192). This results in a conformational change (194) which facilitates its phosphorylation on two Ser/Thr residues by membrane-proximal kinases (195). Now, fully active, Akt phosphorylates several cytoplasmic (196) and nuclear (197) substrates. These substrates include Bad (198), GSK-3 (199) and IKK (200, 201).

#### 1.6.4.3.2 Btk

Bruton's tyrosine kinase (Btk) is a Tec-family kinase expressed in most B cell subsets as well as in innate immune cells (202). Its PH domain specifically binds PIP<sub>3</sub> (203, 204). BCR ligation induces rapid and transient plasma membrane localization that is negatively regulated by both PTEN and SHIP (205, 206). Btk participates in the BCR signalosome (207) and phosphorylates PLC $\gamma$ 2 (124) to promote Ca<sup>2+</sup> signaling (208, 209) and ultimately NF $\kappa$ B activation (210, 211) as well as inside-out activation of integrins (212). Btk also phosphorylates Vav and Wiskott Aldrich syndrome protein (WASP) (213), thereby promoting filamentous- (F-)actin polymerization. The central role of Btk in B cell survival and function is illustrated by a rare human disease, X-linked agammaglobulinemia, caused by loss of function mutations in the PIP<sub>3</sub>-binding pocket of Btk. These patients virtually lack circulating B cells and are unable to produce antibody (214).

#### 1.6.4.3.3 Small GTPases

The Rho family GTPases Rac and Cdc42 exhibit a complex relationship with PI3K, as they have been described to be both upstream PI3K activators and downstream PIP<sub>3</sub> effectors in various systems. What is clear is that they both promote cytoskeletal rearrangements in B cells, stimulating the formation of lamellipodia and filopodia (215).

Rac isoforms 1 and 2 also promote B cell development, BCR signaling (216) and integrin-mediated adhesion through activation of actin nucleation protein Wiskott aldric syndrome protein (WASP) (165). A dependence on upstream PI3K signaling was demonstrated for the adhesion-promoting function of Rac2 (165). One mechanism for Rac1 activation downstream of PI3K was described by our group and depends on the PI(3,4)P<sub>2</sub>-dependent adaptor protein Bam32 (217). BCR-mediated Rac1 activation was impaired in Bam32-deficient B cells, as was B cell adhesion and interaction with T cells. The reverse was observed in Bam32-overexpressing B cells (217). Another mechanism is PI3K-dependent activation of Vav, demonstrated to be a GEF for both Rac1 and Cdc42 (218, 219). *In vitro* and in other cellular systems, interaction of PIP<sub>3</sub> with the PH domain of Vav1 supports an open conformation that permits phosphorylation for further activation (220, 221). However, Vav isoform 3 activity is apparently unaffected by pharmacological inhibition of PI3K in B cells (181). Other isoforms have not been explicitly tested. A more recent study identifies a clear requirement for the PIP<sub>3</sub> effector Btk in efficient phosphorylation of Vav1 and colocalization of Vav1 with the BCR (213). The principal role of these Rho-family GTPases is to bind and activate actin nucleation proteins WASP, neural- (N-)WASP and WASP-family verprolin-homologous protein (WAVE), as will be discussed in section 1.8. The activity of another more recently described small GTPase, Ras-related protein 1 (Rap1), is impaired by pharmacological inhibition of PI3K as well as by deficiency in Vav1, Vav2 or Rac2 (165). Rap1 is known to promote adhesion by activation of integrins (222) and B cell spreading by activation of actin severing protein cofilin (223).

### 1.6.5 BCR signal modulation by co-receptors and phosphatases

The magnitude and duration of BCR signaling required in a given situation depends on several factors, for example the subtype of B cell that is being activated, whether an infection is in early or late stage, and whether other inflammatory or “danger” signals are present in the microenvironment. One important means by which B cells modulate their signaling strength is by way of co-receptors (*Figure 1-5*). CD19 is a co-receptor that lowers the threshold for BCR signaling when bound by C3d complement fragments (224). It forms a complex with CD21 (type 2 complement receptor) and CD81 (tetraspanin) (225). It can be phosphorylated by Lyn and Syk (226, 227) to provide a binding site for PI3K (227). Although co-ligation of the CD19 complex can amplify BCR signaling (224), CD19 becomes phosphorylated after BCR ligation even in the absence of complement and it is critical for effective PI3K activation in this context (228, 229).

In addition to the prominent activating co-receptor CD19, two inhibitory co-receptors have been described to dampen BCR-mediated signals: CD22 and FcγRIIB. CD22, or Siglec-2, is an adhesion molecule of the lectin family that recognizes a variety of glycan ligands containing α2,6-linked sialic acid moieties (230). Soluble IgM is glycosylated in such a way and therefore can serve as a ligand (231). CD22-deficient mice display increased Ca<sup>2+</sup> flux in response to BCR ligation (232). It is not strictly a negative regulator however, as anti-CD22 monoclonal antibody treatment synergizes with BCR ligation to induce a robust proliferative response (232, 233). One important and well described mechanism to explain the negative regulatory role of CD22 is the phosphorylation of its ITIM tyrosines that specifically bind the protein phosphatase SHP-1 (232, 234). It has also been proposed to recruit SHIP (235). Upon

BCR ligation, a complex containing CD22, Shc, Grb2 and SHIP was detected by co-immunoprecipitation. Pull-down experiments with biotinylated peptides mapped the phosphotyrosine binding sites for Shc and Grb2, however a direct binding site was not found for SHIP (235).

Another well-characterized inhibitory co-receptor is Fc $\gamma$ RIIB; it will be discussed at length in chapter three. Briefly, this receptor is ligated by the Fc portion of IgG antibody, found in soluble form at late stages of an immune response or as a component of immune complexes in the context of chronic inflammation (236). When co-ligation occurs, the BCR-associated kinase Lyn phosphorylates the ITIM tyrosine in Fc $\gamma$ RIIB (237), recruiting its binding partner SHIP (238, 239). SHIP is thought to be responsible for most or all of the inhibitory action of Fc $\gamma$ RIIB, evidenced by experiments where co-ligation of Fc $\gamma$ RIIB failed to inhibit BCR-induced Ca<sup>2+</sup> flux in the absence of SHIP (240, 241). As the regulation and function of SHIP is the major topic of this thesis, an extensive background will be provided in section 1.7.

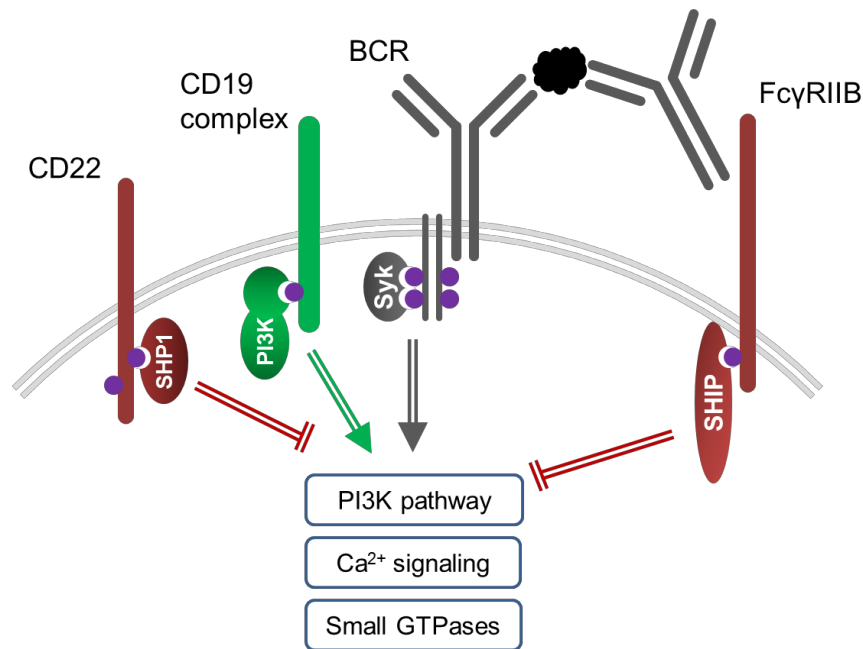


**Figure 1-5. BCR signal modulation by co-receptors.**

*BCR ligation leads to phosphorylation of ITAM tyrosine residues in the BCR signaling chains, recruiting Syk kinase and initiating multiple pathways leading to B cell activation. Positive regulation (green) occurs by co-ligation of CD19, which can directly recruit class IA PI3K via phosphorylated tyrosine residue. Negative regulation (red) occurs by co-ligation of ITIM-bearing receptors. FcγRIIB recruits lipid phosphatase SHIP and CD22 classically recruits protein phosphatase SHP-1.*

### 1.6.6 Abnormal BCR signaling and disease

Since BCR signaling triggers such responses as survival, proliferation, and activation, it not surprising that dysregulation of several key BCR signaling molecules has been described to contribute to both autoimmune disease (242) and to B cell malignancy (243).

Murine models lacking negative regulators of BCR signaling pathways such as CD22 (244, 245), FcγRIIB (62), SHIP (63), PTEN (246) and SHP-1 (247) display B cell hyperactivity and spontaneously develop autoantibodies. A similar phenotype is seen in CD19 transgenic mice (248) and this CD19 overexpression was demonstrated to break tolerance to model autoantigens (249). In humans, increased expression of CD19 on B cells from systemic

sclerosis patients was found to correlate with increased auto antibody titres (250). Autoimmune diseases are complex and involve multiple cell and organ systems, some of which employ the same signaling molecules. Thus it is often difficult to isolate a specific role for the BCR. Some of the above mouse studies address this using B-cell targeted genetic manipulations (63) or examine regulators whose expression is restricted to the B cell compartment (244, 245, 248). These studies in addition to ex-vivo analysis of altered B cell responses support abnormal amplification of BCR signaling as a central driver of autoimmune responses involving antibody.

Enhanced BCR signaling also contributes to B cell malignancy. In a prominent subset of Diffuse large B cell lymphoma (DLBCL) patients, activating mutations are found within the ITAM motifs of Ig- $\alpha$  and Ig- $\beta$  (251). In chronic lymphocytic leukemia (CLL), maintenance of malignant B cells is supported by chronic BCR signaling resulting from low affinity reactivity to self-tissues or microbial antigens (243). Gene expression profiling has identified BCR signaling pathways as by far the most prominently activated pathways in CLL cells isolated from lymphatic tissues (252). In various types of B cell malignancies, increased BCR signaling has been demonstrated to be supported or sustained by increased PI3K enzymatic activity (253), decreased PTEN enzymatic activity (254), increased expression of miRNAs targeting PTEN (17, 255, 256) and SHIP (257), abnormal expression and function of Lyn (258) and upregulation of BLNK (259). Enhanced PI3K pathway activation by the above mechanisms is critical in sustaining CLL cells by promoting cellular and molecular interactions within the permissive microenvironment of lymph nodes and bone marrow (260). This role is being exploited clinically, as both PI3K $\delta$  inhibitors and Btk inhibitors have been

approved for treatment of CLL and mantle cell lymphoma (261). The signaling programs that drive and sustain abnormal function in B cell-driven autoimmunity and malignancy may prove to be their most exploitable Achilles heel.

## **1.7 SH2 domain-containing inositol 5'phosphatase (SHIP)**

### **1.7.1 Discovery of SHIP**

In 1994, several groups reported that a 145-kDa protein became phosphorylated and associated with the adaptor protein Shc1 after BCR (136, 262) or cytokine receptor stimulation (263). Two years later, that protein was identified to be the inositol 5'phosphatase SHIP (264-266), encoded by the gene *INPP5D*.

### **1.7.2 SHIP knock-out models**

The first indication that SHIP was a regulator of BCR signaling came from genetic manipulation of the DT40 chicken B cell line. SHIP<sup>-/-</sup> DT40 cells have increased Ca<sup>2+</sup> flux in response to BCR stimulation which can be rescued by re-expression of wild type but not phosphatase-dead SHIP (267). B cells from SHIP<sup>-/-</sup> mice were studied shortly after (150). The dominant phenotype in these mice is myeloid cell infiltration into the lungs associated with early death (268), however defects in B cell development and activation were apparent in young mice (150). Brauweiler et al. (150) demonstrated reduced numbers of pre- and immature B cells in the bone marrow but increased numbers of B cells in the spleen. By irradiating the animals then following the reconstitution of lymphocyte cell populations, they found evidence for accelerated B cell development and quicker emigration from the bone marrow. When studied in isolation, the SHIP<sup>-/-</sup> B cells were hyper-responsive to BCR



stimulation, displaying increased and sustained PIP<sub>3</sub> production and increased expression of activation markers CD86 and CD69 relative to B cells from wild type mice (150).

Two B cell-specific SHIP knock-outs were later made using a CD79a (Ig $\alpha$ )-cre system in a mixed background (63) and using a CD19-cre system in a C57BL/6 background (269). A similar state of hyper-responsiveness was reported (269). In the mixed background, a severe lupus-like autoimmune disease manifested in the knock-out mice, characterized by high titres of anti-nuclear antibody and by immune complex deposition in kidney glomeruli (63). In C57BL/6 mice, B cell-specific SHIP-deficiency resulted in a shift in B cell populations. The authors found decreased marginal zone B cells but increased germinal centre B cells, B1 cells and plasma blasts. Furthermore, germinal centres formed spontaneously and levels of IgG2 antibodies were increased. Despite this increased responsiveness at rest, the mice responded poorly when challenged. Germinal centres formed but were defective, resulting in reduced isotype switching and the production of only low affinity specific antibody. The authors proposed that the lowered threshold for activation in SHIP<sup>-/-</sup> cells leads to increased negative selection of B cells. The hyper-responsiveness would cause death of intermediate- and high-affinity clones, allowing only low affinity clones to survive and contribute to weakened humoral responses (269). All together, these cell line and murine knock-out systems established a central role for SHIP as a negative regulator of B cell development and responsiveness to antigen.

### **1.7.3 Structure and function**

SHIP is a 1189 amino acid protein encoded by the gene *Inpp5d*. It contains several identifiable domains and motifs that contribute to its cellular functions (**Figure 1-6**).

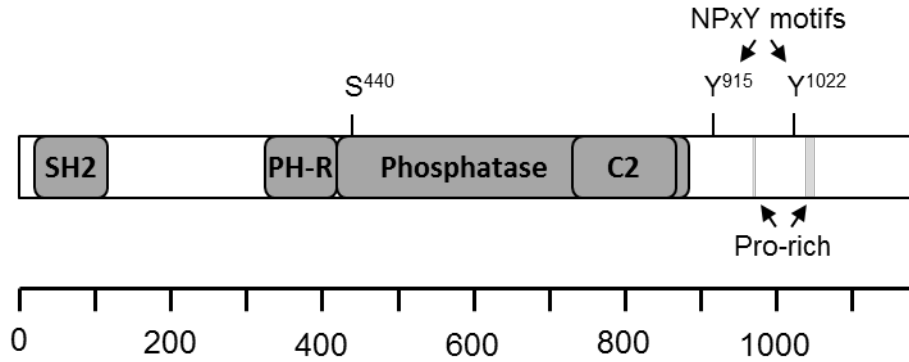


**Figure 1-6. Domain structure of SHIP.**

The N-terminus of SHIP is comprised of an SH2 domain. The central region contains a lipid phosphatase domain that is flanked by a PH-related (PH-R) domain and by an overlapping C2 domain. The C-terminus is largely unstructured yet includes proline-rich regions and two classical PTB domain interaction sites, Tyr 915 and Tyr1022.

### 1.7.3.1 Phosphatase domain

The catalytic domain of SHIP spans amino acids 401-866; it is responsible for recognition of PIP<sub>3</sub> or its soluble equivalent inositol tetrphosphate (IP<sub>4</sub>), and dephosphorylation of these substrates at position D5 of the inositol ring (270, 271). This is the region sharing the highest homology (64%) with related protein SHIP2, encoded by the gene *Inpp1l* (272). Dephosphorylation of PIP<sub>3</sub> prevents the recruitment of PIP<sub>3</sub>-dependent effectors such as Btk, thus inhibiting Ca<sup>2+</sup> flux (206, 271, 273). The production of PI(3,4)P<sub>2</sub> on the other hand promotes recruitment of PI(3,4)P<sub>2</sub>-dependent effectors such as the tandem PH domain containing proteins (TAPPs) (206), implicated in negative feedback regulation of PI3K (274). Both PIP<sub>3</sub> and PI(3,4)P<sub>2</sub> are also critical second messengers for cell migration (151, 153, 275, 276). Early studies re-expressing WT or phosphatase-dead SHIP in SHIP<sup>-/-</sup> chicken DT40 B cells established catalytic activity as the major mechanism by which SHIP regulates BCR-mediated Ca<sup>2+</sup> flux (241). More recent studies in other cell types have

revealed that a phosphatase-dead mutant of SHIP retains significant function (277, 278). This mutant has yet to be studied in lymphocytes.

Overlapping with the phosphatase domain are two allosteric activation sites: The C2 domain (amino acids 725-863) and a phosphorylation site at Serine 440. When exposed to substrate *in vitro*, recombinant SHIP displays sigmoidal reaction kinetics rather than the conventional Michaelis-Menten kinetics (279). In an isolated system, this indicates allosteric activation by the end product. Indeed SHIP activity is enhanced by treatment with PI(3,4)P<sub>2</sub>, and this effect is lost in ΔC2 SHIP (279). Direct binding of PI(3,4)P<sub>2</sub> to the C2 domain was demonstrated (279). This discovery led to the identification of a family of small molecules that bind to SHIP via the same site in the C2 domain and serve as allosteric activators (279). Preclinical studies were performed focusing on effects on mononuclear and mast cells (280, 281). Two phase II clinical trials have also been completed. One of these failed to demonstrate efficacy in chronic obstructive pulmonary disease while the other reported promising results for interstitial cystitis (282).

An allosteric phosphorylation site was first evidenced by a study demonstrating a 2-3 fold increase in SHIP phosphatase activity *in vitro* after treatment with protein kinase A (PKA) (283). Further, pre-treatment of cells with a PKA activating agent inhibited BCR-induced Ca<sup>2+</sup> flux and Akt phosphorylation in the murine A20 B cell line and in SHIP<sup>+/+</sup> but not SHIP<sup>-/-</sup> DT40 B cells (283). A follow-up study identified several serine and threonine residues phosphorylated by PKA *in vitro* and narrowed down the functional site to Serine 440. PKA and PKA activators had no effect on a SHIP S440A mutant protein (284). Thus,

receptors that signal via PKA can modulate BCR signaling pathways by promoting SHIP activity.

### ***1.7.3.2 Src-homology 2 (SH2) domain***

The SH2 domain of SHIP spans amino acids 5-101(265) and shares 54% amino acid identity with homologue SHIP2 (272). One study screened for interactions with a degenerate peptide library and revealed a preference for consensus sequence pY(Y/D)x(L/I/V) (285). Interestingly, this potentially adheres to both ITIM (V/I)xYxx(L/V) and ITAM (YxxL) criteria. Notably, the consensus sequence represents a preference, however not all conforming peptides necessarily bind SHIP. In B cells, the SHIP SH2 domain interacts with phosphorylated ITIM tyrosine residues in FcγRIIB (286), allowing it to mediate downstream inhibitory effects of this receptor (287). In non-B cell types, it has also been shown to bind phosphorylated ITAM tyrosine residues in FcγRIIA, FcγRI-associated zeta-chain (288), TCR zeta chain, FcεRI1 (95), and DNAX-activating protein of 12 kD (DAP12) (289). Although not fully characterized for the other identified binding partners, the functional consequence of FcεRI binding is downregulation of Ca<sup>2+</sup> flux in response to supra-optimal receptor cross-linking (290, 291). In isolation, the SHIP SH2 domain was shown to interact with the phospho-ITAM of Ig-α (103), however association of full length SHIP with Ig-α was undetectable therefore the biological relevance is unclear. In theory, binding of the SH2 domain to the intracellular chains of cell surface receptors is thought to be a critical mechanism controlling the localization of SHIP and therefore access to its substrate PIP<sub>3</sub>. Several phosphorylated cytoplasmic proteins can also interact with the SH2 domain of SHIP, including Shc1 (292, 293) and Dok3 (294). Depending on the context, binding to these proteins can bridge SHIP to receptors (235),

compete with receptors for SHIP binding (295), or co-operate with receptor binding in order to relay signals downstream (235).

### ***1.7.3.3 Pleckstrin homology-related (PH-R) domain***

Another more recently described regulatory domain in SHIP is the PH-related (PH-R) domain (296). Although not evident from examination of the SHIP amino acid sequence, nuclear magnetic resonance (NMR) structural studies revealed an independently folded structure spanning amino acids 292-401. The predicted topology closely resembled that of a PH domain. Phospholipid overlays revealed an interaction between the PH-R domain and phosphoinositides, with a preference for PIP<sub>3</sub>. Unlike the C2 domain, this lipid binding site has no allosteric effect on enzymatic activity and is not targeted by the previously described small molecule agonists. However, mutation of two critical lysine residues in this region abrogated binding to PIP<sub>3</sub>, impaired the localization of SHIP to the phagocytic cup of macrophages, and impaired the ability of SHIP to inhibit phagocytosis in these cells (296). The contribution of this domain to the localization and function of SHIP has not been studied in lymphocytes.

### ***1.7.3.4 C-terminus***

The C-terminus of SHIP diverges from that of SHIP2 considerably (272). It contains several protein-protein interaction motifs that are thought to contribute to the regulation of both catalytic and adaptor activities. In one study, a truncation mutant lacking amino acid 900 onward retained its ability to bind FcγRIIB but displayed reduced ability to inhibit Ca<sup>2+</sup> flux in DT40 B cells (297). Results of later studies in murine and humanized B cells

suggested that some element(s) in the SHIP C-terminus are required to stabilize the interaction with Fc $\gamma$ RIIB (240, 298).

Two specific tyrosine residues in the C-terminus of SHIP were shown to be phosphorylated by Src family kinases, Y917 and Y1020 named for the murine sequence (299-301), corresponding to Y915 and Y1022 in the human sequence. More phosphorylation is seen with Fc $\gamma$ RIIB co-ligation than with BCR ligation alone (264, 302). Mutation of both residues to phenylalanine virtually eliminated all detectable SHIP pTyr signal in T cell receptor-stimulated T cells (301), however this experiment has not been performed in B cells. Much like C-terminal truncation, Y917F/Y1020F SHIP also failed to inhibit Ca<sup>2+</sup> flux in DT40 B cells (297). The authors of this study speculate a role for these residues in stabilizing SHIP at the membrane, therefore facilitating access to its substrate. Other than potentially directing localization, tyrosine phosphorylation has no direct effect on phosphatase activity (300). Despite this, many studies use Y1020 phosphorylation as a marker of SHIP activity.

Two adaptor functions of SHIP, that is functions independent of catalytic activity, have been proposed to depend on the NPxY motifs (illustrated in **Figure 1-7**). The first involves binding of these motifs to the protein tyrosine binding (PTB) domain of Shc, demonstrated by peptide pull-down assays (292, 293). Although the SH2 domain of SHIP can also potentially participate in the interaction by binding tyrosine phosphorylated Shc, the importance of the NPxY motifs at least *in vitro* was illustrated in one early study that demonstrated no detectable interaction of double mutant SHIP Y915F/Y1020F with Shc1

in contrast to a robust interaction detected with WT SHIP (301). The function of the SHIP-Shc interaction in B cells is somewhat debated in the literature. It may interfere with Shc binding to the Grb2-SOS complex, thus negatively regulating Ras-Erk signaling (136, 239, 303). The second proposed adaptor function of the NPxY motifs is binding to p62<sup>dok</sup>, also known as Dok-1. This interaction is proposed to localize a Dok-associated RasGAP to the membrane and thus negatively regulate Ras-Erk signaling (304). Another group confirmed that the SHIP-Dok-1 interaction required the NPxY tyrosines and further demonstrated that unlike WT SHIP, Y917F/Y1020F SHIP failed to inhibit migration of a transformed pro-B cell line (305). Since Dok-1 was previously shown to promote migration (306), the authors propose that SHIP binding inhibits the pro-migratory function of Dok-1 (305).

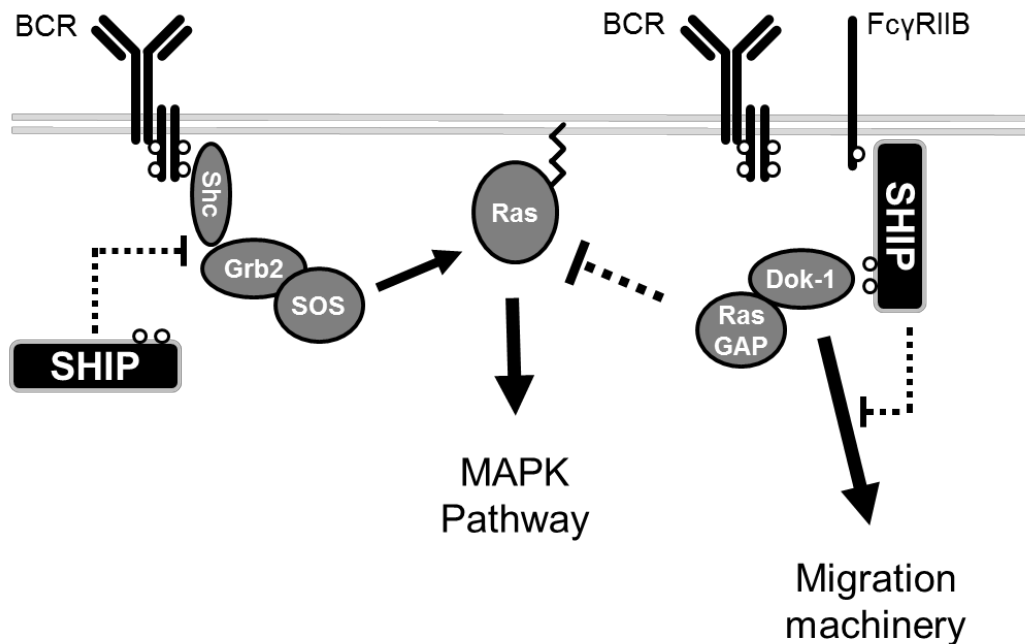


**Figure 1-7. Phosphatase-independent adaptor functions described for SHIP.**

The interaction of SHIP with Shc, via both its SH2 domain and phosphorylated NPxY tyrosine residues, is proposed to obstruct the interaction between Shc and Grb2, thus preventing activation of the Ras/MAPK pathway (303). The interaction of SHIP with Dok-1 via its phosphorylated NPxY residues is proposed to promote the recruitment of a Dok-1-associated RasGAP, thus further dampening Ras/MAPK activation (304). Dok-1 also plays a role in activation of migration machinery and interaction with SHIP is proposed to disrupt this function (305).

Phosphorylation of additional, non-NPxY tyrosine residues at position 867 and 944 is induced in stimulated mast cells (307) and reported in B cells according to publically available mass spectrometry databases ([www.phosphosite.org](http://www.phosphosite.org)). No functional information is currently available for these sites. Chapter 2 of this thesis identifies a potential interaction between phosphorylated Tyr944 of SHIP and the SH2 domain of Nck. Chapter 4 validates this interaction and provides the first examination of Y944 function in B cells.



In addition to tyrosine phosphorylation sites, examination of the amino acid sequence in the SHIP C-terminus reveals a proline-rich region spanning amino acids 920-1148, with SH3-binding domains specifically located at 969-974 and 1040-1051. This was identified as a binding site for the SH3 domain of Grb2 (308). In mouse B cells, an interaction between SHIP and Grb2 or Grb2-related adaptor protein (GRAP) is required to reinforce the association between SHIP and Fc $\gamma$ RIIB (298). Grb2 and GRAP are dispensable for SHIP-Fc $\gamma$ RIIB interaction in human B cells, however an as-yet unidentified protein is presumed to play this role (240).

#### **1.7.4 Regulation of SHIP protein levels**

*Inpp5d*, the gene encoding SHIP, is constitutively expressed in hematopoietic cells. However, SHIP can be regulated by means of micro-RNA (miRNA)-mediated degradation of transcript and proteasome-mediated degradation of protein.

Several groups have reported upregulation of miR-155 in various B cell leukemias and lymphomas (309, 310). Costinean et al. (311) demonstrated that B cell-targeted transgenic expression of miR-155 in mice led to stalled development and accumulation of pre-B cells and with time a mixed leukemia-lymphoma phenotype (311). Based on sequence analysis, SHIP was among the predicted targets of this so-called “onco-miR”. SHIP was later confirmed to be a direct target and a key target of miR-155 in murine B cells (312), human B cell lymphoma cell lines (257) and macrophages (313).

Soon after these discoveries, Rushmann et al. (314) reported that SHIP protein levels decrease in response to ligation of certain receptors and that this can be blocked by both Src family

kinases inhibitors and proteasomal inhibitors. Further investigation revealed that SHIP associates with ubiquitin ligases and becomes polyubiquitinated following receptor ligation, in a Src family kinase-dependent manner. Thus, a model was proposed whereby phosphorylation of SHIP triggers its polyubiquitination and degradation within the proteasome (314).

The identification of multiple mechanisms in place to control SHIP activity, including the regulation of protein levels described here as well as the allosteric regulation of enzymatic activity and recruitment into various complexes described previously suggests that it is of central importance to cellular function. Indeed, disruption of SHIP expression or activity can have destructive consequences for immune homeostasis, as will be discussed in the following section.

### **1.7.5 SHIP in autoimmune and inflammatory disorders**

Fcgr2b polymorphisms that result in decreased expression (315) or loss of function (316) of FcγRIIB have been associated with human lupus. Several mouse models of spontaneous autoimmunity (NZB, MRL, NOD) also share polymorphisms in this gene (317, 318) and the phenotype is reversible by transfer of the wt gene (319). FcγRIIB-deficient mice have increased susceptibility to collagen-induced arthritis (CIA) (320). Depending on the genetic background, FcγRIIB deletion in mice can also cause lupus-like autoimmunity (62, 321) or exacerbate spontaneous autoimmunity caused by other genetic factors (322). Transgenic expression of FcγRIIB in B cells but not macrophages was protective in murine models of CIA and lupus (319, 323).

Direct evidence that SHIP, the main effector of Fc $\gamma$ RIIB, also plays a protective role in autoimmune models was demonstrated more recently. Compared to healthy controls, B cells from a subset of Systemic lupus erythematosus (SLE) patients exhibited decreased phosphorylation of SHIP (324). Antibodies engineered to crosslink CD19 with Fc $\gamma$ RIIB and thereby mimic negative signaling were shown to activate SHIP and suppress BCR signaling in human B cells from healthy donors (325) and SLE patients (326). Moreover, two murine studies demonstrated that natural and antigen-induced anergic B cells have increased basal phosphorylation of SHIP (63) and that SHIP expression is required to maintain anergy (63, 327). Specifically, deletion of SHIP reverses the anergic phenotype in two models of tolerance to self-antigen (63, 327), resulting in autoimmunity. Furthermore, a B cell-targeted deletion of SHIP was sufficient to cause a severe, spontaneous, lupus-like disease in mice (63).

Aside from the “B cell-mediated” autoimmune disorders, a protective role for Fc $\gamma$ RIIB and/or SHIP in other cell types has been demonstrated in *in vivo* models of allergic asthma (328), mast cell-mediated allergic reaction (329) and inflammatory lung disease (330). These findings have fuelled the development and investigation of small molecule SHIP activators (331, 332). Since some of the inhibitory effects of SHIP in B cells may be attributed to adaptor functions rather than enzymatic activity, there is a need to continue defining the molecular mechanisms governing its function in order to find new and better ways to specifically target SHIP in therapeutic settings.

## **1.8 The actin cytoskeleton and B cell signaling**

B cells depend on actin cytoskeleton rearrangements for several processes. The network of actin filaments closely associated with the inner leaflet of the plasma membrane, called the cortical actin network, serves to control and compartmentalize signaling events involving membrane proteins, including the BCR. Additionally, amoeboid-like migration and spreading over antigen-coated surfaces depend on the ability of growing branched actin filaments to exert an outward protrusive force on the cell membrane (333). Migration is essential for B cell homing to tissues and lymphoid organs (334) while spreading is an important mechanism for increasing exposure to antigen (335).

### **1.8.1 Signal initiation**

Antigen binding to BCRs is accompanied by the formation of mobile BCR microclusters from which signaling events are initiated. When the antigen is membrane-bound, microclusters can be observed to merge and move centripetally toward a central contact zone, even while the cell itself is spreading outwards in an effort to gather more antigen (335). The cortical actin network is responsible for the spatiotemporal regulation of these processes. It consists of branched actin filaments and associated binding proteins and is tethered to the plasma membrane through interaction with transmembrane proteins of the ezrin/radixin/moesin (ERM) family (336). Treatment with actin depolymerization agent, even in the absence of antigen, leads to accelerated BCR diffusion in the membrane and initiation of signaling events (337), albeit with slow kinetics (338). Moreover, two different populations of BCRs can be observed in a resting cell, a highly mobile population that tends to be found within actin- and ezrin-poor regions of the membrane and a population with restricted mobility that tends to be

found within actin- and ezrin-rich regions of the membrane. It was postulated that the transiently mobile populations are responsible for the tonic low level signaling that is required for mature B cell survival (337).

Cortical actin rearrangements are also critical in signaling in response to both soluble and membrane-bound antigens. Both complete F-actin depolymerisation and complete F-actin stabilization prior to antigen exposure inhibits BCR microcluster formation (338). Two prominent signals contribute to the required rearrangements: conformational change of ERM proteins (339, 340) and activation of actin severing proteins (223, 338). BCR ligation induces rapid dephosphorylation of ezrin. This induces a conformational change that triggers dissociation of ezrin from both lipid raft domains in the plasma membrane and the cortical actin network in the cytoplasm (339). Thus lipid rafts, containing signaling proteins such as Lyn kinase, are freed from restriction and become more mobile, supporting their association with BCR signaling chains. Uncoupling of cortical actin from the membrane in this manner also allows for a transient increase in BCR diffusion rate in the plasma membrane, promoting microcluster formation. ERM proteins rapidly reorganize upon BCR ligation to surround and support microcluster formation and maturation (340). Moreover, the actin severing proteins cofilin and gelsolin localize to BCR microclusters upon antigen exposure (338). Severing of cortical F-actin essentially makes space for BCRs to interact with cytoplasmic signaling proteins and to coalesce into microclusters. Rap GTPase is a critical upstream activator of cofilin and an essential driver of microcluster formation (223).

Taken together, the current model postulates the existence of discrete compartments or “corrals” underlying the plasma membrane at rest, formed from overlapping F-actin and ERM protein networks. These restrict and confine the lateral mobility of the BCR, preventing extensive interaction with other groups of BCRs, co-receptors, and membrane associated kinases. BCR ligation breaks down these barriers by detaching actin from membrane-bound ERM and by activating actin severing proteins. These processes allow for increased BCR mobility, association with lipid rafts, coalescence of BCR microclusters and the formation of membrane-proximal signaling complexes. Furthermore, F-actin severing serves not only to break down a physical barrier to signal initiation, but also to generate free barbed ends. These are substrates for branched actin filament formation, which is critical for the B cell spreading response (341).

### **1.8.2 Branched actin filament formation**

The formation and outward growth of branched F-actin filaments at the cell periphery, when anchored further inside the cytoskeleton, pushes the plasma membrane outward. This facilitates cell spreading in response to immobilized/membrane bound antigen or lamellipodia formation in response to chemokine stimulation (333). Branching is accomplished when the actin-related protein 2/3 (Arp2/3) complex binds to free barbed ends of actin filaments and nucleates the formation of a new filament at a 70° angle (342, 343). Many of the upstream signals induced by BCR or chemokine receptor ligation are common to other cell types (**Figure 1-8**). Wiskott-Aldrich Syndrome Protein (WASP) and neural- (N-) WASP are actin nucleation promoting factors that activate the Arp2/3 complex (215, 344). These, in turn, are activated by conformational change induced by interaction with GTP-bound Rac and/or Cdc42, with PI(4,5)P<sub>2</sub> (215, 344, 345) and by direct interaction with adaptor protein Nck

(346, 347). *In vitro*, Rac1 and PI(4,5)P<sub>2</sub> only act on N-WASP while Cdc42 acts on both but is more effective for WASP (347).

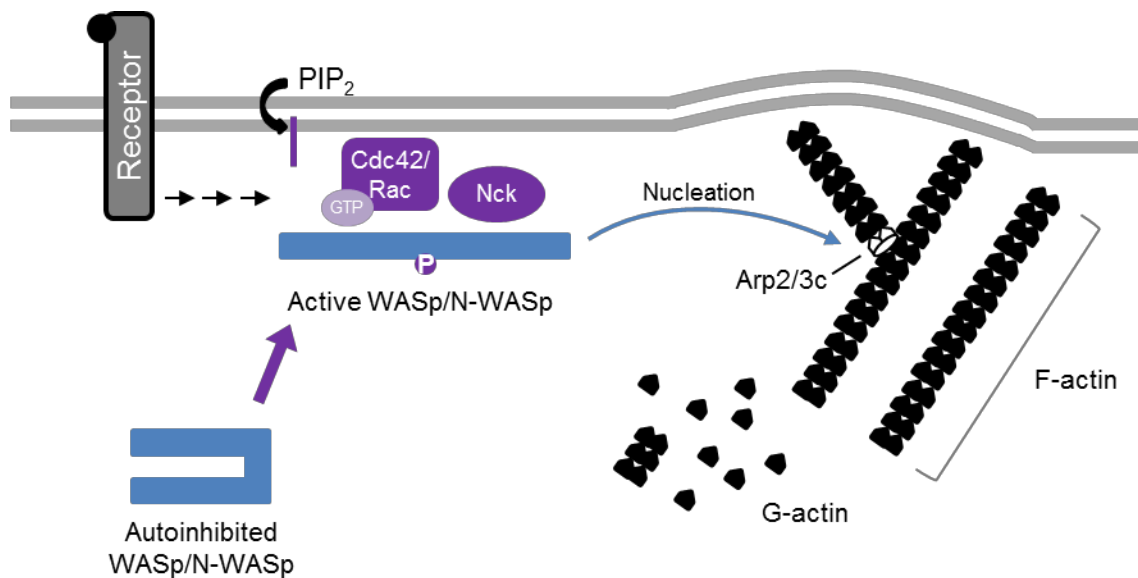


**Figure 1-8. Key signals involved in branched actin nucleation.**

Actin nucleation promoting proteins WASp and N-WASP exist in an autoinhibited conformation at rest, which can be relieved upon interaction with activated (GTP-bound) Cdc42 and/or Rac, PI(4,5)P<sub>2</sub> membrane lipid, and Nck adaptor protein. Nck is thought to both directly activate WASp/N-WASP and indirectly promote activity by recruitment into pTyr-dependent signaling complexes. Tyr phosphorylation also promotes activity. Once active, WASp/N-WASP support nucleation of branched actin filaments by the Arp2/3 complex.

One step further upstream, small GTPases are activated by GEFs. T cell receptor signaling induces the phosphorylation of a scaffold protein called SLP-76, homologous to BLNK. Phospho-SLP-76 binds both Nck and the Rac-GEF Vav1. Nck binds to and stabilizes WASP while Vav1 activates Cdc42. Cdc42 can then further activate WASP, leading to actin branch nucleation (348). In B cells, phosphorylated BLNK has been shown to bind both Nck (349) and Vav1 (120), thus Nck may promote actin polymerization by this scaffolding function in B cells as well, in addition to direct binding and activation of WASP and N-WASP (347). N-WASP is reported to have very similar functions to WASP in other cell types (345), however a recent study indicates this is not the case in B cells (350). WASP was shown to be important

for the spreading and BCR clustering phases of B cell response to antigen (351) while N-WASP was shown to promote the contraction phase, coalescence of microclusters into a central cluster for internalization, and signal attenuation (350). In fact, WASP and N-WASP suppress each other's function in BCR-stimulated murine and human B cells (350).

### **1.8.3 PI3K signaling and actin**

Deletion of several PI3K effectors has been shown to severely impair both BCR microcluster formation and B cell spreading, including PLC $\gamma$ 2, Vav (352), Rac (165) and Btk (17, 213). From mechanistic studies, we know that PIP $_3$ -binding by Vav promotes Rac1 GTPase function, (218, 353, 354), although this might not be a critical mechanism in B cells (181). Btk-mediated phosphorylation of Vav does promote its activity in B cells (213), thus promoting Cdc42 association with GTP and, subsequently, WASP activation (213). Direct phosphorylation of WASP by Btk also activates its actin nucleation activity (351).

SHIP has been shown to negatively regulate WASP phosphorylation in murine B cells, presumably by consuming PIP $_3$  thereby limiting the recruitment of Btk (351). In human T cells, loss of SHIP leads to increased F-actin content (290). Functionally, SHIP has been shown to limit murine B cell spreading on antigen-coated lipid bilayers, a system used to mimic the flexibility of a cellular surface coated with antigen (351). Also, inhibition of cell motility by SHIP has been demonstrated in neutrophils (355). Whether or not these actin-inhibitory mechanisms are dependent on phosphatase activity has never been explicitly tested.

On the other hand, SHIP has been shown to support the formation of adhesive contacts in macrophages in a phosphatase-dependent manner. It does this by promoting certain integrins



to adopt an active conformation (356). SHIP also promotes the formation and/or maintenance of actin-rich microvilli in T cells by an unknown mechanism (290). These positive effects may be explained by considering the double-edged nature of certain PIP<sub>3</sub> binding proteins such as Rac1, which in addition to promoting actin nucleation can also activate protein phosphatases (357, 358). Alternatively, proteins that are specifically recruited to the SHIP product PI(3,4)P<sub>2</sub> may promote F-actin polymerization. The tandem pleckstrin homology domain proteins (TAPPs) (275) and lamellipodin (153, 359) are two candidates. On the other hand, these effects of SHIP may occur entirely independently of its phosphatase activity, depending instead on protein-protein interactions not yet characterized.

## **1.9 Thesis overview**

### **1.9.1 Study Rationale**

Leukocyte activity is controlled by balancing activating and inhibitory signals in order to generate effective immune responses while avoiding tissue damage and autoimmunity. Here we examine an important regulatory circuit in B cells that involves the lipid phosphatase SHIP. Functionally, previous studies have revealed much about how SHIP affects cellular behaviours. It dampens Ca<sup>2+</sup> signaling and thus the expression of Ca<sup>2+</sup>-regulated genes. It inhibits adhesion and migration in certain cell types and regulates B cell spreading and microcluster formation. These were important and informative studies, however if the goal is to target these effects therapeutically, it is essential to also determine exactly *how* SHIP is carrying out these functions. In many cases, the mechanistic explanations have lagged behind the functional descriptions. As is the case in many fields of research, there are certain prevalent assumptions that are affecting how scientists and clinicians approach the question of

therapeutic targeting. The first specific assumption is that the enzymatic activity of SHIP in dephosphorylating PIP<sub>3</sub> accounts for most of its functions. This bias remains even after several studies have demonstrated important exceptions. Indeed the only current therapeutic approaches to targeting SHIP involve direct manipulation of its enzymatic activity. Given the number and variety of domains and motifs found in SHIP, it is likely that this protein has evolved as a multifunctional regulator that carries out its cellular tasks by several distinct means. The dominant mechanism in any given contexts is likely determined by where it is directed to go within the cell and which binding partners are expressed and localized along with it. The second prevalent assumption in the field is that SHIP is primarily controlled by its best described binding partner, the inhibitory receptor FcγRIIB. In the context of BCR-FcγRIIB co-ligation, the binding of SHIP to FcγRIIB is indeed a dominant mechanism by which PIP<sub>3</sub> levels and subsequent Ca<sup>2+</sup> flux are dampened. However, it will be revealed throughout this thesis that SHIP can absolutely be controlled by other means, independent of FcγRIIB, a revelation that has been supported by recent literature.

### **1.9.2 General hypothesis**

SHIP is a multi-functional signaling protein that is controlled by three inter-related factors: interaction with binding partners, phosphorylation and directed subcellular localization.

### **1.9.3 Objectives**

My first objective is to describe novel interaction partners of SHIP and the structural requirements for these interactions. I accomplish this using co-immunoprecipitation assays and surface plasmon resonance screening to selectively investigate proteins involved in related signaling pathways and/or those that are predicted to bind to SHIP, with specific

emphasis of pTyr-SH2 domain pairs. These represent an important class of inducible and reversible interactions commonly triggered by signaling pathways.

My second objective is to examine the role of a novel SHIP phosphorylation site, located at Tyr944, with respect to its binding partners and functional outcomes. I examine its interaction with adaptor protein Nck, first identified via Biacore screening and now validated by pull-down assays. I then compare the effects of WT and Y944F mutant SHIP over-expression on F-actin and actin-dependent cellular processes in human B cells.

My final objective is to describe Fc $\gamma$ RIIB-independent mechanisms by which the subcellular localization of SHIP is controlled, as well as to compare the molecular behaviour of SHIP with and without Fc $\gamma$ RIIB involvement. My main approach employs high resolution imaging techniques to objectively quantify SHIP membrane recruitment in human B cells stimulated via the BCR +/- Fc $\gamma$ RIIB. I assess the effects of structural mutations, pathway inhibitors, and expression/phosphorylation of binding partners.

Together, these studies significantly expand our understanding of how SHIP functions in B cells and therefore how B cell activation is controlled. Many of the mechanistic insights gained likely apply broadly to other immune cell types and open up new avenues for therapeutic manipulation of signaling pathways.

# CHAPTER 2: DEFINING THE INTERACTION NETWORK OF SHIP

## 2.1 Specific Introduction

Interaction partners often change the function of a protein, for example by activating or inhibiting its activity or by directing it to a particular subcellular niche. In some cases, the interaction is the function, providing a scaffold for the assembly of an operational complex. Protein interaction motifs are often “promiscuous”, allowing multiple alternative partners to bind, with the order of preference defined by the expression level, accessibility and rate constant of the interaction. Thus, the functions of a given protein can vary depending on the cellular context. Signal transduction pathways often promote the formation of *de novo*, transient protein-protein interactions. This can result following conformational changes such as those occurring in GPCRs bound by ligand and by post-translational modifications such as when phosphorylation of tyrosine residues create binding sites for specific SH2 and PTB domain-containing proteins. Examining the binding partners of a given protein may inform of its function and/or the context of its function. Reciprocally, examining the function of a protein may provide clues to its interaction network and therefore illuminate the mechanism by which its functions are carried out.

Several direct binding partners of SHIP have been identified and validated (**Figure 2-1**). FcγRIIB (286), Dok-3 (294) and DAP12 (289) bind the SH2 domain. Shc1 binds both the SH2 domain and phosphorylated NPxY tyrosines (292, 293). Grb2 binds the proline-rich region

(308). Dok-1 binds the NPxY tyrosines when phosphorylated (305) (**Figure 2-1**). Still others have been proposed but have not yet been validated (360).

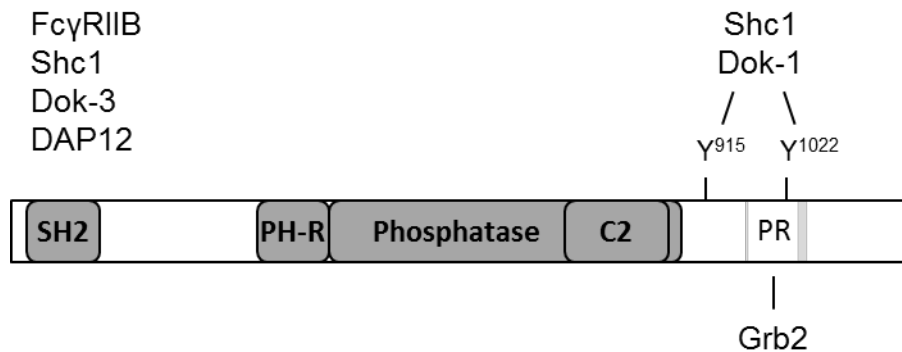


**Figure 2-1. SHIP interaction partners with defined binding sites.**

Some of these interactions have defined functions or at least models of function supported by some experimental evidence. For example, interaction of the SHIP SH2 domain with p-ITIM tyrosines in FcγRIIB is thought to recruit SHIP to the membrane, the site of its catalytic substrate PIP<sub>3</sub> (287, 295). Interaction of the SHIP C-terminus with Dok-1 in sequence brings a RasGAP to the membrane to inhibit the MAPK pathway (304). Other interactions have complex or poorly defined outcomes. Piecing together molecular mechanisms involving protein-protein interactions is tedious work, however a molecular-level understanding of a pathway can guide rational targeting strategies for therapeutic intervention. Indeed a new class of therapeutics has recently emerged, aimed at blocking protein interaction (361).

In this chapter, we seek to identify binding partners of SHIP and to characterize key interactions with respect to the site and strength of interaction. We were at the outset interested in the adaptor protein Bam32, functionally linked to SHIP in mast cells where deficiency in Bam32 resulted in hypo-phosphorylation of SHIP and exaggerated responses to ligation of the high

affinity receptor for IgE (362). We were able to identify an interaction between Bam32 and SHIP in B cells in a co-immunoprecipitation assay detected by selective reaction monitoring (SRM), however binding was not sufficiently robust to detect via traditional western blotting in our hands. Therefore, we broadened our focus to screen for interactions with other proteins functionally linked to SHIP or structurally related to Bam32, using a surface plasmon resonance (Biacore 2000) platform. A number of interactions of varying apparent strength were identified and two were chosen for further analysis: the known interaction between SHIP SH2 and the phospho-ITIM peptide of Fc $\gamma$ RIIB and a novel interaction between SHIP phospho-Tyr944 and the SH2 domain of adaptor protein Nck. The latter phosphorylation event has been reported but remains completely uncharacterized. Together, this chapter provides new insights into SHIP binding partners and their mechanisms of interaction.

## **2.2 Materials and Methods**

### **2.2.1 Cell lines and reagents**

BJAB cells, a human B cell line derived from a female Burkitt Lymphoma patient (363), and a stable cell line derived previously in our laboratory expressing Bam32 with a myc epitope tag (364), were cultured in Roswell Park Memorial Institute (RPMI) medium supplemented with 10% Fetal Bovine Serum (FBS) and penicillin/streptavidin antibiotics. Stimulations were performed using pervanadate, a potent tyrosine phosphatase inhibitor (365) prepared fresh by mixing 2.5mM hydrogen peroxide with 0.25mM sodium orthovanadate (final concentrations).

### **2.2.2 Co-immunoprecipitation, western blotting and selective reaction monitoring**

Cells were lysed at equal numbers with 0.5% Nonidet P-40 (Thermo Fisher) lysis buffer containing protease and phosphatase inhibitor cocktails (Roche). Lysates were precleared for 1h at 4°C then incubated for 1h with 2µg (for detection by western blotting) or 10ug (for detection by SRM) specific antibody against Myc tag (9E10, Millipore), SHIP (P1C1, Santa Cruz), Lyn (44, Santa Cruz), Hck (N-30, Santa Cruz) or SHIP2 (H-300, Santa Cruz). Finally, samples were incubated with protein G sepharose beads (GE) for 1h at 4°C for immunoprecipitation.

For western blotting, equal volume of precipitate was run on a 10% polyacrylamide gel then transferred to nitrocellulose membrane (Bio-Rad). Membranes were probed with anti-SHIP (P1C1, Santa Cruz) or anti-Myc tag (4A6, Millipore) primary antibody, then Horseradish peroxidase-linked goat anti-mouse IgG (Jackson) secondary antibody, followed by chemiluminescence development.

For SRM, proteins were eluted off the beads using 0.1% trifluoroacetic acid (TFA), dried in a speed vacuum evaporator and resuspended in 100mM ammonium bicarbonate. Samples were reduced by adding 100mM dithiothreitol (DTT) and incubating for 35min at 56°C then immediately put on ice. Samples were alkylated by adding 500mM iodoacetamide (IAA) and incubating for 20min at room temperature. Excess IAA was neutralized by the addition of 17.5mM DTT and incubation for 20min at room temperature. Next, the samples were incubated with trypsin for 16h at 37°C at a 1:50 ratio of trypsin:protein then frozen,

evaporated and reconstituted. The samples were then sent to the Manitoba Centre for Proteomics and Systems Biology for SRM analysis, as described previously (366).

### **2.2.3 Bioinformatics prediction tools**

Scansite 3, available at <http://scansite.mit.edu>, was used to identify candidate interaction partners of SHIP, using the amino acid sequence from the UniProtKB database as the query under high stringency conditions (367, 368). Small matrix assisted ligand identification (SMALI), previously available at <http://lilab.uwo.ca/SMALI.htm>, was used to specifically predict SH2 domains likely to interact with phospho-SHIP using the domain scan module (369).

### **2.2.4 Recombinant proteins**

Recombinant SH2 domains fused to Glutathione-S-transferase (GST) were purchased (Thermo Pierce) for Lyn, Hck and Nck and later purified from bacteria for these in addition to SHIP, SHIP2 and Bam32. For in-house preparation, pGEX-5x-2 expression vectors (a gift from Dr Kazuya Machida) were transformed into competent BL21 E. coli cells (Agilent Technologies). Recombinant proteins were purified with glutathione-sepharose beads (Amersham Pharmacia Biotech), dialyzed and verified for purity by SDS-PAGE and Coomassie blue staining.

### **2.2.5 Biacore screening**

For Biacore 2000 assays, biotinylated phospho-peptides (Sigma Aldrich), with sequences specified in (Table 2-1), were reconstituted in 50% acetonitrile/water (vol/vol). Peptides were diluted to a working concentration of 50nM and injected incrementally on streptavidin pre-



coated sensorchip (SA chip, GE) at 5 $\mu$ l/min until 30-50 response units (RU) were captured. Recombinant GST-SH2 proteins or GST control (Thermo Pierce) were diluted to a working concentration of 50nM in HBS-EP and injected over control surface or peptide surface for 2min at a flow rate of 10 $\mu$ l/min. Surfaces were then regenerated with two repeated injections of 1M NaCl at 50 $\mu$ l/min for 30 seconds, each followed by an extraclean cycle. All reagents were filtered through a 0.2 $\mu$ m membrane to remove air bubbles prior to injection.

**Table 2-1. Phosphopeptides derived from candidate proteins**

<b>Protein name</b>	<b>Peptide name</b>	<b>Peptide sequence</b>
Bam32	Y139	EPSI <b>p</b> YESVRVH
SHIP	Y865	REKL <b>p</b> YDFVKTE
	Y915	INPN <b>p</b> YMGVGP
	Y944	TAW <b>S</b> pYDQPPKD
	Y1022	ENPL <b>p</b> YGSLSSF
Lyn	Y32	ERTI <b>p</b> YVRDPTS
	Y193	DNGG <b>p</b> YYISPRI
	Y194	NGGY <b>p</b> YISPRIT
	Y306	LVRL <b>p</b> YAVVTRE
	Y397	EDNE <b>p</b> YTAREGA
	Y473	PDEL <b>p</b> YDIMKMC
	Y508	TEGQ <b>p</b> YQQQP
Hck	Y209	NGGF <b>p</b> YISPRST
	Y411	EDNE <b>p</b> YTAREGA
	Y522	TESQ <b>p</b> YQQQP
Nck	Y105	GERL <b>p</b> YDLNMPA
	Y268	PQCD <b>p</b> YIRPSLT
SHIP2	Y671	SRDT <b>p</b> YAWHKQK
	Y886	RERL <b>p</b> YEWISID
	Y986	NNPA <b>p</b> YYVLEGV
	Y1135	SEVD <b>p</b> YAPAGPA
	Y1162	LPSD <b>p</b> YGRPLSF
FcγRIIB (pos control for SHIP)	Y292	NTIT <b>p</b> YSLLMHP
PDGFR (pos control for Nck)	Y1009	SSVL <b>p</b> YTAVQPNE

### 2.2.6 Biacore steady-state affinity analysis

Peptides were loaded on SA chip surface to 30-50 RU, as described above. Using the Affinity Analysis wizard, four to six dilutions of recombinant GST-SH2 domains were injected serially from lowest to highest concentration over peptide and control surfaces. Each was injected for 2min at 20 $\mu$ l/min followed by a 2.5min wait period, an injection of 1M NaCl at 50 $\mu$ l/min for 0.5min for surface regeneration, and a 0.5min stabilization period. At least two concentrations were performed in duplicate for each analyte. Analysis was performed using Biacore Affinity Analysis software. After subtraction of control surface signal, the averaged equilibrium response ( $R_{eq}$ ) is plotted versus concentration of analyte and curve fit to the steady-state affinity model (BIAevaluation). The dissociation constant ( $K_D$ ) is calculated as the concentration required to reach half the maximal response ( $R_{max}$ ):

$$K_D = \frac{1}{2} R_{max}$$

## 2.3 Results

### 2.3.1 Evidence for an interaction between Bam32 and SHIP in B cells

We performed several co-immunoprecipitation experiments in pervanadate-stimulated BJAB cells overexpressing myc-tagged Bam32, however we consistently failed to detect an interaction between SHIP and Bam32 by western blotting. (**Figure 2-2**. Pervanadate is a potent tyrosine phosphatase inhibitor, thus treatment of cells with this agent rapidly induces phosphorylation of nearly all tyrosine phosphorylation sites within signaling proteins (365). We additionally failed to detect the presence of SHIP in Lyn, Hck, and SHIP2 immunoprecipitates. Importantly, these negative results do not rule out the existence of

interactions between these proteins since it is possible that the stimulation or lysis conditions are not amenable to binding or that binding is transient or of relatively low affinity.

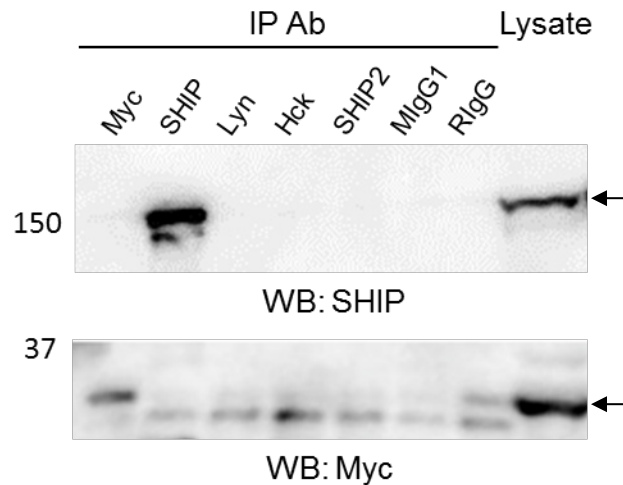


**Figure 2-2. SHIP does not detectably co-immunoprecipitate with Bam32-myc, Lyn, Hck, or SHIP2.**

*1x10<sup>7</sup> cells were stimulated with pervanadate for 1-2min, lysed, precleared, incubated with targeting antibody as indicated or isotype control antibodies mouse IgG<sub>1</sub> (MIgG<sub>1</sub>) or rabbit IgG (RIgG), then precipitated with protein G-sepharose beads. Eluates were separated by SDS-PAGE and western blotting was performed with the indicated antibodies. Blot is representative of a total of 8 repeated co-IPs in Bam32-myc<sup>+</sup> BJAB cells.*

We were especially interested in the potential interaction of SHIP with Bam32 due to the known functional link (362), therefore we developed a mass spectrometry-based selective reaction monitoring (SRM) assay to specifically detect Bam32 in co-immunoprecipitates. Compared to western blotting, this is a more sensitive method for detection of protein in solution. After digesting with trypsin and separating by high performance liquid chromatography (HPLC), the peptides are directed into a time of flight mass spectrometer (Q1). Ions with specified mass/charge ratios are directed into a collision cell (Q2) where they are further cleaved and send through a second time-of-flight mass spectrometer (Q3) for detection. Using purified recombinant Bam32, we identified six tryptic fragments unique to

Bam32 that could be distinguished in the tandem MS system by retention time and mass/charge ratio (**Figure 2-3**). These were the fragments directed through Q2. The presence of Bam32 in the original solution is confirmed if at least 3 y-transitions are present from at least 3 unique tryptic fragments. Bam32 was confirmed to be present in the SHIP IP eluate, the positive control IP eluate (myc-tag IP) and the lysate, but absent in Lyn and isotype control mouse (M) and rabbit (R) IgG IP eluates (Table 2-2).

	10	20	30	40	50
	MGRAELLE <span style="background-color: #cccccc;">GK</span>	MSTQDPSDLW	SRS <span style="background-color: #cccccc;">D</span> G <span style="background-color: #cccccc;">E</span> A <span style="background-color: #cccccc;">E</span> LL	QDLG <span style="background-color: #cccccc;">W</span> Y <span style="background-color: #cccccc;">H</span> G <span style="background-color: #cccccc;">N</span> L	TRH <span style="background-color: #cccccc;">A</span> E <span style="background-color: #cccccc;">A</span> LL <span style="background-color: #cccccc;">L</span> L
	60	70	80	90	100
	S <span style="background-color: #cccccc;">N</span> G <span style="background-color: #cccccc;">C</span> D <span style="background-color: #cccccc;">G</span> S <span style="background-color: #cccccc;">Y</span> LL	R <span style="background-color: #cccccc;">D</span> S <span style="background-color: #cccccc;">N</span> E <span style="background-color: #cccccc;">T</span> T <span style="background-color: #cccccc;">G</span> L <span style="background-color: #cccccc;">Y</span>	S <span style="background-color: #cccccc;">L</span> S <span style="background-color: #cccccc;">V</span> R <span style="background-color: #cccccc;">A</span> K <span style="background-color: #cccccc;">D</span> S <span style="background-color: #cccccc;">V</span>	K <span style="background-color: #cccccc;">H</span> F <span style="background-color: #cccccc;">H</span> V <span style="background-color: #cccccc;">E</span> Y <span style="background-color: #cccccc;">T</span> G <span style="background-color: #cccccc;">Y</span>	S <span style="background-color: #cccccc;">F</span> K <span style="background-color: #cccccc;">F</span> G <span style="background-color: #cccccc;">F</span> N <span style="background-color: #cccccc;">E</span> F <span style="background-color: #cccccc;">S</span>
	110	120	130	140	150
	<span style="background-color: #cccccc;">S</span> L <span style="background-color: #cccccc;">K</span> D <span style="background-color: #cccccc;">F</span> V <span style="background-color: #cccccc;">K</span> H <span style="background-color: #cccccc;">F</span> A	N <span style="background-color: #cccccc;">Q</span> P <span style="background-color: #cccccc;">L</span> I <span style="background-color: #cccccc;">G</span> S <span style="background-color: #cccccc;">E</span> T <span style="background-color: #cccccc;">G</span>	T <span style="background-color: #cccccc;">L</span> M <span style="background-color: #cccccc;">V</span> L <span style="background-color: #cccccc;">K</span> H <span style="background-color: #cccccc;">P</span> Y <span style="background-color: #cccccc;">P</span>	R <span style="background-color: #cccccc;">K</span> V <span style="background-color: #cccccc;">E</span> E <span style="background-color: #cccccc;">P</span> S <span style="background-color: #cccccc;">I</span> Y <span style="background-color: #cccccc;">E</span>	S <span style="background-color: #cccccc;">V</span> R <span style="background-color: #cccccc;">V</span> H <span style="background-color: #cccccc;">T</span> A <span style="background-color: #cccccc;">M</span> Q <span style="background-color: #cccccc;">T</span>
	160	170	180	190	200
	G <span style="background-color: #cccccc;">R</span> T <span style="background-color: #cccccc;">E</span> D <span style="background-color: #cccccc;">D</span> L <span style="background-color: #cccccc;">V</span> P <span style="background-color: #cccccc;">T</span>	A <span style="background-color: #cccccc;">P</span> S <span style="background-color: #cccccc;">L</span> G <span style="background-color: #cccccc;">T</span> K <span style="background-color: #cccccc;">E</span> G <span style="background-color: #cccccc;">Y</span>	L <span style="background-color: #cccccc;">T</span> K <span style="background-color: #cccccc;">Q</span> G <span style="background-color: #cccccc;">G</span> L <span style="background-color: #cccccc;">V</span> K <span style="background-color: #cccccc;">T</span>	W <span style="background-color: #cccccc;">K</span> T <span style="background-color: #cccccc;">R</span> W <span style="background-color: #cccccc;">F</span> T <span style="background-color: #cccccc;">L</span> H <span style="background-color: #cccccc;">R</span>	N <span style="background-color: #cccccc;">E</span> L <span style="background-color: #cccccc;">K</span> Y <span style="background-color: #cccccc;">F</span> K <span style="background-color: #cccccc;">D</span> Q <span style="background-color: #cccccc;">M</span>
	210	220	230	240	250
	<span style="background-color: #cccccc;">S</span> P <span style="background-color: #cccccc;">E</span> P <span style="background-color: #cccccc;">I</span> R <span style="background-color: #cccccc;">I</span> L <span style="background-color: #cccccc;">D</span> L	T <span style="background-color: #cccccc;">E</span> C <span style="background-color: #cccccc;">S</span> A <span style="background-color: #cccccc;">V</span> Q <span style="background-color: #cccccc;">F</span> D <span style="background-color: #cccccc;">Y</span>	S <span style="background-color: #cccccc;">Q</span> E <span style="background-color: #cccccc;">R</span> V <span style="background-color: #cccccc;">N</span> C <span style="background-color: #cccccc;">F</span> C <span style="background-color: #cccccc;">L</span>	V <span style="background-color: #cccccc;">F</span> P <span style="background-color: #cccccc;">F</span> R <span style="background-color: #cccccc;">T</span> F <span style="background-color: #cccccc;">Y</span> L <span style="background-color: #cccccc;">C</span>	A <span style="background-color: #cccccc;">K</span> T <span style="background-color: #cccccc;">G</span> V <span style="background-color: #cccccc;">E</span> A <span style="background-color: #cccccc;">D</span> E <span style="background-color: #cccccc;">W</span>
	260	270	280		
	<span style="background-color: #cccccc;">I</span> K <span style="background-color: #cccccc;">I</span> L <span style="background-color: #cccccc;">R</span> W <span style="background-color: #cccccc;">K</span> L <span style="background-color: #cccccc;">S</span> Q	I <span style="background-color: #cccccc;">R</span> K <span style="background-color: #cccccc;">Q</span> L <span style="background-color: #cccccc;">N</span> Q <span style="background-color: #cccccc;">G</span> E <span style="background-color: #cccccc;">G</span>	T <span style="background-color: #cccccc;">I</span> R <span style="background-color: #cccccc;">S</span> R <span style="background-color: #cccccc;">S</span> F <span style="background-color: #cccccc;">I</span> F <span style="background-color: #cccccc;">K</span>		

**Figure 2-3. Amino acid sequence of Bam32**

Amino acids 1-280 are shown for human Bam32 protein. Tryptic peptides are highlighted in grey.

**Table 2-2. Multiple reaction monitoring to identify Bam32-Myc in co-IP samples.**

Peptide	Retention time LC	Q1	y-transition	Q3	IP Ab					Lysate
					SHIP	Lyn	Myc	MIgG 1	RIgG	
AELLE GK	14min	380.22	2y4	446.26	+	-	-	-	-	+
			2y5	559.34						
			2y6	688.39						
DQMSPEP IR	15min	536.76	2y6	698.38	+	-	+	-	-	+
			2y7	829.42						
			2y8	957.48						
VEEPSIYE SVR	20min	654.33	2y7	853.44	+	-	+	-	-	+
			2y8	950.49						
			2y9	1079.54						
TGVEADE WIK	21min	574.29	2y6	761.38	+	-	+	-	-	+
			2y7	890.43						
			2y8	989.49						
DSNETTG LYSLSVR	23min	771.38	2y8	894.5	-	-	+	-	-	+
			2y9	995.55						
			2y10	1096.6						
FGFNEFSS LK	26min	588.29	2y7	824.41	-	-	+	-	-	+
			2y8	971.48						
			2y9	1028.5						

### 2.3.2 Identification of potential SHIP interaction partners using prediction tools

Although an interaction between SHIP and Bam32 could be detected by co-IP paired with SRM, it was not sufficiently robust to detect by standard western blotting in our hands. Thus, we set out to broaden our search for candidate binding partners of SHIP using bioinformatics tools. Scansite3 (<http://scansite3.mit.edu>) is an open web tool developed at the Massachusetts Institute of Technology that uses results from oriented peptide library and phage display experiments to construct position-specific scoring matrices (PSSM). These PSSMs can be used to identify protein motifs and determine the probability of any given protein in its database binding to that motif (367, 368). This is then converted into a score where a higher

score is associated with higher probability of binding. For pTyr-SH2 domain interactions, positions +1 to +3 relative to pTyr are considered for selectivity. Using high stringency search conditions, 29 interactions with 12 unique proteins were predicted (Table 2-3). The hits involving phosphotyrosine residues are highlighted in gray. Bam32 was not among the predicted interactions, however the cytoskeletal adaptor protein Nck was predicted to bind at two sites (bolded), at a proline rich region via its 2<sup>nd</sup> SH3 domain and at pTyr944 via its SH2 domain.

**Table 2-3. SHIP interaction partners predicted by Scansite3.**

<b>Motif in</b>	<b>Motif in partner</b>	<b>Partner</b>	<b>Score</b>
Pro127	SH3	CAP	0.6136
Pro955	SH3	CAP	0.6018
Pro1135	SH3	Itk	0.5681
Pro127	SH3 (1 <sup>st</sup> )	Intersectin	0.5157
Pro955	SH3 (3 <sup>rd</sup> )	p85	0.5124
Pro1139	SH3	PLC $\gamma$	0.5043
Tyr915	PTB	Shc	0.4748
Thr1087	Basophilic S/T Kinase	Akt	0.4586
Ser1127	Basophilic S/T Kinase	AMP	0.4586
Pro250	SH3 (1 <sup>st</sup> )	p85	0.4559
Ser971	Pro-dependent S/T kinase	Erk1	0.4447
Pro1141	SH3	Crk	0.4316
Thr1138	Pro-dependent S/T kinase	Erk1	0.4303
Ser1057	Pro-dependent S/T kinase	Erk1	0.4219
Pro250	SH3	Src	0.4160
Ser971	Pro-dependent S/T kinase	Cdc2	0.4106
Thr963	Pro-dependent S/T kinase	Erk1	0.3953
Thr1136	Pro-dependent S/T kinase	Erk1	0.3933
Tyr944	SH2	CRK	0.3903
Thr988	DNA damage kinase	DNA PK	0.3844
Tyr221	Y kin	Lck	0.3789
Thr739	Basophilic S/T Kinase	PKC $\alpha/\beta/\gamma$	0.3659
Tyr1022	PTB	Shc	0.3571
<b>Pro962</b>	<b>SH3 (2<sup>nd</sup>)</b>	<b>Nck</b>	<b>0.3561</b>
Ser971	Pro-dependent S/T kinase	Cdk5	0.3559
Thr451	DNA damage kinase	DNA PK	0.3505
<b>Tyr944</b>	<b>SH2</b>	<b>Nck</b>	<b>0.3434</b>
Thr108	Acidophilic S/T kinase	Casein	0.3218
Tyr944	SH2	Abl	0.3116



Another web-based prediction tool available is Small matrix assisted ligand identification (SMALI), which also uses previously generated results from oriented peptide array library screening experiments (370) to determine the probability of a given SH2 domain to bind a given phosphopeptide sequence, based on the surrounding sequence (369). The PSSM incorporates selectivity information for positions -2 to +4, relative to the pTyr residue. This database contains selectivity information for 76 SH2 domains (of the 120 encoded in the human genome), a significant improvement on the 14 SH2 domains included in the Scansite search. For this, we input the amino acid sequence for SHIP and several SH2 domain proteins were identified as candidate interaction partners of various tyrosine residues. Those involving known phosphorylation sites are listed in Table 2-4. Higher scores are associated with higher probability of binding.

**Table 2-4. Phospho-SHIP interaction partners predicted by SMALI**

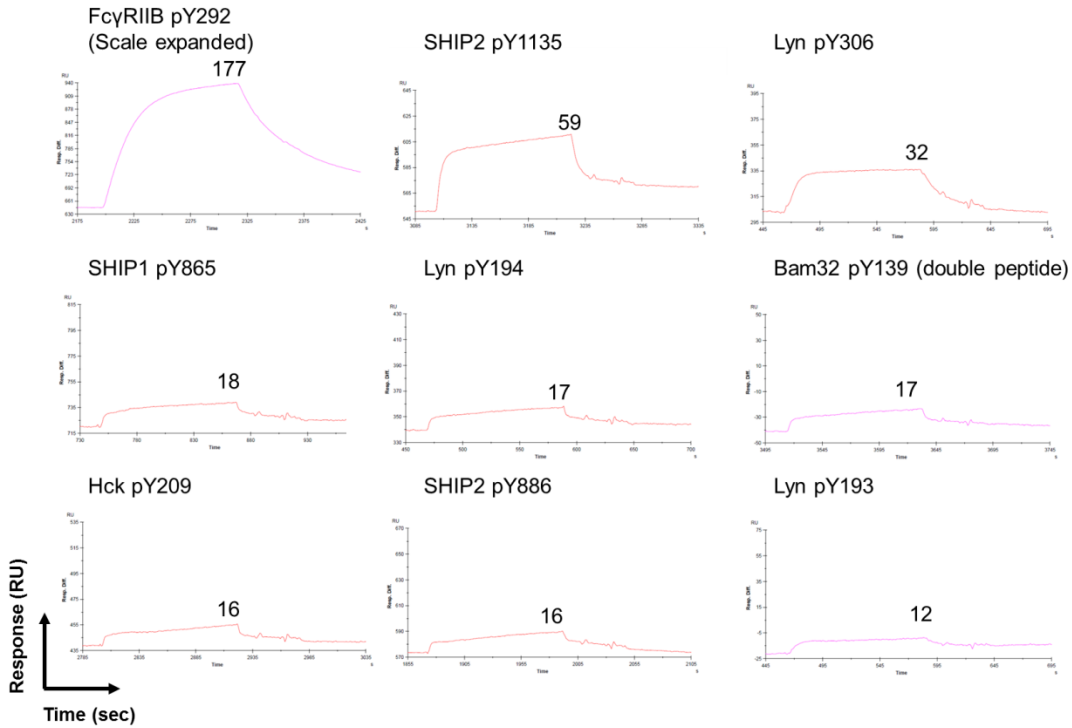
<b>pTyr in SHIP</b>	<b>SH2 domain Partner</b>	<b>Score</b>
Y866	BLNK	1.32
	Tec	1.20
	Txk	1.14
	<b>Nck1</b>	<b>1.13</b>
	Brk	1.07
	Nck2	1.04
Y915	Abl1	1.16
	Crk	1.14
	SH2D1A	1.10
	SRMS	1.00
Y944	Rasa1 (C-terminal)	1.23
	<b>Nck1</b>	<b>1.16</b>
	BLNK	1.16
	Crk	1.11
	CrkL	1.05
	Tec	1.05
	<b>Nck2</b>	<b>1.01</b>
Y1022	Syk (C-terminal)	1.13
	Abl1	1.03
	Crk	1.01

### 2.3.3 Identification of SHIP interaction partners by a Biacore screening assay

Along with bioinformatics prediction, we set out to screen our pool of candidates for interaction with SHIP experimentally, focusing on pTyr-SH2 domain pairs. We individually immobilized each biotinylated phosphotyrosine-containing 11-mer peptide (Table 2-1) on a

streptavidin-conjugated sensorchip surface, then individually injected each SH2 domain analyte. Several *in vitro* binding partners of SHIP were identified by this screening assay and are listed in Table 2-5, with the raw sensorgrams shown in **Figure 2-4**. The response depends on refractive index changes on the sensorchip surface, which in turn depends on changes in mass at the surface. Since the peptides were immobilized within a fairly tight range of response units (RUs) and since the SH2 domains all have approximately the same mass, it is possible to compare the relative estimated affinity of each interaction based on the relative response at equilibrium. Thus, the interactions in Table 2-5 are ranked based on their relative estimated affinity. In total, the SH2 domain of SHIP was screened for binding to all 24 peptides listed in the Materials and Methods section (Table 2-1) and the four known pTyr sites in SHIP were each screened for binding to all six recombinant SH2 domains. Thus, the list of 15 positive hits obtained using a cut-off value of 10RU at equilibrium was derived from a total of 48 experimental pairings.

**Interactions with SHIP1 SH2 domain**



**Interactions with SHIP1 phospho-peptides**

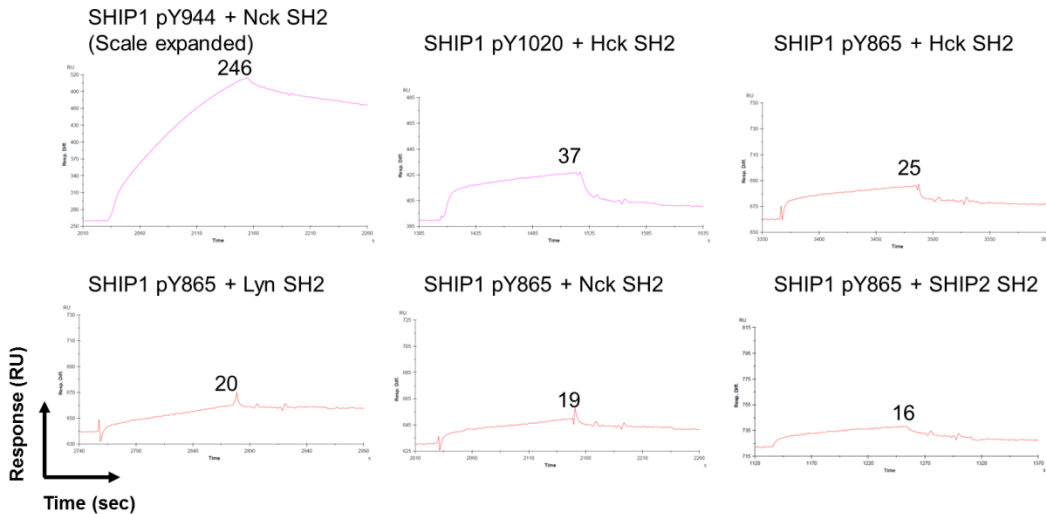


**Figure 2-4. Potential SHIP interaction partners identified in a Biacore screening experiment.**

Biotinylated phospho-peptides were immobilized on an SA sensorchip surface to 30-50 RU and SH2 domain analytes were injected for 2min. Response (RU, y-axis) is plotted over time (sec, x-axis). The response at equilibrium ( $R_{eq}$ ) is indicated for each graph. All are plotted to the same scale, except where indicated, to facilitate estimated comparisons.

**Table 2-5. Interaction partners of SHIP identified by Biacore screening assay**

Motif in SHIP	Motif in partner	Partner	Relative binding
pY944	SH2	Nck	++++
SH2	pY292	FcγRIIB	+++
SH2	pY1135	SHIP2	++
SH2	pY139	Bam32	+
SH2	pY209	Hck	+
pY865	SH2	Hck	+
pY1020	SH2	Hck	+
SH2	pY193	Lyn	+
SH2	pY194	Lyn	+
SH2	pY306	Lyn	+
pY865	SH2	Lyn	+
pY865	SH2	Nck	+
SH2	pY865	SHIP1	+
SH2	pY886	SHIP2	+
pY865	SH2	SHIP2	+

+ 10-50RU  
 ++ 50-100RU  
 +++ 100-200RU  
 ++++ 200<sup>+</sup> RU

### 2.3.4 Biacore affinity analysis of SHIP-FcγRIIB and SHIP-Nck interactions

Two interactions were chosen for further analysis and comparison of dissociation constant: the interaction between SHIP SH2 and FcγRIIB pY292 and the interaction between Nck SH2 and SHIP pY944 (**Figure 2-5**). In this assay, phospho-peptide is again immobilized on a sensorchip surface then multiple rounds of binding-dissociation are repeated, at increasing analyte concentration. The response at equilibrium, normalized to control surface, increases as concentration increases, until a plateau is reached. The dissociation constant ( $K_D$ ) is calculated to be the analyte concentration required to attain half of the maximal response; it was found to be 120nM for both interactions.

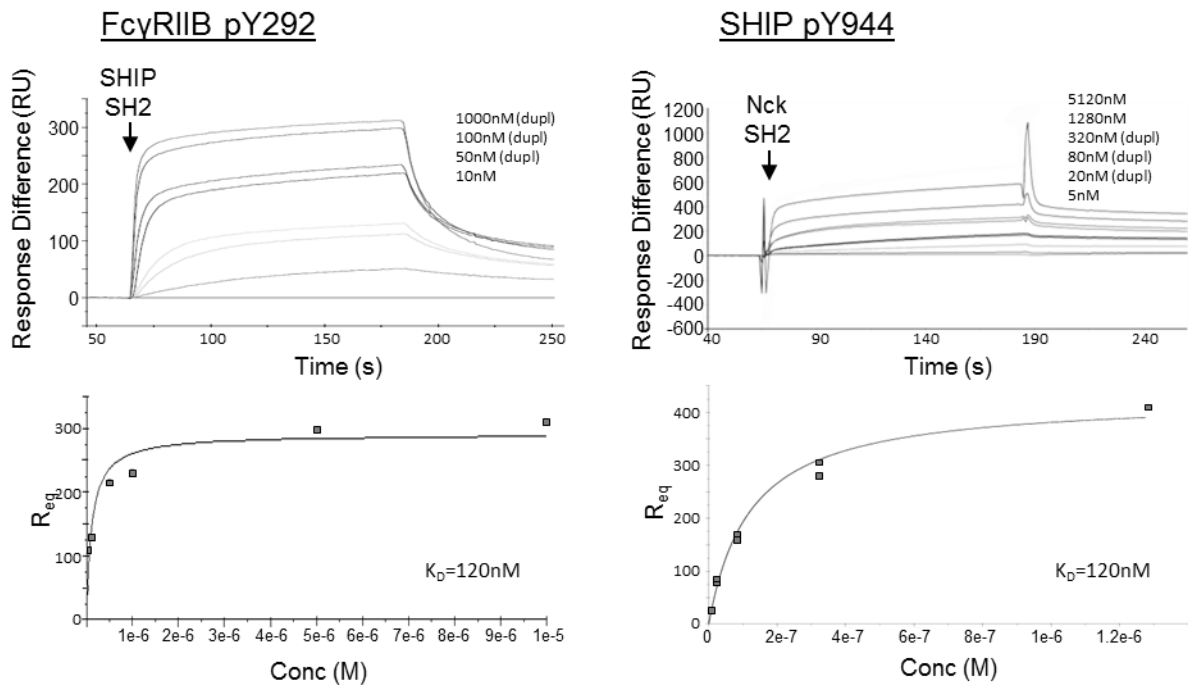


**Figure 2-5. Steady-state affinity analysis of selected interactions.**

Biotinylated-phosphopeptide was captured on an SA sensorchip surface to 30-50RU then the Biacore Affinity Analysis wizard was used to inject SH2 domain analyte at increasing concentrations, as indicated, with surface regeneration performed after each injection. Upper panels show sensorgram overlays and lower panels show response at equilibrium for FcγRIIB-SHIP (A) and SHIP-Nck (B) direct interactions.

## 2.4 Discussion

Our first set of experiments identified Bam32 as a bona fide SHIP interaction partner, as Bam32 was detected in anti-SHIP co-immunoprecipitates by a custom mass spectrometry-based SRM assay. However, we were consistently unable to confirm this finding by the traditional western blotting method of detection. This suggests that the interaction between SHIP and Bam32 is likely weak and/or transient in our system, and perhaps indirect. Our Biacore screening experiments suggests a direct interaction between Bam32 phospho-Y139 and the SH2 domain of SHIP can occur, however it appears relatively weak. Since much more robust binding partners were identified in this *in vitro* assay with potentially interesting functional implications, we opted not to pursue the Bam32-SHIP interaction any further and focused instead on a newly identified interaction between Nck and SHIP involving the SH2 domain of the former and phospho-Y944 of the latter. This interaction was predicted by both the Scansite3 and SMALI prediction tools and the dissociation constant was calculated here to be comparable to the well-characterized interaction of SHIP SH2 with FcγRIIB pITIM peptide. The dissociation constant of the SHIP-FcγRIIB interaction has been reported previously for the murine proteins (295). An interaction between SHIP and Nck was reported in a previously published paper as detected by co-immunoprecipitation in stimulated mast cells (371). The paper describes their binding in the context of a larger protein complex, thus it is not clear whether the interaction is direct or mediated by other proteins. Our results complement this previous work and further provide support for a direct interaction, one mediated by a previously unappreciated phosphotyrosine residue in the C-terminus of SHIP.

Given the identification of SHIP Tyr944 as a potential site for Nck binding with relatively high affinity, we believe it warrants further experimentation. Phosphorylation at this site has been reported in mass spectrometry studies (307), but nothing further is known. Previously, only the NPxY tyrosine residues in the SHIP C-terminus were recognized as important. This was perhaps rooted in results from early T cell receptor signaling experiments demonstrating an abrogation of total SHIP pTyr signal in SHIP Y915F/Y1022F double mutant T cells (301). One might be tempted to speculate that these two residues are then responsible for close to 100% of the tyrosine phosphorylation events in SHIP, leaving no room for Tyr944 phosphorylation. However, these experiments were performed in stable cell lines, did not include analysis of other tyrosine mutants, and have not been repeated in other cell types. Thus they should not bias further investigation in B cells.

According to the bioinformatics tools used here, a total of seven potential SH2 domain interaction partners were identified for SHIP Y944. Both Scansite3 and SMALI predicted an interaction with Nck SH2. Nck is an important regulator of cytoskeletal dynamics first described in non-hematopoietic cells but also functioning in lymphocytes (372). Interaction with Nck may explain some of the effects of SHIP on the cytoskeleton. Nck is a potent and direct activator of the actin nucleation promoting factors WASP and N-WASP (347). Furthermore, in T cells, the SH2 domain of Nck binds to the BLNK-like scaffolding molecule SLP-76, bridging WASP to the T cell signalosome (348). It is easy to imagine that disruption of the Nck-SLP76 interaction by competition with SHIP might have important functional consequences.



Interestingly, examination of the amino acid sequence of human and mouse Y944 reveals a potentially important distinction – the presence of a proline residue at Y+3 in human but not mouse. Proline residues cause a bend in three-dimensional structure, which could affect binding of protein partners. Studies have shown that as far as Y+6 may be important for specific interactions (373). There are known differences in the mechanisms employed by human and mouse B cells to recruit and retain SHIP to Fc $\gamma$ RIIB (240). Species-specific binding preferences provide one possible explanation for these differences.

Here, we use two different web tools for prediction SHIP interaction partners, Scansite3 and SMALI. These are useful tools for hypothesis building, however the potential for false negatives should be considered as a limitation. For instance, the phosphopeptide SHIP2 pY1135 bound to SHIP SH2 with the second highest Biacore response in our screening experiment, weaker only than ITIM binding. This interaction was not predicted by either web tool, nor does it conform to the previously described consensus sequence for SHIP SH2 (95, 370). Of note, Scansite and SMALI use information extending to the Y+3 and Y+4 positions, respectively, while specificity has been reported to extend as far as Y+6 for some SH2 domains (373). False positive predictions can also potentially arise, however only one positive hit was further tested (and subsequently confirmed) in our Biacore screening experiment since we limited our screening to selected specific candidates. One likely cause of false positives theoretically is negative selection against specific residues near the tyrosine, which is not accounted for in either prediction tool. For example the presence of a positively charged residue might repel the essential arginine in an SH2 domain. It is also important to note that these prediction tools are limited to only a subset of SH2 domains for which peptide screening experiments were performed previously. Scansite has

prediction information available for only two of our six candidate SH2 domains (SHIP and Nck) while SMALI has information for five of six (SHIP, SHIP2, Lyn, Hck, Nck), lacking only Bam32 SH2.

Finally, it is vital to keep in mind, both for bioinformatics prediction tools and *in vitro* assays such as Biacore, that a given cellular context may or may not allow for an interaction to occur even if strongly predicted or having a high measured affinity. Many additional inter-related factors are at play including expression levels, conditions required for tyrosine phosphorylation, co-localization within the cell, binding kinetics, and competition with other interaction partners. Thus, the identification of an interaction *in vitro* is not sufficient to conclude the presence of an interaction *in vivo*, nor is it sufficient to extrapolate physiological relevance. Some of these factors will be examined in more detail in chapter three (for the Nck-SHIP interaction) and chapter four (for the SHIP-Fc $\gamma$ RIIB interaction)

# **CHAPTER 3: A NOVEL PHOSPHORYLATION SITE IN SHIP INDUCES BINDING TO NCK AND REGULATES ACTIN DYNAMICS IN B CELLS**

## **3.1 Specific Introduction**

The actin cytoskeleton is a fundamental component of cellular structure and response to extracellular cues. It directs such key activities as spreading, migration and adhesion of B lymphocytes. These functions are critical to the immune response as B cell trafficking through tissues and lymph nodes permits encounter with antigen and B cell spreading produces the increased surface area required to gather as much antigen as possible and/or to make maximal cell:cell contacts. Both of these processes depend on the induction of branched filamentous actin (F-actin) polymerization that drives the cell membrane outward (333).

Many of the upstream signals induced by BCR or chemokine receptor ligation are common to other cell types. Wiskott-Aldrich Syndrome Protein (WASp) and neural- (N-) WASp are actin nucleation promoting factors that activate the Arp2/3 complex, which bind to existing filaments and nucleate a new branch (215, 344). WASP and N-WASP require several signals to become fully activated, including binding to active (GTP-bound) GTPases Cdc42 and Rac (347, 374, 375) and to the SH3 and SH2 domain-containing adaptor protein Nck (347). Tyrosine phosphorylation of WASP and N-WASP is also associated with increased activity (376-378). Actin severing proteins such as cofilin are proposed to promote extensive branching by generating free barbed ends (223), the preferred site of Arp2/3-mediated filament nucleation

(379). In B cells, both WASP and N-WASP contribute to cell spreading, however N-WASP was demonstrated to play an additional, more dominant role in cell contraction and signal attenuation (350).

B cell receptor (BCR) signaling promotes remodelling of cellular F-actin. The rate of peripheral F-actin turnover is increased in stimulated cells (223), which likely reflects both continuous addition of actin monomers onto growing filaments and continued addition of new branches. Phosphatidylinositol 3-kinase (PI3K) is a key signaling enzyme activated upon ligation of the BCR. It phosphorylates the membrane lipid PI(4,5)P<sub>2</sub> to produce PI(3,4,5)P<sub>3</sub>. PI(3,4,5)P<sub>3</sub>-dependent effector molecules contribute to the actin nucleation pathway by several means. Btk, a PIP<sub>3</sub>-binding tyrosine kinase, phosphorylates Vav, a PIP<sub>3</sub>-binding guanine nucleotide exchange factor, which activates Cdc42 and subsequently WASp (213). Btk also phosphorylates WASP directly and contributes to its full activation (351).

Pathways independent of PI3K also play an important role in actin dynamics. The adaptor protein Nck is recognized as a crucial link between tyrosine kinase associated receptor signaling and localized actin polymerization (380, 381). Nck interacts with WASp (382) and N-WASP (383, 384) which serves to recruit them into receptor-associated signaling complexes (348, 385, 386), in addition to directly activating their actin nucleation activity (347). By contributing to the activation of actin nucleation proteins, Nck promotes branched actin formation (346). In lymphocytes, Nck is recruited via interaction with phosphorylated scaffolding molecules (348, 349) or, as more recently demonstrated, via direct interaction with the BCR (177).

The lipid phosphatase SHIP is a key regulator of actin dynamics. SHIP-deficiency results in increased F-actin content in B cells (351), T cells (290) and neutrophils (355) and more effective B cell spreading (351). In B cells, this negative regulatory role of SHIP is proposed to depend on hydrolysis of PI(3,4,5)P<sub>3</sub>, triggering a loss of Btk membrane recruitment (351). However, this hypothesis has not been thoroughly examined. Paradoxically, another study showed that primary T cells deficient in SHIP had reduced numbers of microvilli and decreased basal motility compared to their wild type counterparts (290). These positive effects of SHIP may be explained by considering the double-edged nature of certain PIP<sub>3</sub> binding proteins such as Rac, which in addition to promoting actin nucleation can also activate protein phosphatases (357, 358). Alternatively, proteins that are specifically recruited to the SHIP product PI(3,4)P<sub>2</sub> may promote F-actin polymerization. The tandem pleckstrin homology domain proteins (TAPPs) (275) and lamellipodin (153, 359) are two candidates. On the other hand, these effects of SHIP, both positive and negative, may occur entirely independently of its lipid phosphatase activity, depending instead on protein-protein interactions not yet characterized.

In chapter 2 of this thesis, we identify and characterize a direct interaction that forms *in vitro* between SHIP Tyr944 phosphopeptide and the SH2 domain of Nck, as detected by surface plasmon resonance. Here, we provide further support for this interaction in a cellular system and provide evidence that Tyr944 is required. Using a fluorescence recovery after photobleaching (FRAP) assay, we demonstrate that SHIP overexpression is associated with decreased dynamic turnover of fluorescently tagged actin. According to our data, this effect is lost by mutation of Tyr944 to phenylalanine (Y944F) or by co-overexpression of Nck. The loss of inhibitory function associated with Y944F mutation does not seem to be associated with reduced enzymatic

activity or defective recruitment to the cell membrane. Thus we propose instead that SHIP inhibits actin dynamics by binding to Nck and disrupting its function in promoting branched F-actin polymerization.

## **3.2 Materials and Methods**

### **3.2.1 Cell culture and reagents**

Ramos (Ra 1) cells, a human B cell line derived from a male Burkitt Lymphoma patient (387), Ramos clonal cell lines expressing Fc $\gamma$ RIIB generated and described previously (388), and A20 cells, a murine B cell line derived from BALBc mice with reticulum cell sarcoma (389), were both cultured in Roswell Park Memorial Institute (RPMI) medium supplemented with 10% Fetal Bovine Serum (FBS) and penicillin/streptavidin antibiotics. 50nM 2-mercaptoethanol was also added to A20 cultures. Stimulations were performed using F<sub>(ab')<sub>2</sub></sub> goat anti-human IgM (Jackson Immunolabs or Southern Biotechnology) or pervanadate, which was prepared fresh by mixing 2.5mM hydrogen peroxide with 0.25mM sodium orthovanadate (final concentrations).

### **3.2.2 Plasmids and transfections**

Actin-pTagRFP vector was purchased from Evrogen and Nck-pCMV6-Entry vector was purchased from Origene. Human SHIP-pEGFP-C1 construct was a gift from Dr M. Jücker (390). Site-directed mutagenesis was performed using the QuikChange II XL kit (Agilent Technologies) to convert Tyr944 to phenylalanine (Y944F) with the following primers:

5'-ACAGCCTGGAGCTTCGACCAGCCGC-3'

5'-GCGGCTGGTTCGAAGCTCCAGGCTGT-3'

Mutagenesis was confirmed by sequencing (Robarts Research Institute). Transfections were performed using the Neon® transfection system (Invitrogen) to electroporate  $5 \times 10^6$  cells per 100µl reaction with 20µg SHIP vector and/or 10µg Actin pTagRFP. Cells were cultured in antibiotic-free medium and used for experiments 24-48h post-transfection.

### **3.2.3 Generation of stable cell lines**

Expression vectors were linearized by single cutting with MluI enzyme (New England Biolabs) and, after purification using QiaQuick columns (Qiagen) and verification by agarose gel electrophoresis, transfected into Ramos cells. After 24h, Geneticin (Thermo Fisher) was added at 1.5mg/ml for drug selection. After 1-2 weeks, cells were sorted by fluorescence activated cell sorting (FACS) using a FACSAria III cell sorter (BD) then cloned into 96-well plates after a brief rest period. Once single cell colonies were visible, EGFP expression was verified by flow cytometry and EGFP or SHIP-EGFP expression was verified by western blotting using anti-EGFP antibody (4B10, Cell Signaling Technologies).

### **3.2.4 GST pull-downs**

Cells were stimulated with either pervanadate or anti-IgM, then lysed in equal numbers with 0.5% Nonidet P-40 (Thermo Fisher) lysis buffer containing protease and phosphatase inhibitor cocktails (Roche). Lysates were precleared with glutathione-sepharose beads prior to pull-down with fresh beads plus recombinant Nck-GST or GST control (Abnova). Eluates were separated by SDS-PAGE using precast 4-15% polyacrylamide gradient gels (Bio-Rad), transferred to nitrocellulose membrane (BioRad) and probed with anti-SHIP (P1C1, Santa Cruz) or anti-BLNK (3587, Cell Signaling Technologies) antibody. Horseradish peroxidase-

linked goat anti-mouse (Jackson) or anti-rabbit (Cell Signaling Technologies) IgG was used as secondary antibody, followed by chemiluminescence development.

### **3.2.5 FRAP assay for actin turnover**

Transfected cells expressing actin-TagRFP together with either EGFP, SHIP-EGFP or Y944F-EGFP were adhered for 30min on coverglass surfaces coated with 10µg/ml anti-IgM. Cells were mounted on a stage-top incubator and three peripheral regions of interest (ROIs) were chosen for photobleaching using a 405nm laser (100% intensity, 100ms, Rapp OptoElectronic) concurrent with confocal imaging on a Zeiss AxioObserver spinning disc microscope. TagRFP signal intensity within the bleached ROI was normalized to intensity values from an unbleached control region of the same cell. The curves were also y-transformed to (0,0) at t=0 (bleaching event) so that individual recovery curves begin at the intensity minimum. Each group of recovery curves were then fit to the following equation, with the constraint that  $Y_0=0$ :

$$Y = Y_0 + (Plateau - Y_0) * (1 - e^{-K*x})$$

The rate constant (K) was derived by nonlinear regression analysis using GraphPad Prism software.

### **3.2.6 Membrane recruitment assay**

FcγRIIB<sup>+</sup> Ramos cells were serum-starved at 1x10<sup>6</sup>/ml for 3h. Stimulations were performed in a cell culture incubator and stopped with 2% ice cold paraformaldehyde (PFA). Membrane recruitment was measured by co-localization analysis in ImageJ. The Cell Outliner plugin was used to define individual cells and the Colocalization Indices plugin was used to calculate



Pearson's coefficient of correlation between green and red signals. The red signal arises from the membrane marker fmem. The green signal arises from ectopic EGFP control or EGFP fused to SHIP protein.

### **3.2.7 Intracellular staining**

For PI(3,4)P<sub>2</sub> staining, cells were incubated at 1x10<sup>7</sup>/ml in warm PBS with LIVE/DEAD Fixable Aqua stain (Molecular Probes) at 1:1000 dilution for 20min at 37°C and 5% CO<sub>2</sub>, then centrifuged and resuspended in the same volume RPMI. After a 30min recovery period, cells were stimulated with F<sub>(ab')<sub>2</sub></sub> anti-IgM then fixed and permeabilized with BD Fix/Perm solution (BD Biosciences) for 20min on ice. Cells were incubated with anti-PI(3,4)P<sub>2</sub> (Echelon) diluted to 1:200 for 1h at room temperature, followed by Alexafluor647-conjugated goat anti-mouse IgG secondary antibody (Life Technologies) diluted to 1:500 for 30min at room temperature. Detection was performed by flow cytometry.

For F-actin staining, spread cells were fixed with 2% PFA for 30min on ice and permeabilized with 0.1% saponin for 10min at room temperature. Cells were incubated overnight at 4°C with Alexafluor647-Phalloidin diluted to 1:100. Detection was performed by confocal microscopy and quantitation was performed using ImageJ software.

### **3.2.8 Spreading assay**

8-well coverglass bottom slides (Nunc) were coated with 5µg/ml F<sub>(ab')<sub>2</sub></sub> anti-IgM overnight at 4°C then washed in PBS followed by RPMI. 40-44h post-transfection, EGFP<sup>+</sup> transfected cells were purified by FACS and rested a minimum of 2h in a cell culture incubator. Cells were then transferred to coated surfaces at 5x10<sup>4</sup> cells per well and incubated for 30min.

Spreading was stopped by transfer to ice and addition of 2% PFA. After washing and F-actin staining, cells were imaged on a confocal microscope. Cells were traced based on red signal using the Cell Outliner plugin for ImageJ and the relative surface area was quantified.

### **3.2.9 Statistical Analysis**

GraphPad Prism software was used for all statistical analyses and comparisons. For all figures, \*=p<0.05, \*\*=p<0.01, \*\*\*=p<0.001 and \*\*\*\*=p<0.0001.

## **3.3 Results**

### **3.3.1 SHIP interacts with the cytoskeletal adaptor protein Nck**

In chapter 2 of this thesis, we reported an interaction between phospho-Y944 of SHIP and the SH2 domain of Nck, detected in an *in vitro* Biacore 2000 assay. To validate this interaction in a cellular system, we stimulated cells with the potent tyrosine phosphatase inhibitor pervanadate, lysed them and performed pull-down assays using recombinant Nck-GST. In both murine A20 and human Ramos cells, endogenous SHIP protein was able to bind Nck-GST and was detected by western blotting (**Figure 3-1**). BLNK was used as a positive control since it is known to interact with the Nck SH2 domain (120).

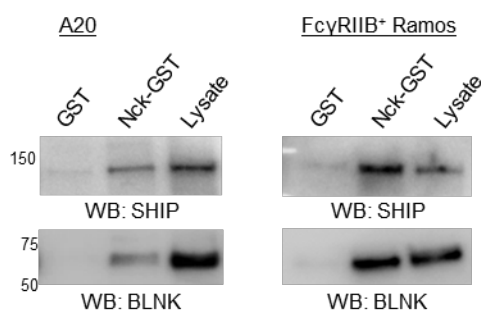


**Figure 3-1. Endogenous SHIP binds recombinant Nck-GST.**

*A20 (left) or Ramos cells (right) were stimulated for 2min with pervanadate, lysed then incubated with GST control or recombinant Nck-GST. Glutathione sepharose beads were used to pull-down binding partners, which were detected by SDS-PAGE and western blotting for SHIP and BLNK. Blots are representative of at least two repeated experiments in each cell line.*

To define the dependence on BCR stimulation and the contribution of Y944, we developed clonal cell lines which overexpress EGFP, SHIP-EGFP or SHIP Y944F-EGFP (**Figure 3-2A**) and performed GST pull-down experiments in unstimulated and BCR-stimulated cells (**Figure 3-2B**). Background binding to GST control was high, however in one experiment SHIP-EGFP bound to Nck-GST appreciably more than to GST control. The interaction was observed only after stimulation through the BCR and it was greatly reduced when Y944 was mutated to phenylalanine (**Figure 3-2**).

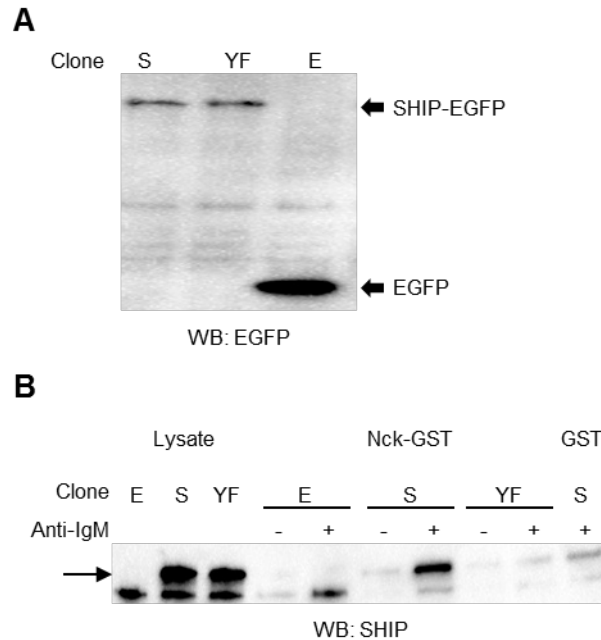


**Figure 3-2. Interaction between SHIP and Nck is stimulation-dependent and supported by Tyr 944.**

(A) Clonal cell lines expressing SHIP-EGFP (S), SHIP Y944F-EGFP (YF) and EGFP (E) were lysed. Western blotting was performed with anti-EGFP antibody. (B) The indicated clonal cell lines were left unstimulated or stimulated with 10  $\mu$ g/ml  $F_{(ab)2}$  anti-IgM for 5min then lysed. Lysates were incubated with recombinant Nck-GST or GST control. The binding fraction was separated with glutathione-sepharose beads and subjected to SDS-PAGE followed by western blotting with anti-EGFP antibody. Note that SHIP-EGFP can be identified above background in stimulated cells expressing WT SHIP but not in unstimulated cells or those expressing SHIP Y944F.

**3.3.2 SHIP inhibits actin turnover by a mechanism seemingly dependent on Tyr944**

Since our data supports that Tyr944 is the major motif required for interaction of SHIP with Nck and since Nck is a regulator of the actin cytoskeleton, we aimed to determine the effects of SHIP overexpression on F-actin turnover and the requirement for Y944. We adopted an assay previously developed in the laboratory of Dr Michael Gold that allows for direct visualization and measurement of fluorescently-tagged actin turnover in live cells by FRAP (223). We transiently transfected cells to express actin-TagRFP plus either EGFP control, SHIP-EGFP or SHIP Y944F-EGFP, then allowed them to spread on anti-IgM-coated

coverglass for 30-40min. Live cells were kept in a stage-top incubator with temperature, humidity and CO<sub>2</sub> control and imaged at high magnification and high-resolution with a spinning-disc confocal microscope. Three regions of interest (ROIs) were chosen at the periphery of EGFP<sup>+</sup> cells, where actin is assembled into filaments and theoretically turning over to promote cell spreading over the antigen-coated surface. A high intensity, 405nm laser was directed to the ROIs, which locally bleached the fluorescent signals. The cells were imaged as the bleached regions recover their fluorescence over time. The kinetics with which the TagRFP fluorescence signal recovered reflects the rate of tagged-actin turnover. We found that SHIP-EGFP overexpression was associated with slower actin turnover relative to control EGFP, as indicated by a decrease in the rate constant of fluorescence recovery. The reduction was not seen in cells overexpressing SHIP Y944F-EGFP (*Figure 3-3*). This was statistically significant and consistently observed in four independent experiments.

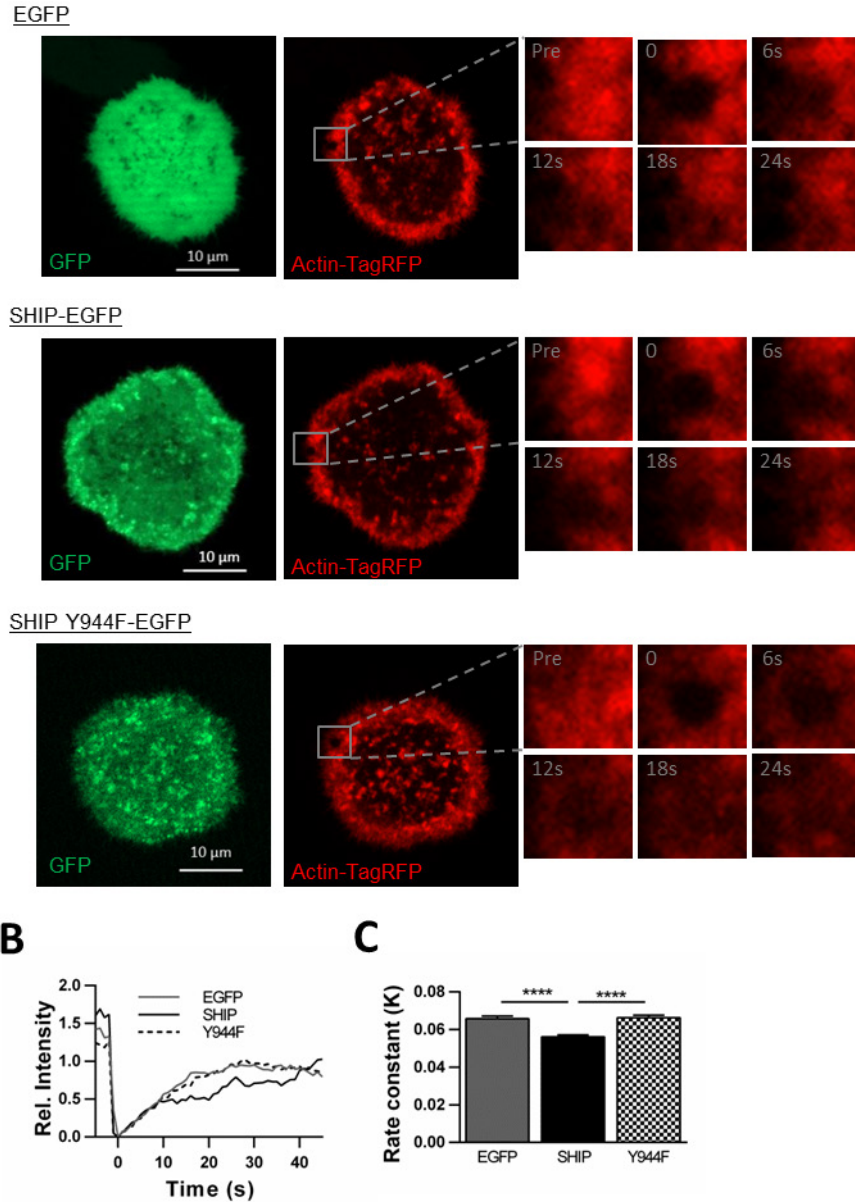


**Figure 3-3. SHIP inhibits actin turnover rate in a Tyr944-dependent manner.** (A) Example cells, (B) representative recovery curves and (C) rate constant quantification pooled from four independent FRAP experiments (48 bleaching events total per group). Ramos cells were co-transfected with actin-TagRFP2 plus either EGFP, WT SHIP-EGFP or Y944F SHIP-EGFP and spread on anti-IgM for 30-40min before photobleaching of peripheral ROIs. Rate constants and *p* values were obtained by nonlinear regression analysis.

### 3.3.3 Effect of SHIP-EGFP on actin turnover is overcome by co-overexpression of Nck

If the proposed function of SHIP in slowing actin turnover is accomplished by binding to Nck as we predict, then we would expect that co-overexpression of Nck would abrogate the effect of SHIP overexpression. This is indeed what we observed in two independent experiments (*Figure 3-4*). Since the Nck expression vector had no fluorescent indicator it was transfected at a ratio of 3:1 relative to EGFP/SHIP-EGFP expression vector to ensure that most EGFP<sup>+</sup> cells also received the Nck vector.

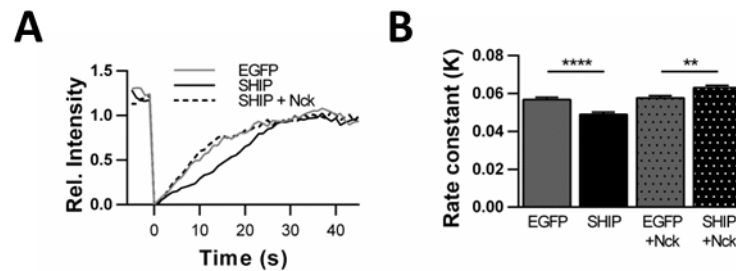


**Figure 3-4. Co-overexpression of Nck abrogates the inhibitory effect of SHIP-EGFP on actin turnover.**

Ramos cells were transfected with Actin-TagRFP2 plus either EGFP or SHIP-EGFP and a 3x excess of Nck. Spreading and photobleaching were performed as in Figure 3-3. (A) Representative recovery curves. (B) Rate constant quantification pooled from two independent experiments with 24 bleaching events total per group. Rate constants and *p* values were obtained by nonlinear regression analysis.

### 3.3.4 SHIP membrane recruitment and enzymatic activity are not diminished by Y944F mutation

The observation made here that Y944 is required for the function of SHIP in slowing actin turnover could potentially be explained if this tyrosine residue was important for localization of SHIP to the cell periphery or if it somehow inhibited the catalytic activity of SHIP.

To address the effect on localization, we co-expressed either WT or Y944F SHIP-EGFP along with a red fluorescent membrane marker in Fc $\gamma$ RIIB<sup>+</sup> Ramos cells. The cells were stimulated, fixed, and imaged by confocal microscopy. Membrane localization was quantitatively assessed by Pearson's coefficient, which measures the overlap between green and red signals. Both WT and mutant forms are induced to accumulate at the plasma membrane upon stimulation through the BCR (F<sub>(ab')</sub><sub>2</sub> anti-IgM) or through co-ligation of the BCR with Fc $\gamma$ RIIB (Intact anti-IgM, **Figure 3-5A**). Both forms of SHIP-EGFP could be recruited to a similar extent.

To address the effect on catalytic function, Ramos cells were transiently transfected with EGFP, SHIP-EGFP, or SHIP Y944F-EGFP, stimulated via the BCR, and stained with an anti-PI(3,4)P<sub>2</sub> antibody as well as a fixable viability dye. As expected, SHIP-EGFP overexpression resulted in increased PI(3,4)P<sub>2</sub> production upon stimulation, relative to EGFP control. Overexpression of the mutant version had the same effect, perhaps even more potently, demonstrating no evidence that enzymatic activity is impaired by Y944F mutation. Further repeated experiments will determine if this result is supported by statistical comparison.



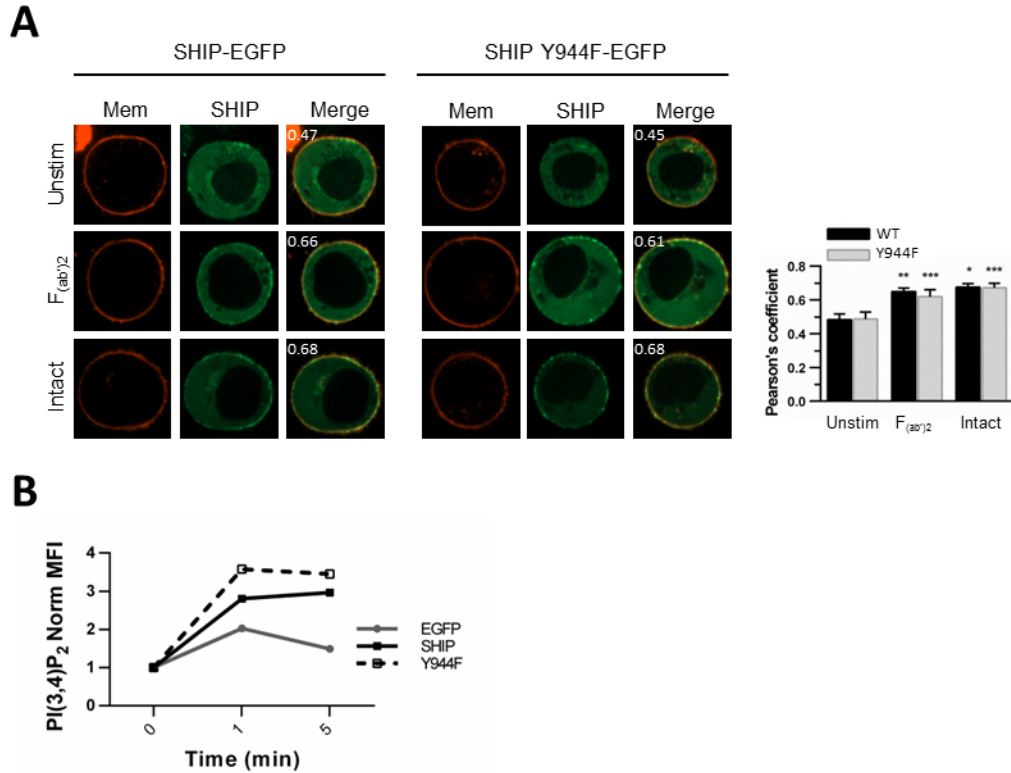


**Figure 3-5. Mutation of Tyrosine 944 to phenylalanine does not impair membrane recruitment of SHIP or its  $PIP_2$ -hydrolyzing function.**

(A) Transiently transfected,  $Fc\gamma RIIB^+$  Ramos cells expressing WT or Y944F SHIP-EGFP and red membrane marker were stimulated in a cell culture incubator for 5min, fixed and imaged by confocal microscopy. Representative images and quantitation of green/red colocalization by Pearson's coefficients are shown, analyzed for 14 cells per condition by one-way Anova using GraphPad Prism. Asterisks indicate statistical significance relative to unstimulated control in the same group. (B) Transiently transfected Ramos cells expressing EGFP, SHIP-EGFP or SHIP Y944F-EGFP were stained with a fixable viability dye (AmCyan), stimulated with  $F_{(ab)2}$  anti-IgM, fixed, stained for intracellular  $PI(3,4)P_2$  lipid and analysed by flow cytometry. Graph shows normalized  $PI(3,4)P_2$  staining intensity gated on  $EGFP^+$ ,  $AmCyan^-$  population.

### 3.3.5 Overexpression of SHIP-EGFP has no measurable effect on cell spreading in a transient transfection system

To test the functional consequence of SHIP's role in slowing actin turnover in Ramos cells, we performed a cell spreading assay. Here, a coverglass surface is coated with anti-IgM and transiently transfected, FACS purified cells are allowed to adhere for 30min before fixation

and phalloidin staining, which binds specifically to F-actin. We find no difference in either total area of spreading or total F-actin staining intensity between controls cells and cells overexpressing WT or mutant SHIP-EGFP (*Figure 3-6*).

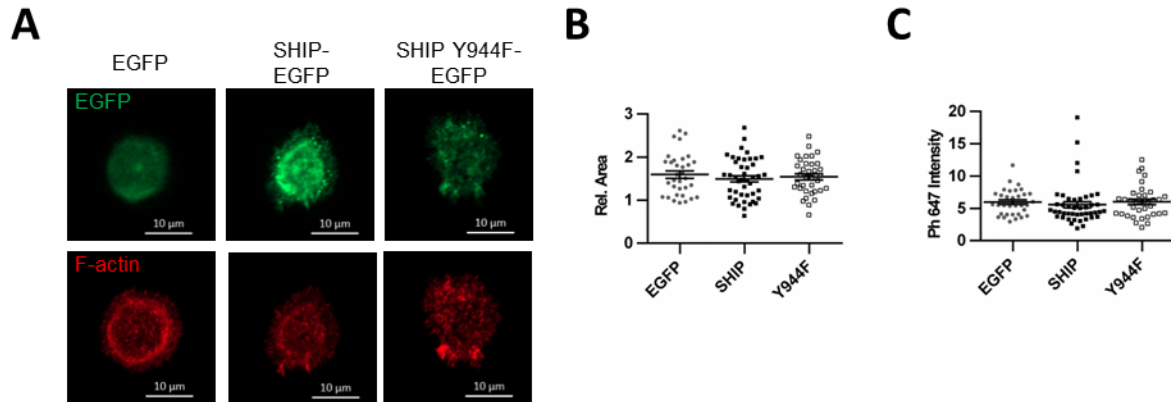


**Figure 3-6. Overexpression of SHIP-EGFP has no measurable effect on Ramos cell spreading.**

Transiently transfected Ramos cells expressing the indicated construct were sorted by FACS, rested a minimum of one hour, then spread on anti-IgM coated coverglass surfaces. Following fixation and permeabilization, cells were stained with Alexafluor647-Phalloidin and imaged on a confocal microscope. Relative area and Phalloidin intensity were measured using ImageJ. Representative cells (A) and quantitation of relative area (B) and F-actin content (C) are shown. Statistical analysis was performed by one-way Anova test using GraphPad Prism software.

### 3.3.6 Cell viability after transfection is variable and vector-dependent

Several experiments were performed to examine potential mechanisms by which SHIP might affect actin turnover in a Y944-dependent manner. These include flow cytometry-based measurements of WASP and N-WASP phosphorylation and F-actin content after stimulation. Further functional assays were also performed, including chemokinesis experiments and spreading assays in other cell lines. The results were inconsistent between experiments, thus are inconclusive to date and are not shown here. These inconsistencies may be explained by variability in cell viability after transfection. As shown in *Figure 3-7A*, EGFP-expressing

transfected populations had more surviving cells compared to SHIP-EGFP and SHIP Y944F-EGFP-expressing transfectants, and even proliferated over the course of 24h in some experiments. When compared directly, SHIP-Y944F vector had a more profound negative effect on cell viability compared to the WT version (**Figure 3-7B**). We also consistently observed dimmer expression of SHIP Y944F-EGFP compared to WT SHIP-EGFP (observation, not shown).

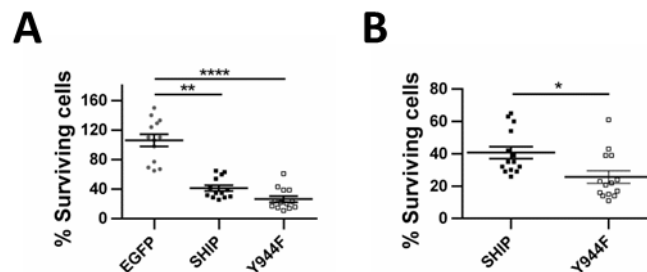


**Figure 3-7. Cell viability is negatively affected by transient transfection with SHIP and Y944F constructs.**

Ramos cells transiently transfected with the indicated pEGFP-C1 construct were cultured at  $5 \times 10^5$ /ml for 18-24h then counted with a hemocytometer using trypan blue to exclude dead cells. Each dot represents an independent transfection. Percent surviving cells were compared by a paired one-way Anova (A) or by a paired t-test (B) using GraphPad Prism software.

Measures taken to overcome these differences, including FACS sorting based on forward and side scatter and the inclusion of a viability indicator, were insufficient to instill confidence in the results since cells in early stages of apoptosis cannot be excluded by these methods. The differences in cell viability observed in the current experimental system make it difficult to assess the differential effects of SHIP and SHIP Y944F on cellular signaling and function. Caution is also required in the interpretation of FRAP experiments presented earlier, however for this experiment it was possible to select morphologically normal, well-spread cells from each group prior to manipulation and measurement.

### 3.4 Discussion

Our data supports the existence of a SHIP-Nck complex that is induced to form in B cells upon stimulation and that depends, at least in part, on Tyr944 of SHIP. In a FRAP assay, we demonstrate a role for SHIP in slowing actin turnover. This function is apparently lost with either mutation of Tyr944 to Phe or with co-overexpression of Nck. The dependence on Tyr944 does not seem to be due to an effect on SHIP localization or catalytic function, although further experimentation is required to substantiate this finding. Experiments so far fail to demonstrate a functional effect of SHIP or SHIP Y944F overexpression on B cell spreading, however shortcomings of the transient transfection system currently used may be a limiting factor in the detection of potential differences. The limitations of the current system include differences in cell viability after transfection with different expression vectors, as well as the fact that SHIP is expressed endogenously in these cells at relatively high levels. The over-expression that is achieved over and above endogenous expression may not be sufficient to detect overall changes in function.

Importantly, the key data demonstrating an interaction between SHIP and Nck and demonstrating a differential effect of SHIP WT and Y944F on actin turnover are less vulnerable at least to the cell viability issue. For the interaction studies, this is true because they are performed in stable cell lines expressing similar levels of exogenous protein. For the Actin FRAP experiments, this is true because morphologically normal, viable and well-spread cells from each condition can be visualized and chosen for further photobleaching and analysis without experimental bias.

We have provided evidence that Tyr944 of SHIP is linked to the actin cytoskeleton physically through interaction with cytoskeletal adaptor protein Nck and functionally by supporting the role of SHIP in slowing actin turnover. At this point, two major points remain to be confirmed: the presence of this complex *in vivo* and the link between its existence and the proposed functional consequence. GST pull-down experiments support the ability of SHIP and Nck to interact in a cellular context, however these experiments were performed either after non-physiological stimulation with pervanadate or in BCR-stimulated cells with non-physiological levels of overexpressed SHIP and recombinant Nck. Further experimentation should be performed to confirm the presence of a SHIPpY944-Nck SH2 interaction *in vivo*. The demonstration that SHIP-EGFP overexpression is no longer associated with slower kinetics of actin turnover when Nck is co-overexpressed is consistent with our hypothesis that binding of SHIP to Nck is the mechanism by which SHIP alters the cytoskeleton, or at least that it lies somewhere upstream.

One could imagine several reasons why mutation of Tyr944 could result in loss-of-function of SHIP with respect to its effect on actin. First, Tyr944 could be important in localizing SHIP to the plasma membrane where it can access and hydrolyze its substrate PIP<sub>3</sub>. Our data does not support this hypothesis since SHIP Y944F-EGFP is recruited to the membrane as well as WT SHIP-EGFP. Second, Y944 could somehow promote enzymatic activity either directly by some cross-domain allosteric mechanism or indirectly by directing it to specific PIP<sub>3</sub>-containing membrane compartments via binding partners. Our preliminary data does not support this hypothesis either, since SHIP Y944F-EGFP overexpression results in an equivalent or even greater increase in stimulation-induced PI(3,4)P<sub>2</sub> production over control transfectants, compared to WT SHIP-EGFP overexpression. Although further supporting experiments are required, it is

tempting to speculate that mutation of Y944 may uncouple SHIP from the cytoskeleton by releasing it from Nck. This might result in more “free” SHIP molecules available for PIP<sub>3</sub> hydrolysis, which could account for the qualitative increase in PI(3,4)P<sub>2</sub> production observed and perhaps the increased cell death.

The specific mechanism by which SHIP binding to Nck disrupts actin turnover can be speculated based on previous studies. The SH2 domain of Nck is known to bind to phosphorylated BLNK, a molecular scaffold that binds several BCR signaling proteins. The model below (*Figure 3-8*) illustrates how pSHIP could compete with pBLNK for Nck SH2 and inhibit downstream signaling events. The BLNK-related molecule SLP-76 has been shown in T cells to bind both Nck SH2 and the guanine nucleotide exchange factor Vav upon T cell receptor stimulation. Nck recruits WASP into the signalosome while Vav recruits and activates Cdc42. Cdc42 can then activate the actin nucleation function of WASP, inducing branched actin formation (348). Although an equivalent process has not been extensively characterized in B cells, it is likely to occur since BLNK, like SLP-76, inducibly associates with both Nck and Vav (120). Furthermore, Nck can directly activate both Cdc42 and Rac if brought into proximity (347). Thus, our model predicts that SHIP inhibits actin polymerization by excluding Nck from the BCR signalosome. This model depends not on the catalytic activity of SHIP but rather on an adaptor function of a novel tyrosine phosphorylation site, Y944.

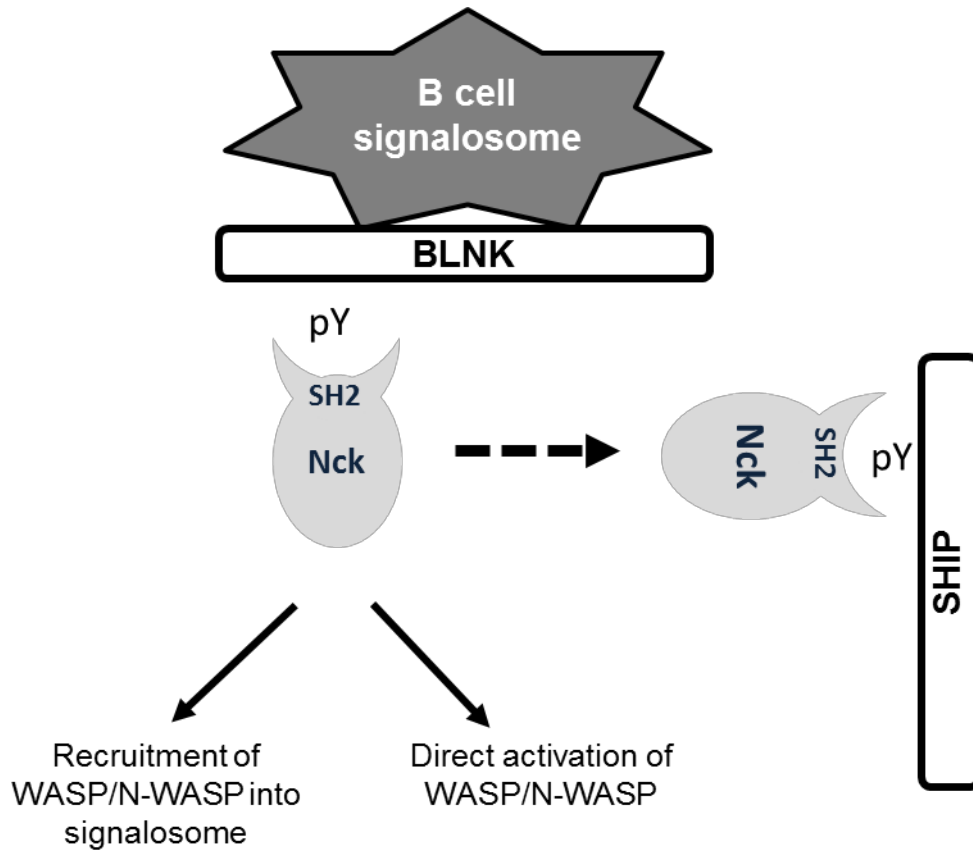


**Figure 3-8. Model demonstrating how binding of SHIP to Nck via Y944 could inhibit F-actin dynamics.**

*Upon BCR ligation, a large complex of signaling molecules forms, known as the signalosome. A key scaffolding molecule in this complex is BLNK. Phosphorylated BLNK binds Nck via its SH2 domain. Nck associates with WASP/N-WASP, promoting an active conformation and bridging these actin nucleation promoting factors to the signalosome. By providing an alternative binding site for the Nck SH2 domain, SHIP phospho-Tyr944 may inhibit this function of Nck and subsequently inhibit nucleation of branched actin filaments.*

In brief, the data presented here supports that an interaction is induced to form between SHIP and the cytoskeletal adaptor protein Nck by way of Tyr944, a newly described tyrosine phosphorylation site in SHIP. Furthermore, our data suggests that SHIP inhibits actin turnover in a manner dependent on Tyr944 and seemingly independent of its inositol polyphosphatase enzymatic activity. Although the physiological consequences of Tyr944 phosphorylation are as-

yet unclear, these results provide exciting justification for further characterization of this site and its contribution to SHIP function in lymphocyte signaling.



# CHAPTER 4: CONTROLLING THE INTRACELLULAR LOCALIZATION DYNAMICS OF SHIP

## 4.1 Specific Introduction

Activation of immune cells is controlled by an intricate balance of activating and inhibitory signals, which collectively direct effective immune responses while avoiding damage to self tissues. Understanding how activating and inhibitory signals are balanced requires a detailed determination of the multiple inputs controlling activity of regulatory signaling molecules. Many of the fundamental signaling pathways leading to B cell activation via the BCR have been elucidated, however the integration of activating and inhibitory signaling mechanisms are still not well understood.

The BCR signaling chains  $Ig\alpha$  and  $Ig\beta$  each contain two ITAMs that can be phosphorylated upon receptor cross-linking by the Src family kinase Lyn and, in some contexts, Syk (103, 105). Doubly phosphorylated  $Ig\alpha/\beta$  ITAMs provide binding sites for Syk, thereby initiating its activation (104). These two early signaling kinases phosphorylate a variety of target proteins, initiating multiple independent and overlapping signaling cascades, ultimately resulting in activation of the B cell (105). One key Syk-dependent pathway is the PI3K pathway. Upon BCR ligation, Syk phosphorylates CD19 and BCAP, providing binding sites at the membrane for class IA PI3K adaptor subunits (142, 158). PI3K catalytic subunits then convert the membrane lipid phosphoinositol 4,5-bisphosphate ( $PI(4,5)P_2$ ) to the second messenger phosphoinositol 3,4,5-trisphosphate ( $PI(3,4,5)P_3$ ) (147), which is of critical importance for cell proliferation, survival, antigen presentation, class switching and migration (158)

Late in the immune response, both in the context of a protective response to pathogens or a pathological response to self-antigen, complexes of antigen and previously-generated IgG are present and can co-ligate Fc $\gamma$ RIIB along with the BCR (236). This leads to phosphorylation of ITIM tyrosines in Fc $\gamma$ RIIB and subsequent recruitment of SH2 domain containing inositol-5'-phosphatase (SHIP) (239). SHIP controls the accumulation of PI3K products at the plasma membrane by converting PI(3,4,5)P<sub>3</sub> to PI(3,4)P<sub>2</sub> (150, 265). SHIP was found to mediate most of the inhibitory functions of Fc $\gamma$ RIIB in B cells (240). Together these findings established the paradigm that SHIP recruitment to the ITIM of Fc $\gamma$ RIIB is a dominant mechanism controlling SHIP activity and thus B cell activation via the PI3K pathway. Since both Fc $\gamma$ RIIB and SHIP are implicated in control of autoreactive B cells (62, 63) this regulatory circuit is critical. However SHIP is also phosphorylated and functional after triggering activating receptors such as cytokine receptors and the BCR, indicating that it can also function independently of Fc $\gamma$ RIIB (150, 265).

SHIP recruitment to the plasma membrane is required for its function in hydrolyzing PIP<sub>3</sub> substrate, and the current model predicts that inhibitory receptor engagement enhances SHIP membrane recruitment via phosphorylated ITIMs. Unexpectedly, we find here that after BCR stimulation SHIP is indistinguishably recruited to the plasma membrane in the presence or absence of Fc $\gamma$ RII co-ligation, however Fc $\gamma$ RII co-ligation impacts the mobility of engaged SHIP molecules once at the cell surface based on fluorescence recovery after photobleaching (FRAP) analysis. BCR-induced membrane recruitment requires the SH2 domain of SHIP and an intact C-terminus containing tyrosine phosphorylation sites and proline rich region, while with Fc $\gamma$ RIIB co-ligation SHIP recruitment becomes less dependent on the C-terminal region. The kinase activity of Syk is strictly required for SHIP recruitment in either stimulation context, and

for the association of SHIP with another well-characterized binding partner. Together our findings provide new insight into the regulation of SHIP by BCR and Fc $\gamma$ RIIB and identify a novel and essential role for Syk kinase as an upstream regulator of SHIP.

## **4.2 Materials and Methods**

### **4.2.1 Cell culture and reagents**

Ramos clonal cell lines expressing full length or cytoplasmic truncated Fc $\gamma$ RIIB were generated previously (388). A20 cell culture conditions are described elsewhere (205). Primary human B cells were isolated from healthy donor blood using the EasySep Direct B cell Isolation Kit (Stem Cell Technologies) and were rested 1h before manipulation. Where indicated, coverglass slides were coated with 5 $\mu$ g/ml fibronectin (FN, Sigma Aldrich) overnight at 4°C. Stimulations were performed using goat anti-human IgM or goat anti-mouse IgG antibodies (Jackson Immunolabs and Southern Biotechnology) at 10 $\mu$ g/ml (F<sub>(ab')<sub>2</sub></sub>) or 20 $\mu$ g/ml (intact). Inhibitors used were as follows: 3AC (10 $\mu$ M, Calbiochem, GDC-0980 (1  $\mu$ M, Selleck Chemicals), Bafetinib (1 $\mu$ M; Selleck Chemicals), PP2 (10 $\mu$ M; Sigma Aldrich), R406 (10 $\mu$ M; Selleck Chemicals) and GS-9973 (5 $\mu$ M; Selleck Chemicals). Vehicle controls were used at the same dilution and consisted of ethanol (Commercial Alcohols) for 3AC or DMSO (Sigma) for all others.

### **4.2.2 Plasmids and transfections**

Human SHIP-pEGFP-C1 construct was a gift from Dr M. Jücker (390). The membrane marker used was pmKate2-f-mem (Evrogen), where f-mem is a 20 amino acid farnesylation

signal from c-Ha-Ras (391). Site-directed mutagenesis was performed using the QuikChange II XL kit (Agilent Technologies). Primer sequences are as follows:

SH2 domain inactivated SHIP R31G (293):

5'-GAGCTTCCTCGTGGGTGCCAGCGAGTC-3'

5'-GACTCGCTGGCACCCACGAGGAAGCTC-3';

Phosphatase –deficient SHIP D673G (278, 392):

5'-CCTTCCTGGTGTGGCCGAGTCCTCTGG-3'

5'-CCAGAGGACTCGGCCCACACCA GGAAGG-3';

For truncated SHIP 909<sup>Trunc</sup>, a stop codon was introduced using

3'-GTGGCTCCAGCATCACTTAAATCATCAACCCCAAC-5'

3'-GTTGGGGTTGATGATTAAAGTGATGCTGGAGCCAC-5'.

All newly generated constructs were verified by sequencing (Robarts Research Institute). Transient expression of constructs was achieved using the Neon® transfection system (Invitrogen) to electroporate  $5 \times 10^6$  cells per 100  $\mu$ l reaction with 20  $\mu$ g SHIP vector and/or 10  $\mu$ g pmKate2-f-mem. Cells were cultured in antibiotic-free medium and used for experiments 18-24h post-transfection.

#### **4.2.3 Membrane recruitment experiments**

For live cell imaging experiments, transfected cells were plated at  $1 \times 10^5$ /well on uncoated (A20) or fibronectin-coated (Ramos) coverglass slides, mounted in a stage-top incubator and stimulated while imaging on a Zeiss AxioObserver spinning disk confocal microscope. For fixed cell experiments, cells were serum-starved at  $1 \times 10^6$ /ml for 3h (Ramos) or 1h (primary cells) and inhibitors were added during the final hour. Stimulations were performed in a cell culture incubator and stopped with 1-2% ice cold paraformaldehyde (PFA). Membrane

recruitment in transfected cell lines was measured by co-localization analysis in ImageJ. The Cell Outliner plugin was used to define individual cells and the Colocalization Indices plugin was used to calculate Pearson's coefficient of correlation between green and red signals. The red signal arises from the membrane marker fmem. The green signal arises from either ectopic EGFP or anti-SHIP staining using anti-SHIP (P1C1, Santa Cruz) as primary antibody at 1:200 plus goat anti-mouse Alexafluor 488 (Molecular Probes) as secondary antibody at 1:500.

Membrane recruitment in primary cells was estimated using a modification of the previously described "maximal method" (205). Briefly, for each cell the maximal intensity membrane pixel (within 2 pixels of the cell edge) is divided by the average pixel intensity of the entire cell to calculate a maximal membrane/average pixel intensity ratio.

#### **4.2.4 Statistical Analysis**

Correlation coefficient data from 10 cells per condition (live cell time courses) or 20 cells per condition (fixed cell imaging) were analyzed by ANOVA to identify any significant differences in means among multiple conditions. Post-tests for pairwise significance were applied depending on the comparison being made. For comparison of three stimulation conditions, one-way Anova with Tukey post-test was used; for comparison of multiple stimulation time points to unstimulated, non-parametric one-way Anova with Dunn's test was used; for multiple time points and two stimulation conditions, or for three stimulations conditions and two drug treatments, two-way Anova with Sidak's test was used. All calculations were performed using GraphPad Prism software. For all figures, \*=p<0.05, \*\*=p<0.01, \*\*\*=p<0.001 and \*\*\*\*=p<0.0001.

#### 4.2.5 FRAP experiments

Ibidi  $\mu$ -slides were coated with 5 $\mu$ g/ml FN plus 5 $\mu$ g/ml F<sub>(ab')<sub>2</sub></sub> or 10 $\mu$ g/ml Intact anti-IgM where indicated. Cells were serum-starved for 2-3h then plated at 2.5x10<sup>5</sup>/well and spread for 30-40min. Peripheral regions of interest were bleached with a 405nm laser (Rapp OptoElectronic), concurrent with high speed confocal imaging. Intensity values were obtained using the Time Series V3 plugin for ImageJ. To account for initial intensity differences as well as minor whole-cell photobleaching resulting from the 488nm imaging laser, intensity values within the bleached regions of interest were normalized to intensity values from an unbleached control region of the same cell. The curves were also y-transformed to (0,0) at t=0 (bleaching event) so that individual recovery curves begin at the intensity minimum. Each group of recovery curves were then fit to the following equation, with the constraint that Y<sub>0</sub>=0:

$$Y = Y_0 + (Plateau - Y_0) * (1 - e^{-K*x})$$

The rate constant (K) was derived and statistical comparisons between groups were performed using GraphPad Prism software. Two peripheral regions of interest were bleached in at least 8 cells per stimulation condition per experiment.

#### 4.2.6 Co-immunoprecipitation experiments

Equal numbers of Fc $\gamma$ RIB<sup>+</sup> Ramos cells were stimulated as indicated and lysed with 0.5% Nonidet P-40 (Thermo Fisher) lysis buffer containing protease and phosphatase inhibitor cocktails (Roche). 3 $\mu$ g specific antibody, either anti-SHIP (P1C1, Santa Cruz) or anti-Shc (PG-797, Santa Cruz), was used for immunoprecipitation with protein G sepharose beads (GE). Equal volume of precipitate was run on mini-protean 7-15% polyacrylamide precast gels (Bio-Rad) and transferred to nitrocellulose membrane (Bio-Rad). Membranes were

probed with anti-SHIP (P1C1, Santa Cruz), anti-Shc (H-108, Santa Cruz) or anti-pTyr (4G10, Millipore) primary antibody then HRP-linked goat anti-mouse IgG (Jackson) or goat anti-rabbit IgG (Cell Signaling Technologies) secondary antibody, then developed by chemiluminescence.

#### **4.2.7 Antibodies and staining**

For surface staining, FITC-conjugated anti-FcγRIIB/CD32 (BD Pharmingen), Cy3-conjugated anti-IgM (Jackson ImmunoResearch) and APC-conjugated anti-CD19 (BD Pharmingen) were all used at 1:200. For intracellular phosphoflow staining, cells were prepared at  $1 \times 10^6$ /ml in warm serum-free RPMI and starved for 3h before stimulation as indicated. Cells were centrifuged briefly for harvest, re-suspended in Fix/Perm solution (BD Biosciences), washed and finally stained with Alexafluor488-conjugated anti-phospho Syk (BD Biosciences) at 1:5 or rabbit monoclonal anti-phosphoSHIP (EPR425, Abcam) at 1:200 in combination with Alexafluor 488-conjugated donkey anti-rabbit IgG secondary antibody (BD) at 1:500. For phospho-SHIP western blot, anti-pY1020 (Cell Signaling Technologies, named for mouse sequence) was used at 1:1000.

#### **4.2.8 Lentivirus-mediated shRNA silencing**

pGIPz vector alone or coding for two distinct Shc1-targeting shRNAs (V3LHS\_319056 and V3LHS\_319060 from GE Dharmacon) were packaged and prepared as concentrated viral preparations by the University of Manitoba Lentiviral Core Facility. Ramos cells were seeded in a 24-well plate at  $5 \times 10^4$  cells/well in 0.2ml complete medium overnight. The next day, 15μl concentrated viral prep and 2μl polybrene were added to the cells and the total volume was adjusted to 300μl with medium. HEPES buffer (Gibco) was added to a final concentration of

25mM. Plates were centrifuged at 800xg for 1h at room temperature, then cells were re-suspended in 500µl fresh medium and incubated for 3 days. Transductants were selected with 1µg/ml puromycin for 24h. Transduction was verified in intact cells by flow cytometry (EGFP marker) and in cell lysates by SDS-PAGE followed by western blotting with anti-Shc1 antibody (Santa Cruz).

## 4.3 Results

### 4.3.1 SHIP is recruited to the plasma membrane after BCR stimulation with and without FcγRIIB co-engagement

Previous studies report that SHIP-mediated inhibition of PIP<sub>3</sub> and Ca<sup>2+</sup> flux is most active when FcγRIIB is co-ligated with the BCR (238, 240). SHIP is also more highly phosphorylated in its C-terminus with FcγRIIB co-ligation (302). However, the impact of co-ligation on SHIP recruitment to the plasma membrane has not been directly determined. To assess SHIP recruitment in the presence or absence of FcγRIIB we utilized human Ramos B cell lines lacking endogenous expression of FcγRIIB but transfected with either wild-type FcγRIIB or a truncation mutant lacking the ITIM motif (**Figure 4-1A-B**). As expected, co-ligation of FcγRIIB using intact anti-IgM led to increased phosphorylation of SHIP on tyrosine 1022, relative to BCR ligation alone using F<sub>(ab')<sub>2</sub></sub> anti-IgM, and this increased phosphorylation required the ITIM motif (**Figure 4-1C**, left). In contrast, phosphorylation of Syk was unaffected by FcγRIIB co-ligation (**Figure 4-1C**, right). SHIP-EGFP fusion protein also showed increased phosphorylation in FcγRIIB-expressing Ramos cells stimulated with intact anti-IgM (**Figure 4-1D**).



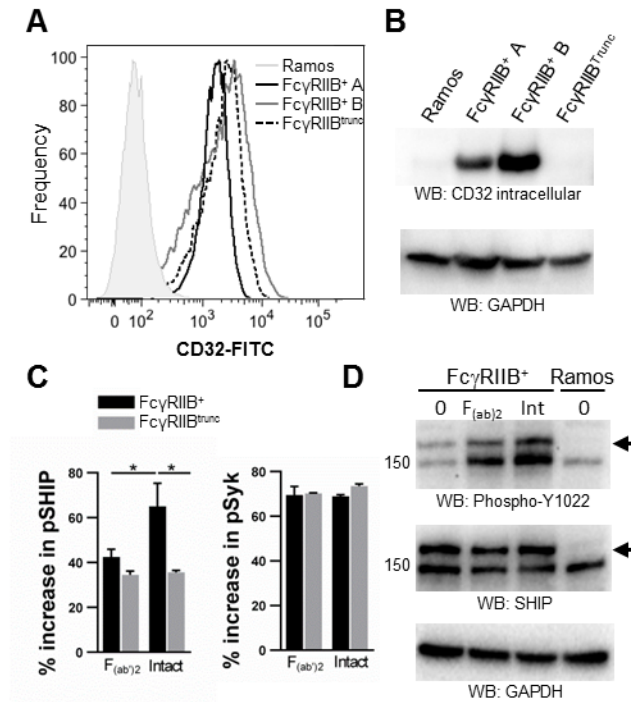


**Figure 4-1. Defining an experimental system to test the influence of  $Fc\gamma RIIB$  on BCR-induced recruitment of SHIP.**

(A-B)  $Fc\gamma RIIB/CD32B$  expression in Ramos-derived cell lines. (A) Ramos cell cultures were cell surface stained with anti-CD32 antibody and analyzed by flow cytometry. (B) Cell lysates were probed with antibody that specifically detects the C-terminus of anti-CD32B and analyzed by western blotting. Note that  $Fc\gamma RIIB^{trunc}$  is not detected with this antibody as expected. (C) Stimulation with intact anti-IgM leads to increased SHIP phosphorylation dependent on the  $Fc\gamma RIIB$  cytoplasmic tail. The indicated Ramos-derived cell lines were serum-starved then stimulated as indicated. Intracellular staining was performed for phospho-Y1022 SHIP or phospho-Y348 Syk and detection was performed by flow cytometry. Percent increase in mean fluorescence intensity relative to unstimulated cells was determined for triplicate samples. (D) SHIP-EGFP is phosphorylated on Y1022 after  $F_{(ab)2}$  and intact anti-IgM stimulation. 24h after transfection with SHIP-EGFP vector,  $Fc\gamma RIIB^+$  Ramos cells were serum-starved and stimulated for 5min with anti-IgM. Lysates were subjected to SDS-PAGE and western blotting was performed with the indicated antibodies. EGFP-tagged SHIP (upper band, arrow) and endogenous SHIP (lower band) can be distinguished by size.

In  $Fc\gamma RIIB^+$  Ramos cells, we unexpectedly found that SHIP-EGFP is significantly recruited to the plasma membrane when the BCR is ligated alone, and there is in fact no measurable difference in the magnitude of recruitment induced by  $F_{(ab)2}$  or intact anti-IgM (**Figure 4-2A**).

In addition, SHIP recruitment still occurs in Ramos cells expressing truncated FcγRIIB that lacks the ITIM-motif (**Figure 4-2B**).

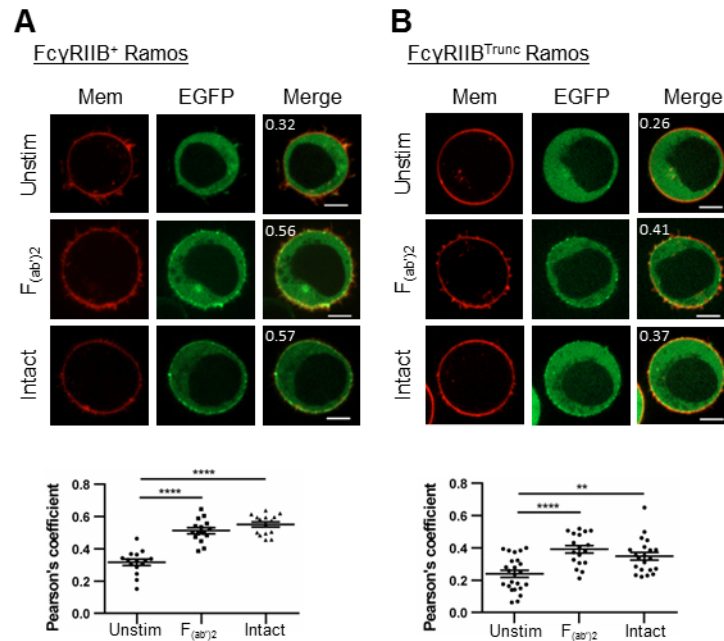


**Figure 4-2. SHIP-EGFP is recruited to the plasma membrane with BCR ligation alone or with FcγRIIB co-ligation.**

Transiently transfected FcγRIIB<sup>+</sup> (A) or FcγRIIB<sup>Trunc</sup> (B) Ramos cells expressing SHIP-EGFP and red membrane marker were serum-starved, stimulated in a cell culture incubator for 2min, fixed and imaged by confocal microscopy. Representative images and quantitation of green/red co-localization by Pearson's coefficients is shown, analyzed by one-way Anova with Tukey's multiple comparisons test for pairwise comparisons. Data are representative of at least 3 independent experiments for FcγRIIB<sup>+</sup> cells or 2 for FcγRIIB<sup>Trunc</sup> cells, with 20 cells per group. Scale bars indicate 5μm.

We examined whether FcγRIIB co-ligation impacted the kinetics of SHIP membrane recruitment. Live cell imaging of FcγRIIB<sup>+</sup> Ramos co-expressing SHIP-EGFP and a red fluorescent membrane marker indicated that recruitment occurs within the first minute of stimulation with either F<sub>(ab)<sup>2</sup></sub> or intact anti-IgM and did not reveal any significant differences between these stimuli (**Figure 4-3A**). A similar analysis was conducted in murine A20 cells, which express IgG BCR and endogenous FcγRIIB and are an established model for inhibitory

signaling (273). A20 cells also did not show significant differences in the magnitude or kinetics of SHIP recruitment (*Figure 4-3B*).

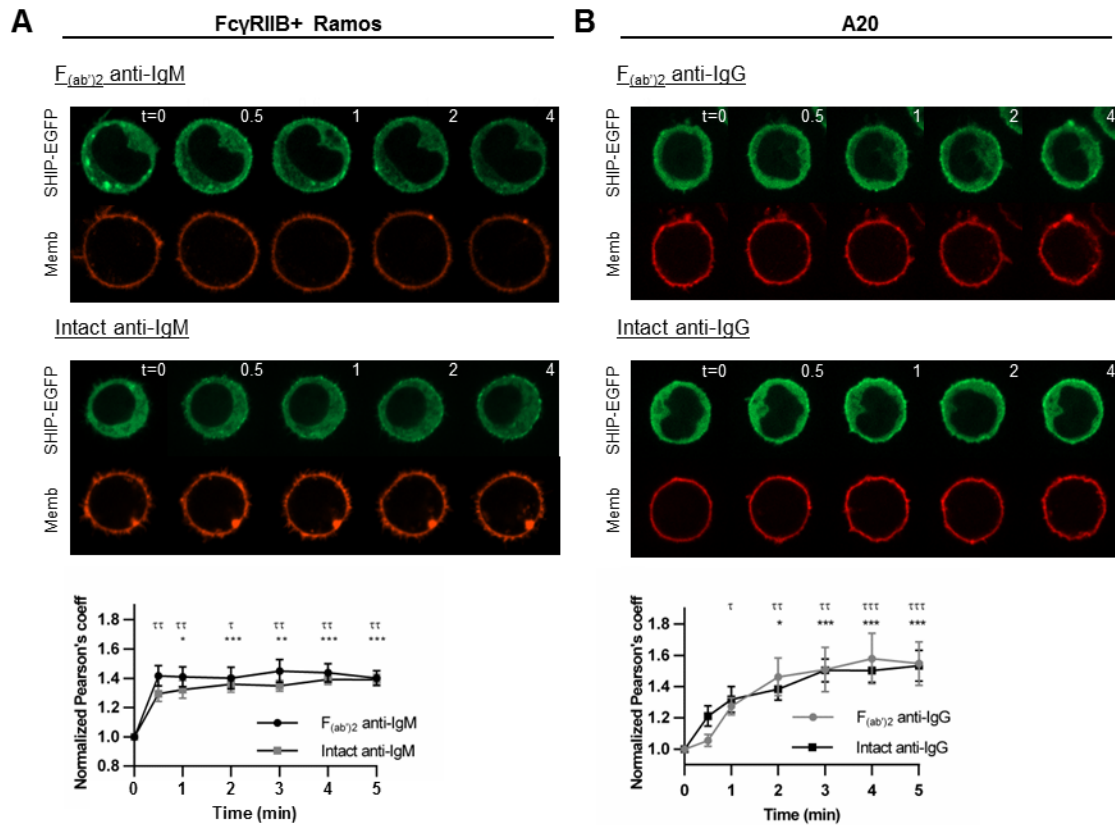


**Figure 4-3. Kinetics of SHIP-EGFP membrane recruitment in live cells.**

(A)  $Fc\gamma RIIB^+$  Ramos cells or (B) A20 cells were transiently transfected with plasmids encoding SHIP-EGFP plus a red fluorescent membrane marker and stimulated with anti-Ig while imaging in a stage-top incubator. Graphs show change in SHIP membrane localization over time, expressed as average Pearson's correlation coefficient of 10 cells per condition (normalized to time 0). Significance relative to pre-stimulation, as assessed by Dunn's test is indicated by \* (Intact) or  $\tau$  ( $F_{(ab')_2}$ ). Two-way ANOVA did not reveal any significant difference between  $F_{(ab')_2}$  and Intact anti-Ig.

We further examined membrane association of endogenous SHIP detected by intracellular staining and colocalization with a membrane marker and found results consistent with those using SHIP-EGFP (*Figure 4-4A*). Examination of primary human B cells also revealed that

BCR stimulation alone triggers membrane recruitment of SHIP that is indistinguishable from that induced in the presence of Fc $\gamma$ RIIB co-ligation (*Figure 4-4B*). Together these results indicate that neither expression nor engagement of Fc $\gamma$ RIIB are essential for SHIP accumulation at the plasma membrane during B cell activation, counter to the prevailing paradigm.

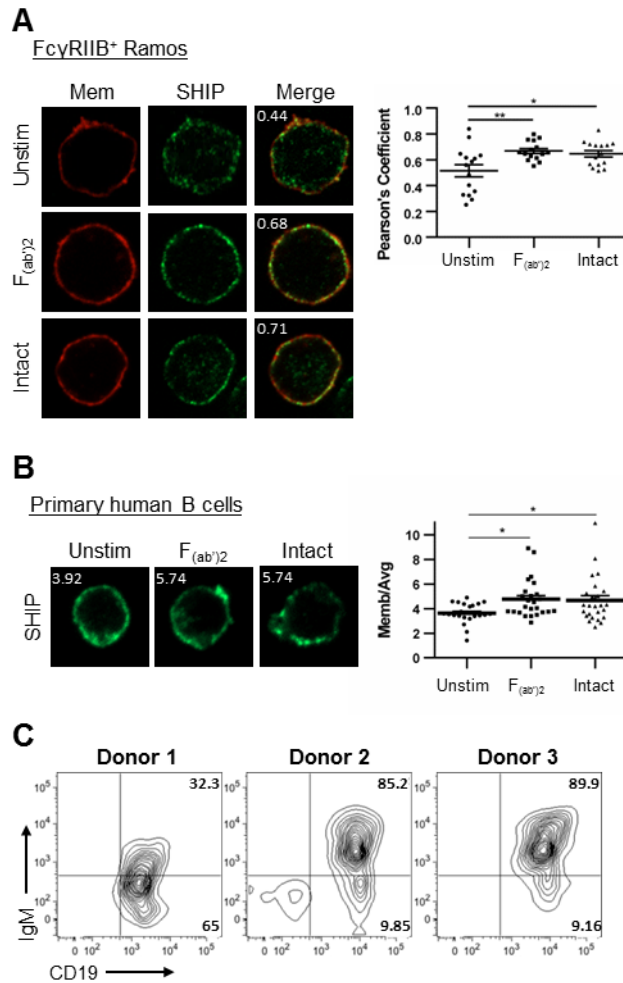


**Figure 4-4. Endogenous SHIP is recruited to the plasma membrane after BCR ligation with or without FcyRIIB co-ligation.**

(A) FcyRIIB<sup>+</sup> Ramos cells transfected with membrane marker only were serum-starved, stimulated, fixed, permeabilized and stained with anti-SHIP Ab. Representative images and quantitation of green/red co-localization by Pearson's coefficients is shown, analyzed by one-way ANOVA with Tukey's multiple comparisons test for pairwise comparisons. (B) Primary human B cells were enriched from healthy donor blood and serum-starved prior to stimulation, fixation and staining with anti-SHIP antibody. Membrane recruitment of SHIP was calculated as the ratio of maximal membrane intensity to average fluorescence (Memb/Avg) in each cell and statistical differences were calculating by one-way ANOVA with Tukey's test. Images and analysis are representative of at least 3 independent experiments with 20 cells per group. (C) Analysis of B cell population purified from three human donors. Fluorophore-conjugated anti-IgM and anti-CD19 antibodies were used for cell surface staining ex-vivo.

### 4.3.2 Mobility of SHIP-EGFP is altered by stimulation

While BCR ligation appears sufficient to recruit SHIP to the plasma membrane, Fc $\gamma$ RIIB co-ligation can impact SHIP phosphorylation and activity (238, 240). We thus speculated that engagement of this inhibitory receptor may allow SHIP to enter into functionally distinct protein complexes at the membrane. One measurable parameter that can be influenced by signaling complex formation is dynamic protein mobility or diffusion rate. We employed FRAP to determine whether stimulation conditions alter the mobility of SHIP-EGFP molecules at the cell periphery. We bleached regions of interest and subsequently monitored the fluorescence recovery over time. By curve fitting, rate constants were derived for the recovery, reflective of how quickly the molecules redistribute within the bleached area. Our results in Fc $\gamma$ RIIB<sup>+</sup> Ramos B cells indicate that the mobility of SHIP-EGFP is significantly reduced when cells are stimulated with intact anti-IgM relative to F<sub>(ab')<sub>2</sub></sub> anti-IgM (**Figure 4-5B**). This difference was not seen in Fc $\gamma$ RIIB<sup>Trunc</sup> Ramos cells (**Figure 4-5C**).

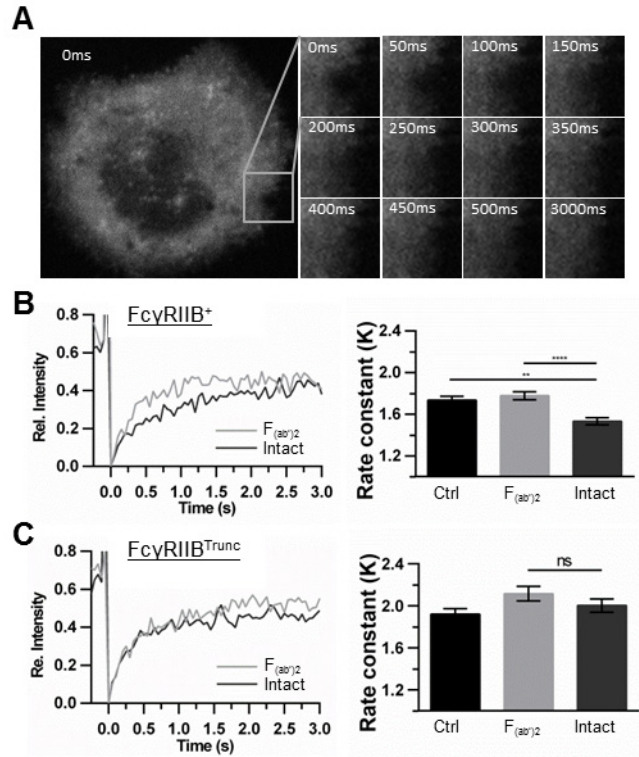


**Figure 4-5. Fluorescence recovery after photobleaching analysis of SHIP-EGFP.** *FcγRIIB*<sup>+</sup> or *FcγRIIB*<sup>Trunc</sup> Ramos cells transiently transfected to express SHIP-EGFP were plated on either *F*<sub>(ab)<sup>2</sup></sub> or Intact anti-IgM for 30-40min before photobleaching of peripheral regions of interest. (A) Representative images showing recovery from bleaching over time. (B) FRAP analysis of *FcγRIIB*<sup>+</sup> Ramos cells. Left panel shows example recovery curves and right panel shows quantification of rate constants pooled from four experiments (100-120 bleaching events total). (C) FRAP analysis of *FcγRIIB*<sup>Trunc</sup> cells. Right panel shows data pooled from two experiments (50-60 bleaching events total). Rate constants and *p* values were obtained by nonlinear regression analysis.

### 4.3.3 Dependence of SHIP membrane recruitment on protein interaction motifs

We tested the sensitivity of the membrane recruitment process to disruption of key elements of SHIP structure (**Figure 4-6**). It was found that a functional SH2 domain is required for SHIP membrane recruitment irrespective of *FcγRIIB* co-ligation, as SH2 mutated (SH2mut) SHIP is not significantly recruited to the plasma membrane. (**Figure 4-6B,C**). A phosphatase-

deficient mutant was recruited normally (**Figure 4-6B,D**). Interestingly, a C-terminal truncation mutant failed to be recruited upon stimulation with  $F_{(ab)2}$  Ab, but could be recruited after intact Ab stimulation (**Figure 4-6B,E**). This differential effect was not observed in cells expressing truncated  $Fc\gamma RIIB$  lacking the ITIM motif; In these cells, truncated SHIP failed to be recruited under either stimulation condition (**Figure 4-6F**). Mutagenesis of Y1022, the best-characterized pTyr in the SHIP C-terminal domain, revealed that this tyrosine is not essential for membrane recruitment (**Figure 4-6G**). These results suggest that tyrosines other than Y1022, or other motifs in the C-terminal region, can play a role together with the SH2 domain in facilitating BCR-induced SHIP recruitment.



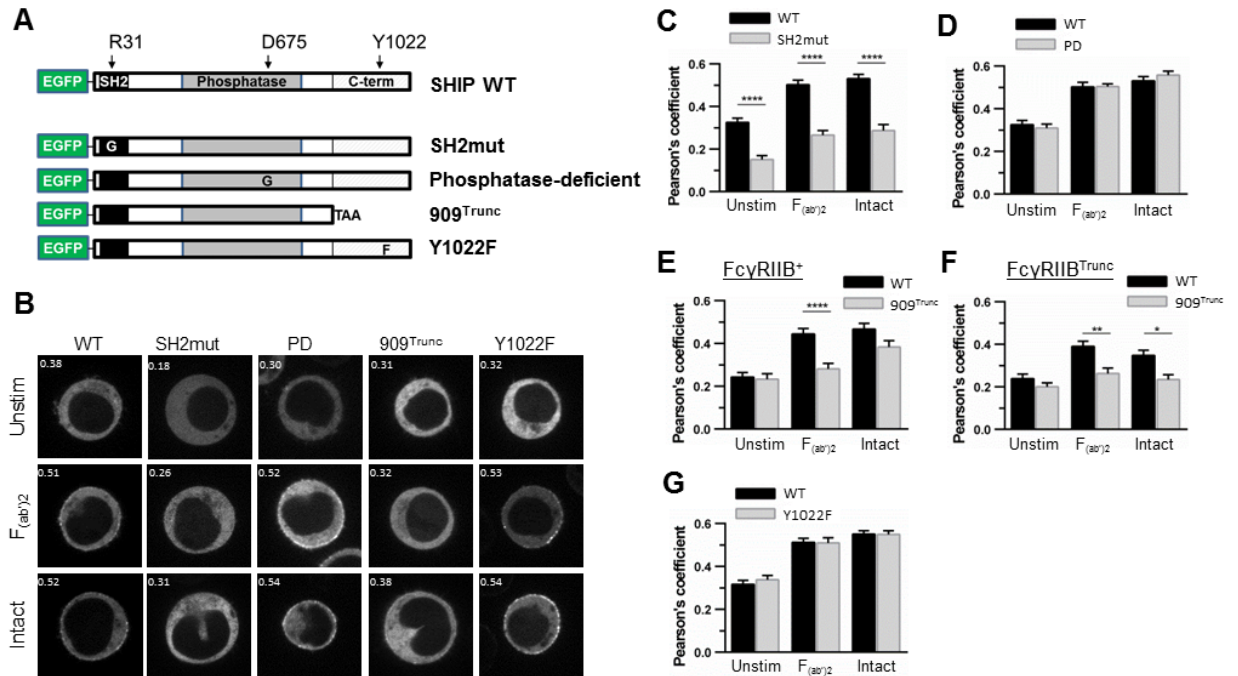


**Figure 4-6. Structural requirements for SHIP-EGFP membrane recruitment.**

(A) Schematic of fusion proteins derived from SHIP-EGFP vector by site-directed mutagenesis. (B)  $Fc\gamma RIIB^+$  Ramos cells expressing membrane marker plus WT or mutant SHIP-EGFP, as indicated, were serum-starved, stimulated, fixed and imaged by confocal microscopy. The SHIP-EGFP images and Pearson's correlation coefficient of representative cells are shown. Quantitation is shown for (C) SH2 mutant (D) phosphatase-deficient (PD) mutant, (E) C-terminal truncation (909<sup>Trunc</sup>) mutant or (G) Y1022F mutant SHIP-EGFP. (F) 909<sup>Trunc</sup> mutant expressed in  $Fc\gamma RIIB^{Trunc}$  Ramos cells. Statistical analyses were performed by two-way ANOVA with Sidak's multiple comparisons test. Data are representative of at least 3 independent experiments for  $Fc\gamma RIIB^+$  cells or 2 for  $Fc\gamma RIIB^{Trunc}$  cells, with 20 cells per group.

#### 4.3.4 Dependence of SHIP membrane recruitment on upstream kinases

We next examined whether SHIP recruitment is influenced by its own activation state or requires activation of Syk, Src or PI3K kinases (**Figure 4-7**). Neither the SHIP inhibitor 3AC (**Figure 4-7A,B**) nor the pan-PI3K inhibitor Apatolisib (GDC-0980, **Figure 4-7A,C**) had any effect, suggesting that binding to phosphoinositides or PI-binding proteins are not essential for SHIP recruitment. Unexpectedly, membrane association of SHIP was not strongly inhibited by the potent Lyn inhibitor Bafetinib or by the pan-Src kinase inhibitor PP2, even in the

presence of Fc $\gamma$ RIIB co-ligation (**Figure 4-7A,D**). However, pre-treatment with the Syk kinase inhibitor Fostamatinib (R406) strongly inhibited membrane recruitment of SHIP-EGFP in Fc $\gamma$ RIIB<sup>+</sup> Ramos cells (**Figure 4-7A,E**). Similar results were obtained using a distinct Syk inhibitor Entospletinib (GS-9973; **Figure 4-7F**). While Syk inhibition significantly reduced membrane recruitment with either F<sub>(ab)2</sub> or intact anti-IgM stimulation, we noted a trend of decreased percent inhibition under the latter condition (**Figure 4-7G**).

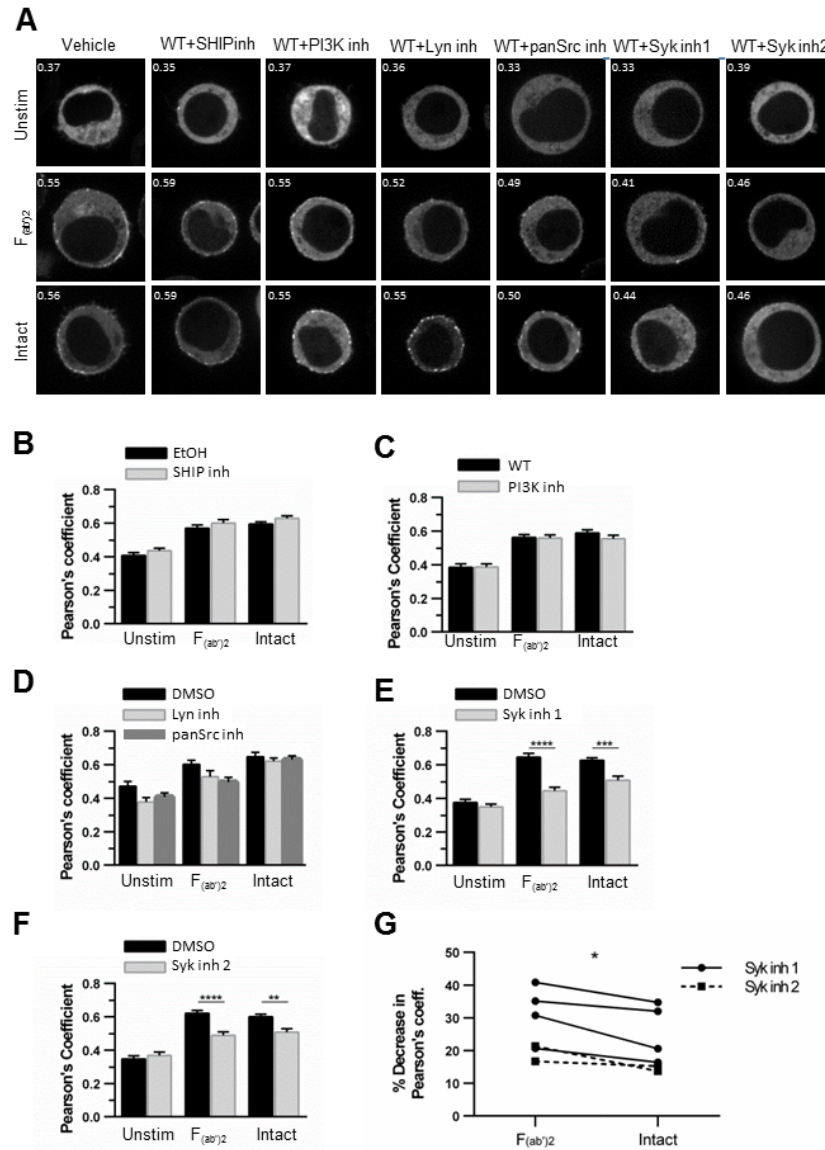


**Figure 4-7. Signaling requirements for SHIP-EGFP membrane recruitment.** (A)  $Fc\gamma RIIB^+$  Ramos cells expressing membrane marker plus WT SHIP-EGFP were serum-starved, pre-incubated with inhibitors, stimulated as indicated, then fixed and imaged. SHIP-EGFP images and Pearson's correlation coefficient of representative cells are shown. Quantitation of Pearson's coefficient is shown for (B) SHIP phosphatase inhibitor 3 alpha-aminocholestane (3AC), (C) PI 3-kinase inhibitor Apatolisib (GDC-0980), (D) Lyn inhibitor Bafetinib or pan-Src kinase inhibitor PP2, (E) Syk inhibitor 1 Fostamatinib (R406), (F) Syk inhibitor 2 Entospletinib (GS-9973). Statistical analyses were performed by two-way ANOVA with Sidak's multiple comparisons test. Data are representative of at least 3 independent experiments with 20 cells per group. (G) Comparison of the effect of Syk inhibitor on SHIP-EGFP membrane localization induced by  $F_{(ab)2}$  versus intact anti-IgM stimulation, assessed by non-parametric paired t-test. Percent decrease in Pearson's coefficient relative to DMSO control was calculated for 4 experiments with R406 (Syk inh 1) and 2 experiments with GS-9973 (Syk inh 2).

Syk inhibition also blocked membrane recruitment of endogenous SHIP in both Fc $\gamma$ RIIB<sup>+</sup> Ramos cells (**Figure 4-8A**) and primary human B cells (**Figure 4-8B**). Together these results identify a novel role for Syk kinase activity in recruitment of SHIP to the membrane of human B cells.

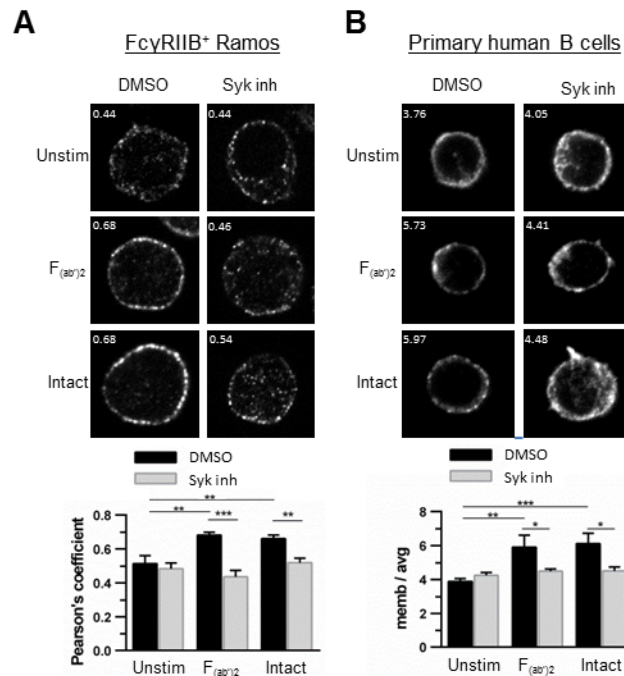


**Figure 4-8. Syk inhibition prevents membrane recruitment of endogenous SHIP.**

(A) Fc $\gamma$ RIIB<sup>+</sup> Ramos cells expressing red membrane marker were serum-starved, pre-incubated with Syk inhibitor R406, then stimulated, fixed and stained for endogenous SHIP. Example images and co-localization analysis are representative of 3 independent experiments with 20 cells per group. (B) Primary human B cells derived from healthy donor blood were serum-starved, pre-incubated with Syk inhibitor R406, then stimulated, fixed and stained for endogenous SHIP. Example images and maximal method analysis are representative of 3 donors with 20 cells per group for each donor. Statistical analyses between treated and untreated groups were performed by two-way ANOVA with Sidak's multiple comparisons test.

#### 4.3.5 Syk activity is required for phosphorylation and association of SHIP with Shc

Stimulation with intact anti-Ig induces a robust interaction between SHIP and the adaptor protein Shc1 (136, 301). Here, we report that F<sub>(ab')<sub>2</sub></sub> anti-Ig induces a comparable interaction

detected by reciprocal co-immunoprecipitation (**Figure 4-9A**). Interestingly, pre-treatment with the Syk inhibitor R406 abrogates the interaction between SHIP and Shc and substantially reduces the total tyrosine phosphorylation of both proteins (**Figure 4-9C**). A second Syk inhibitor, GS-9973, had a similar effect (**Figure 4-9D**). Phospho-flow cytometry confirms that inhibition of Syk significantly reduces SHIP phosphorylation at Y1022; however this inhibition appears incomplete in the presence of Fc $\gamma$ RIIB co-ligation (**Figure 4-9B**). Inhibition of Src family kinases, which are directly responsible for phosphorylating Y1022 (299, 300), abrogated phosphorylation (**Figure 4-9B**). Together these results suggest that Syk activity is required for SHIP to form a complex with Shc and facilitates SHIP phosphorylation by Src kinases at the plasma membrane.

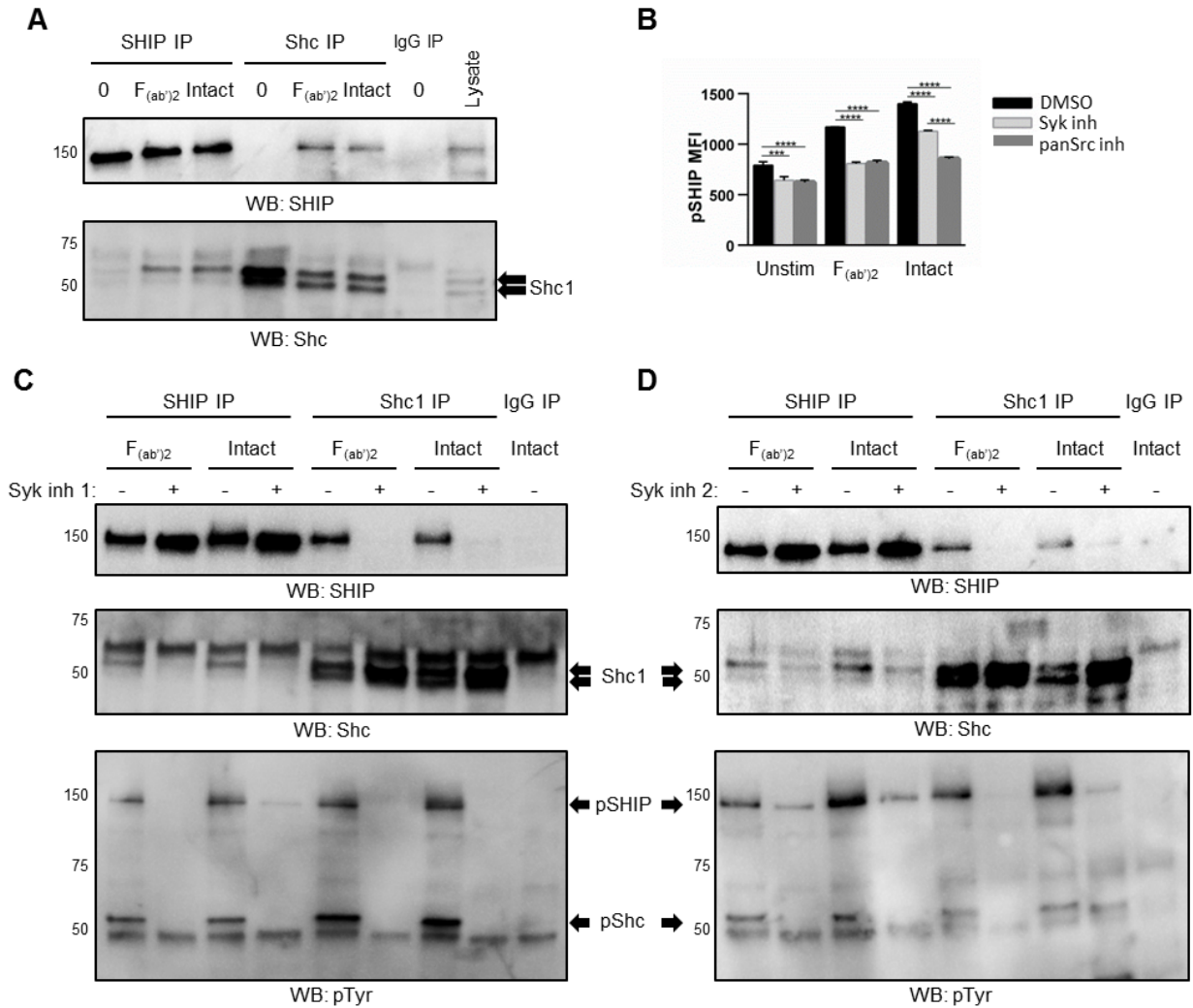


**Figure 4-9. Syk inhibition prevents SHIP phosphorylation and association with Shc1.**

(A) *FcγRIIB*<sup>+</sup> Ramos cells were serum-starved, stimulated for 5min with the indicated anti-IgM antibody, lysed, and subjected to co-immunoprecipitation with specific antibody or isotype control. Eluates were separated by SDS-PAGE and western blotting was performed with the indicated antibodies. (B) *FcγRIIB*<sup>+</sup> Ramos cells were serum-starved, pre-treated with Syk inhibitor R406 or Src family kinase inhibitor PP2 then stimulated for 5min, fixed, stained for intracellular phospho-SHIP (Y1022) and analyzed by flow cytometry. Quantitation is based on triplicate samples. (C-D) Cells were pre-treated with Syk inhibitor 1 R406 (C) or Syk inhibitor 2 GS-9973 (D) prior to stimulation and protein extracts analyzed as above. Blots are representative of 3 experiments for C and two experiments for D.

### 4.3.6 A lower stimulation threshold is required for SHIP membrane recruitment compared to SHIP phosphorylation

Most previous studies use a standard dose of 10 $\mu$ g/ml (F<sub>(ab')2</sub>) or 20 $\mu$ g/ml (Intact) anti-IgM for *in vitro* B cell stimulation (241, 393), an equimolar ratio of the two antibodies. Some studies use even higher doses (298, 302). In a preliminary experiment, we found that a 10x lower dose of anti-BCR antibody (“low anti-IgM”) resulted in the same magnitude of SHIP-EGFP membrane recruitment as the standard dose (“high anti-IgM”, **Figure 4-10A**). However, low dose stimulation was not able to induce SHIP phosphorylation at Tyr1020 (**Figure 4-10B**). This suggests that the two events - recruitment and phosphorylation - are uncoupled in the context of weak BCR stimulation.

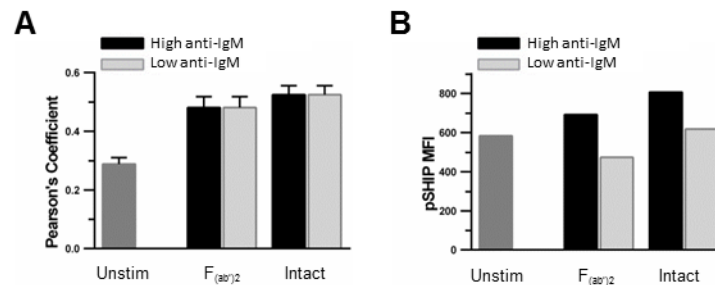


**Figure 4-10. Low dose anti-BCR stimulation is sufficient for SHIP membrane recruitment but not phosphorylation.**

(A) Fc $\gamma$ RIIB<sup>+</sup> Ramos cells expressing membrane marker plus WT SHIP-EGFP were serum-starved, stimulated for 2min, fixed and imaged by confocal microscopy. Quantitation of Pearson's coefficient was performed for 15 cells per group in one experiment. Two-way ANOVA with Sidak's multiple comparisons test revealed no difference between high and low dose anti-IgM. (B) Fc $\gamma$ RIIB<sup>+</sup> Ramos cells were serum-starved and stimulated for 5min, then intracellular staining was performed using anti-SHIP phospho-Y1022 primary antibody and Alexafluor488-conjugated secondary antibody. MFIs were measured by flow cytometry.

#### **4.3.7 Reducing Shc1 expression has no measurable impact on SHIP membrane recruitment**

As we observed, SHIP membrane recruitment is dependent on Syk kinase activity. Since the interaction between SHIP and Shc1 is also Syk-dependent, we wanted to determine if this complex is in fact required for directed localization of SHIP in B cells. Thus, we used lentivirus-mediated shRNA silencing to reduce Shc1 protein levels in Ramos cells (*Figure 4-11A*). Compared to empty vector control, Shc1 knockdown had no measurable effect on SHIP membrane localization (*Figure 4-11B*). Since the inception of this study, three distinct mechanisms that were predicted to contribute significantly to SHIP membrane recruitment failed to be identified as important in our experiments. These were: a) phosphorylation of ITIMs and/or ITAMs by Src family kinases, b) PIP<sub>3</sub> levels and c) interaction with Shc1. In light of this we reasoned that the contributions of these mechanisms might be partially redundant, making ablation of one of them alone insufficient to cause mis-localization of SHIP. Thus, we tested their redundancy by combining Src and PI3K pharmacological inhibitors in an FcγRIIB-deficient system with reduced Shc1 expression. Still we found no measurable effect on SHIP membrane recruitment (*Figure 4-11C*).



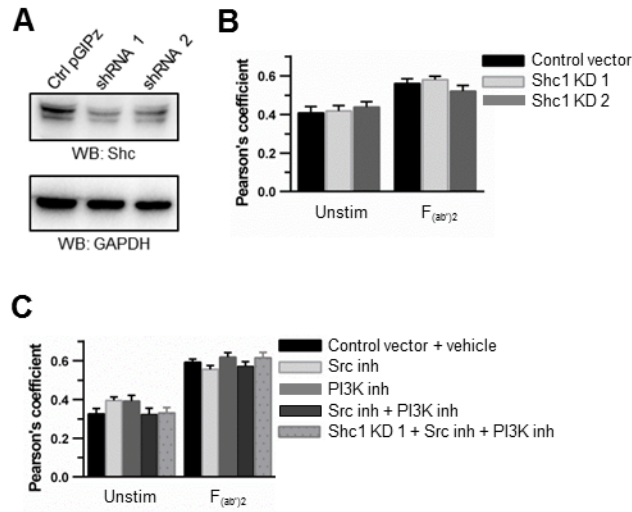


**Figure 4-11. Knockdown of *Shc1* has no measurable effect on SHIP membrane recruitment.**

(A) Ramos cells were transduced with control lentivirus or lentivirus encoding two distinct shRNA constructs targeting *Shc1*. SDS-PAGE and western blotting was performed to verify *Shc1* knockdown. (B) Transduced cells were transfected with red fluorescent membrane marker, serum-starved, stimulated for 2min, then stained with anti-SHIP primary antibody and Alexafluor647-conjugated secondary antibody. Co-localization analysis was performed to calculate overlap of SHIP signal with membrane marker and is representative of two independent experiments with 20 cells per group. (C) Parental or *Shc1* knockdown Ramos cells were transfected with membrane marker, serum-starved, pre-incubated for 1h with the indicated pharmacological inhibitor(s), then stimulated for 2min and stained as above. Co-localization analysis was performed for one experiment. Two-way ANOVA with Sidak's multiple comparison test revealed no significant differences between control and any of the knockdown/treatment groups.

## 4.4 Discussion

Engagement of Fc $\gamma$ RIIB provides a critical control mechanism to attenuate B cell activation in the presence of antigen complexed with pre-existing IgG antibody. This feedback circuit plays essential roles in preventing inappropriate activation and preventing autoimmunity and immune complex mediated inflammatory disease (323, 394, 395). SHIP is also strongly implicated in control of autoreactive B cells and inflammation (63), and this is most often attributed to its role as mediator of Fc $\gamma$ RIIB inhibitory signaling. Our results demonstrate that in the absence of Fc $\gamma$ RIIB involvement BCR ligation alone can trigger robust membrane recruitment of SHIP via protein-protein interactions driven by Syk. These results are consistent with a model where SHIP is directly recruited by the BCR and acts primarily as an intrinsic brake on BCR signaling, and can secondarily be modulated by Fc $\gamma$ RIIB - and likely other receptors as well. Indeed this example of a negative signal initiated from an activating receptor is one of several recent challenges to the elegant but simplistic ITAM-ITIM dogma (98, 396). Other activating receptors have been found to recruit SHIP (289, 397).

The established model for SHIP membrane recruitment and activation predicts the central importance on the Src family kinase Lyn, which can phosphorylate the ITIM motif on Fc $\gamma$ RIIB that binds to the SHIP SH2 domain (398, 399). However our results indicate that activity of this kinase is dispensable for SHIP recruitment after BCR or BCR/Fc $\gamma$ RIIB ligation, while inhibition of Syk abrogates membrane recruitment of SHIP under these conditions. We determined that the Src family kinase inhibitors were indeed functional as they were able to prevent stimulation-induced phosphorylation of known target SHIP Tyr1022. We saw that weak BCR stimulation (low dose anti-IgM) is sufficient to induce membrane recruitment but not phosphorylation of

SHIP. It would be useful to test whether there is a differential requirement for Syk/Src family kinases for the induction of SHIP membrane recruitment at low versus high dose stimulation conditions.

Conceptually these results indicates that the “activating kinase” Syk rather than the “inhibitory kinase” Lyn can serve as the primary driver of SHIP membrane recruitment in human B cells. Mechanistically, this result could be interpreted in several ways. As Syk is upstream of PI3K (142), the requirement for Syk activity might reflect a requirement for either PI(3,4,5)P<sub>3</sub> or PI(3,4)P<sub>2</sub> as an alternate ligand for plasma membrane docking. Indeed SHIP contains a pleckstrin homology-related domain that is required for localization to the phagocytic cup of RAW264.7 macrophages (296) and a C2 domain that can interact with its own lipid product to promote enzymatic activity via an allosteric positive feedback mechanism (279). However, we found that inhibition of PI3K or SHIP enzymatic activity had no effect on BCR-induced SHIP membrane recruitment, arguing against this mechanism. Alternatively, Syk might be responsible for phosphorylation of a SHIP binding partner that is required for its recruitment to, or retention at, the plasma membrane.

The latter hypothesis led us to test the sensitivity of known interactions to Syk inhibition. We focused on Shc1 since previous studies report an inducible association with SHIP upon ligation of various receptors (400) and that its phosphorylation is impaired in the absence of Syk (401). We found that pre-treatment with Syk inhibitor abrogates the anti-IgM-induced interaction between SHIP and Shc1. However, a partial knockdown of Shc1 had no measurable impact on BCR-mediated SHIP recruitment. Furthermore, global tyrosine phosphorylation of both SHIP

and Shc1 is substantially reduced in the presence of Syk inhibitor. This may to some extent reflect direct phosphorylation by Syk, which has been reported previously for Shc1 (402). We also found that phosphorylation of SHIP at Y1022 is blocked by both Syk and Src kinase inhibitors. As Lyn or other Src family kinases are directly responsible for phosphorylating Y1022 (299, 300), this result is consistent with a model where Syk-dependant translocation of SHIP to the membrane is prerequisite to phosphorylation by membrane-associated Src family kinases.

Our structure-function analysis indicates that BCR induced SHIP recruitment requires both its SH2 domain and its C-terminal domain. The latter contains NPxY motifs at Y917 and Y1022, PxxP motifs, and several other poorly characterized tyrosine phosphorylation sites. Any or all of these sites might contribute to interaction with membrane-proximal signaling complexes. The SHIP SH2 domain was reported to bind directly to Ig- $\alpha$  (403); however an intramolecular and/or oligomeric interaction between SHIP's SH2 domain and its C-terminus was also found to compete for Ig- $\alpha$  binding (403). Thus, it is possible that direct recruitment of SHIP to the BCR complex may require disengagement of SHIP's SH2 domain from its C-terminus, and perhaps engagement of the C-terminus with other binding partners could promote such disengagement. The identity of the key binding partner(s) eludes us still as Shc1 appears not to contribute, at least in preliminary experiments. Three alternate models of SHIP membrane recruitment that are consistent with our data are depicted in **Figure 4-12**. According to our experiments, both the SH2 domain and C-terminus of SHIP are required, Syk is required either for phosphorylation of binding partner(s) or as a binding partner itself (371), and PIP<sub>3</sub> and PI(3,4)P<sub>2</sub> contribute minimally or not at all in this context.

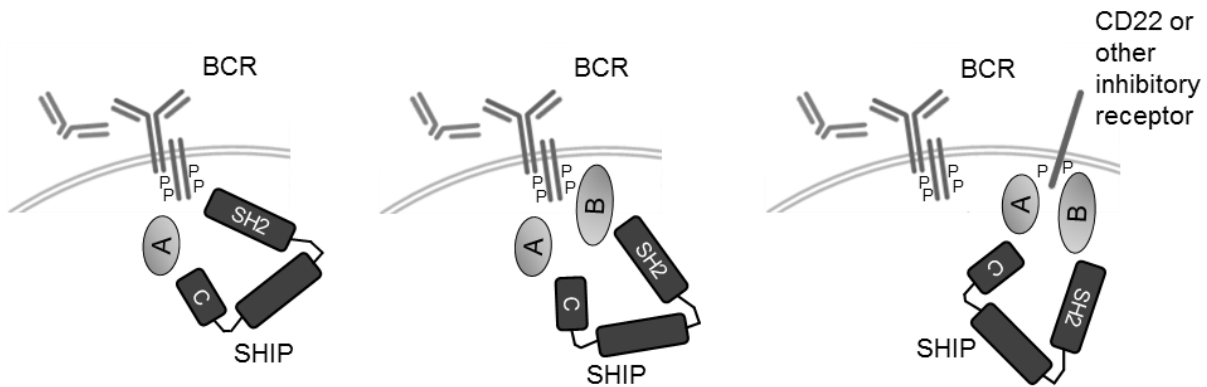


**Figure 4-12. Visualizing BCR-mediated SHIP recruitment.**

*The SH2 domain of SHIP can bind directly to BCR ITAMs or might be bridged to the BCR via an interaction partner. Alternatively, it may be bridged to an inhibitory receptor such as CD22 that can associate closely with the BCR. In all cases, a C-terminal binding partner is additionally required.*

Our data indicate that co-ligation of Fc $\gamma$ RIIB modulates BCR-induced SHIP recruitment such that it becomes less dependent on C-terminal interactions and immobilized to a greater degree. The most straightforward interpretation of these results is that SHIP preferentially binds to phospho-ITIMs when they are available, and this promotes SHIP interaction with distinct protein complexes that promote increased phosphorylation on Y1022 and increased or prolonged enzymatic activity. Our finding that Fc $\gamma$ RIIB co-ligation decreases mobility of SHIP-EGFP is consistent with inhibitory receptor driving formation of distinct membrane associated protein complexes. Surprisingly, SHIP recruitment, phosphorylation and interaction with Shc1 remains dependent on Syk activity with co-ligation of Fc $\gamma$ RIIB, suggesting an “upstream” requirement for Syk in generation of both activating and inhibitory signaling complexes.

Since modulation of SHIP activity by Fc $\gamma$ RIIB cannot be explained by an increase in access to phosphoinositide substrate at the plasma membrane, more subtle regulatory mechanisms must be at play to control the activities of this key enzyme. One current model of SHIP recruitment to

the membrane after BCR/ Fc $\gamma$ RIIB co-ligation describes the formation of a stable tri-molecular complex containing Fc $\gamma$ RIIB, SHIP and Grb2 and/or GRAP in murine B cells (298). In human B cells, Grb2 and GRAP are dispensable but an as-yet unidentified interaction partner that bridges the C-terminus of Fc $\gamma$ RIIB to the C-terminus of SHIP is proposed to exist (240). We were unable to detect SHIP/Grb2 interaction and found that the C-terminal region of SHIP is less critical for recruitment in the case of BCR/Fc $\gamma$ RIIB co-ligation of human B cells, suggesting that this complex may not have a major role in the human B cell context, however we cannot rule out the possibility. While our data suggests that this region is more quantitatively significant for SHIP membrane targeting upon BCR ligation alone, it remains possible that the C-terminus is also engaged in protein interactions within the inhibitory signaling complex that are important for control of enzymatic activity. Indeed previous studies demonstrated reduced functionality of C-terminally truncated SHIP (297). The best characterized tyrosine phosphorylation site within the C-terminus of SHIP, Y1022, is clearly phosphorylated to a greater extent with BCR/Fc $\gamma$ RIIB co-ligation, perhaps indicating that the inhibitory complex is more accessible to Lyn, which phosphorylates this site. However, the functional role of Y1022 is unclear, and we find that mutation of this tyrosine has no effect on membrane recruitment.

Given its established ability to control autoimmune and inflammatory reactions, SHIP is an attractive drug target (280, 404), highlighting the need to further define mechanisms controlling SHIP activity. Together our results refine the classical paradigm for modulation of SHIP activity by inhibitory receptor and suggest that SHIP might be more accurately viewed as an intrinsic regulator of immunoreceptor signaling whose recruitment is intimately associated with engaged ITAM-bearing receptors.

## CHAPTER 5: GENERAL DISCUSSION

### 5.1 Summary of findings

The data presented in this thesis informs several novel aspects of the molecular regulation and function of SHIP in B cells. First, potential interaction partners of SHIP were examined using both unbiased bioinformatics prediction tools and an *in vitro* candidate screening approach. Several novel partners were identified. The list included Nck, revealed by both methods. The interaction was mapped to the SH2 domain of Nck and phospho-Tyr944 of SHIP. The dissociation constant was measured by affinity analysis and revealed to be approximately equal to the dissociation constant of a well-characterized interaction between SHIP SH2 and Fc $\gamma$ RIIB ITIM phosphopeptide.

Next, I examined the function of SHIP Y944 with respect to regulation of the actin cytoskeleton. Endogenous SHIP derived from stimulated B cell lysates was demonstrated to interact with recombinant Nck. Further experiments in stable cell lines overexpressing WT or Y944F SHIP-EGFP supported a requirement for BCR engagement and for Y944. In a FRAP assay which measures actin dynamics, transient overexpression of WT but not Y944F SHIP-EGFP in Ramos cells resulted in a reduced rate of tagged actin turnover. The reduction could be overcome by co-overexpression of Nck. The defect demonstrated with mutation of Tyr944 is likely not due to a defect in enzymatic activity or membrane recruitment, supporting instead a role for Nck binding. I present a model whereby SHIP binding to Nck disrupts the recruitment of Nck into signaling complexes, where it normally serves to promote the function of actin nucleation promoting proteins.

Finally, I use confocal imaging techniques to examine the mechanisms controlling subcellular localization dynamics of SHIP after ligation of the BCR with or without co-ligation of Fc $\gamma$ RIIB, an inhibitory receptor and a well-known SHIP interaction partner. The data demonstrates that SHIP is recruited to the plasma membrane after stimulation, however contrary to expectation recruitment is not measurably enhanced by co-ligation of Fc $\gamma$ RIIB with the BCR. We confirm this unforeseen finding by meticulous testing, carefully validating stimulation antibodies obtained from distinct sources, examining both SHIP-EGFP and endogenous SHIP in multiple independently repeated experiments, and testing two cell lines as well as primary cells. Since previous studies have extensively demonstrated a role for Fc $\gamma$ RIIB in promoting the inhibitory function of SHIP, at least with respect to PIP<sub>3</sub> hydrolysis and Ca<sup>2+</sup> flux (238, 240), we propose that Fc $\gamma$ RIIB does so not by enhancing the overall recruitment of SHIP to the membrane but rather by recruiting SHIP into distinct signaling complexes. This model is supported by FRAP experiments demonstrating an effect of Fc $\gamma$ RIIB co-ligation on the dynamic mobility of SHIP-EGFP molecules at the cell periphery. Further experiments assess which structural elements in SHIP and which upstream signals are required for SHIP recruitment after BCR stimulation with or without Fc $\gamma$ RIIB co-ligation. I demonstrate that the SH2 domain of SHIP is required in both cases, as is the kinase activity of Syk. Syk activity is also required for interaction of SHIP with known binding partner Shc1 and for phosphorylation of both SHIP and Shc1. The C-terminus of SHIP is required for BCR-induced recruitment but has no statistically significant role in the case of co-ligation. Phosphoinositide moieties produced upon stimulation appear to have no role, as neither inhibition of PI3K activity nor disruption of SHIP activity by mutagenic and pharmacological means had any effect on SHIP localization. The precise identity of SHIP



binding partner(s) required for association with membrane-proximal signaling complexes in the context of BCR ligation alone is still under investigation.

## **5.2 Impact and implications**

This thesis examines the regulation and function of SHIP in B cells and the role of specific structural elements and binding partners. As therapeutics designed to target the PI3K pathway as a whole or SHIP activity in particular are emerging as promising treatments against autoimmune and inflammatory disorders, it is essential to gain a molecular-level understanding of these pathways and how they are regulated in order to guide and refine pharmacological applications. It is also essential to verify that previous conclusions made using chicken or mouse B cell systems hold true for human B cells and human SHIP protein. This thesis addresses both of these concerns and provides important novel insight into the mechanisms by which SHIP contributes to B cell signaling and how its function is controlled.

One major impact of this thesis work is in challenging the multiple, persistent biases that exist in the field. These biases originated from informative but limited early studies on the biochemistry and function of SHIP. One is the long-held notion that SHIP carries out its inhibitory functions almost exclusively by its enzymatic activity in hydrolyzing PIP<sub>3</sub>. This is likely true for inhibition of Ca<sup>2+</sup> flux, which was the focus of early studies (238, 298), however it has not been examined for other functions such as the effect of SHIP on the cytoskeleton. Here, we propose and examine a role for SHIP in regulating actin dynamics, relying not on enzymatic activity but rather on interaction with cytoskeletal adaptor protein Nck. This data, in addition to previous studies demonstrating protein interactions as a major mechanism by which SHIP regulates MAPK

signaling in B cells (303, 304) and demonstrating functional activity of phosphatase-dead SHIP in other cell types (277, 278), should be sufficient to cast doubt on the absolute importance of SHIP enzymatic activity and to re-evaluate the expected results of therapeutic manipulation. New therapies targeting protein-protein interactions rather than enzymatic activity might be beneficial in some contexts and should be explored.

Another persistent bias, one that we ourselves assumed to be true prior to carefully experimentation, is that interaction with the FcγRIIB ITIM, phosphorylated only after co-ligation of this receptor with the BCR, is the major mechanism for SHIP recruitment to the plasma membrane. This assumption was based on early studies demonstrating a robust interaction between SHIP SH2 and the ITIM motif and demonstrating increased SHIP phosphorylation (302), enhanced PIP<sub>3</sub> hydrolysis and greater inhibition of Ca<sup>2+</sup> flux (238, 240) with co-ligation of BCR/FcγRIIB relative to BCR ligation alone. Despite this, my data demonstrates that SHIP is recruited to the plasma membrane equally after BCR ligation with or without FcγRIIB co-ligation. FcγRIIB likely promotes SHIP function in PIP<sub>3</sub> hydrolysis by more subtle influences such as by controlling association into particular membrane sub-domains and/or participation in distinct protein/lipid complexes.

In addition to challenging these biases in the field, the data presented here also serves to refine some of the models of SHIP regulation proposed by other groups. For example, one group performed an elegant study demonstrating that both the SH2 domain and C-terminus of SHIP participate in an inter- or intra-molecular interaction at rest, forming an auto-inhibited conformation that can be relieved upon interaction with other proteins (403). The Biacore

interaction screen performed here estimated only a very weak interaction of SHIP's SH2 domain with one of its uncharacterized C-terminal phospho-tyrosine residues, Tyr886. However, in this same screening experiment, an interaction of appreciably higher apparent strength was identified between the SH2 domain of SHIP and a well-characterized phosphorylation site of homologous protein SHIP2. Thus, perhaps it is a hetero-oligomeric rather than or in addition to a homo-oligomeric structure that retains SHIP in a cytoplasmic-localized, inhibited conformation at rest.

Another model of SHIP regulation put forward by others suggested that the mechanism by which SHIP is recruited to the membrane upon BCR ligation is by interaction with Dok-1, which in turn binds to PIP<sub>3</sub> in the plasma membrane (405). Although neither they nor we have explicitly tested the effect of Dok-1 silencing/deficiency on SHIP localization, the data presented here does not support a role for PIP<sub>3</sub>. Neither PI3K inhibitors nor SHIP inhibitors, both of which substantially alter the balance of PIP<sub>3</sub>/PI(3,4)P<sub>2</sub> phosphoinositides, have any measurable effect on SHIP recruitment. Neither did mutation of the SHIP phosphatase domain. These results also imply that there is no significant requirement for direct phosphoinositide binding by the PH-R (296), C2 (279) or SH2 domains (406) of SHIP under the conditions tested.

Finally, the prevalent ITAM-ITIM model postulates that phosphorylated ITAM residues (targets of both Src family and Syk kinase activity) bind activating kinases such as Syk and initiate positive signaling pathways, while phosphorylated ITIM residues (targets of only Src family kinase activity) bind inhibitory phosphatases such as SHIP or SHP and initiate negative signaling. We demonstrate here, as others have before us (289, 397), that ITAM-containing receptors such as the BCR can directly initiate negative signaling pathways. Moreover, we

demonstrate a critical role for Syk, the “activating kinase”, in initiating inhibitory signaling. Syk activity was categorically required for membrane recruitment of SHIP while inhibition of Src family kinases had little impact under the conditions tested. Syk was also required for SHIP phosphorylation, best explained if membrane localization is a pre-requisite to phosphorylation by Src family kinases. These results should inspire a re-evaluation of the role of Syk in other inhibitory signaling pathways as well.

### **5.3 Limitations and future research directions**

The conclusions presented in this thesis could be strengthened and extended in several ways. In chapter 2, I screen for interactions between SHIP and candidate interaction partners using a Biacore assay. More information could be gathered using an unbiased approach. For example, a Biacore assay could be established whereby structural elements of SHIP (SH2 domain, phosphotyrosine sequences, or other motifs) or full-length SHIP protein are immobilized on a sensorchip surface and whole cell lysate is sent through the fluidics system in place of recombinant analyte. The fraction that binds to SHIP can be eluted for mass spectrometry detection. This type of assay would generate more candidate interaction partners and map their interaction sites. It would require considerably less recombinant SHIP protein compared to a more traditional pull-down assay and could be performed more easily with low numbers of primary cells.

In chapter 3, I examine a potential role for SHIP phospho-Tyr944 in slowing actin turnover by mediating an interaction with Nck. First, complementary approaches could be taken to validate the SHIP-Nck interaction in cells, such as an *in-situ* proximity ligation assay. It would also be

informative to describe the conditions of Tyr944 phosphorylation more thoroughly. The generation of a specific antibody would allow us to characterize the kinetics of Tyr944 phosphorylation after ligation of the BCR and other receptors and to define the kinase(s) and phosphatase(s) that act on this site. An attempt was made to generate such an antibody, however it detected phosphorylation even of Y944F mutant SHIP and therefore had poor specificity.

Furthermore, as discussed in chapter 3, the transient transfection system used to explore the role of Tyr944 has important limitations. One is the variation in cell viability that is observed from experiment to experiment and from one construct to another. To account for this potentially complicating factor, one must have a method to clearly distinguish live, healthy cells from dead or dying cells. In some assays such as the FRAP assay performed for measuring actin dynamics, this can be accomplished by observation of cell morphology and spreading behaviour. For other assays, a fluorescent live-cell marker can be used theoretically; however these typically mark only late stages of cell death. A second key limitation is the presence of relatively high levels of endogenous SHIP protein. A role for Tyr944 might be masked in SHIP Y944F-expressing cells if there is sufficient endogenous WT SHIP present to perform its Tyr944-dependent function. Other drawbacks of transient transfection include variability of vector expression and the presence of a large fluorescent tag fused to the protein of interest, SHIP. We have attempted to account for these factors by excluding excessively dim or excessively bright cells and by testing the ability of SHIP-EGFP to be phosphorylated and to act on its substrate PI(3,4,5)P<sub>3</sub>. On the other hand, there are some advantages to a transient transfection approach. Experiments can be repeated quickly and with relative ease. Furthermore, unlike with a stable transfection or knock-

in approach, cells have little time to change their genetic programs to compensate for the manipulation.

For future experiments, we will first attempt to overcome the viability in a transient system by relatively simple modifications, for example by FACS sorting and a longer recovery period or by using improved early apoptosis markers. An alternate option is to generate multiple stable clones expressing each construct. Unfortunately, the number of cell lines required to compensate for potential clonal anomalies would make this approach time-consuming and it would not solve the problem of endogenous SHIP expression. Another possibility is the generation of a knock-in SHIP Y944F mutant in a SHIP-deficient system using either chicken DT-40 B cells or an in-vivo mouse model. However, careful interpretation of results would be required as species-specific SHIP binding partners have been described in previous studies (240) and the sequence surrounding Tyr944 is similar but not identical between human, mouse and chicken SHIP protein. With newly emerging CRISPR-Cas9 technology, a knock-in mutation could conceivably be generated in human cells. However, this approach is still limited by transfectability and would likely also require the generation of clonal cell lines. Unfortunately, there is no perfect experimental system for studying the effects and requirements of small motifs such as phosphotyrosine sequences, therefore results obtained using any chosen model must be cautiously interpreted.

Finally, in Chapter 4 I examine the localization dynamics of SHIP and how they are controlled. I found that co-ligation of the BCR with FcγRIIB had no effect on the magnitude or kinetics of SHIP recruitment to the plasma membrane, however the mobility of SHIP molecules was

reduced by co-ligation in a manner dependent on the Fc $\gamma$ RIIB ITIM. This is consistent with the inference that SHIP participates in distinct protein and/or lipid complexes depending on Fc $\gamma$ RIIB involvement. A more informative experiment would be to directly measure the rate of SHIP-EGFP diffusion by single particle tracking. We could also co-label SHIP and Fc $\gamma$ RIIB or the BCR in these experiments to examine their spatial relationships under different stimulation conditions. Another key follow-up study would be to perform a detailed examination of the complexes that form. The least biased approach would be to differentially label BCR- and BCR/Fc $\gamma$ RIIB-stimulated cells with heavy and light amino acid isotopes, then perform co-immunoprecipitation experiments with anti-SHIP antibody followed by detection via mass spectrometry.

In addition to the direct follow-up studies proposed here, there are still many big picture questions that remain unanswered. For example, it would be a large but extremely informative undertaking to carefully dissect and compare the contributions of SHIP phosphatase activity versus adaptor elements to function *in vitro* and *in vivo*. This could be accomplished using knock-in mutants of phosphatase-dead, Y915F/Y1022F, Y944F SHIP and more to study basic differences in downstream signaling, interaction with protein partners including BCR, Fc $\gamma$ RIIB and cytoskeletal regulators, as well as their contribution to disease susceptibility in whole animal models. The influence of regulatory factors such as Fc $\gamma$ RIIB and other co-receptors that tip the balance toward either inhibitory or activating signaling pathways should also be examined. A mouse knock-in model of SHIP Y944F would be especially informative to assess effects of Tyr944 on B cell development, tissue homing, immune response to pathogens and susceptibility to autoimmunity or other diseases.

Furthermore, future translational studies should focus on other therapeutic mechanisms to manipulate SHIP function, complementing the use of enzymatic modulators currently under investigation. One obvious focus would be to promote or inhibit membrane localization, which could affect both enzymatic and adaptor functions of SHIP. Conceptually, it is easier to imagine how recruitment could be inhibited rather than promoted, which might be relevant to treatment of some cancers in which SHIP inhibition seems to paradoxically promote leukemic cell death (407). This could be accomplished by blocking the interaction between SHIP and ITIM/ITAM phospho-tyrosines, perhaps using specific SH2 domain “superbinders” (408) to bind exposed phospho-tyrosines in a dominant negative fashion. Strategies to promote membrane recruitment in contexts where SHIP plays a protective role are less intuitive but could be explored nonetheless. For example, if we determine that interaction of SHIP with a specific phospho-protein is required for membrane recruitment, then inhibiting the dephosphorylation of that protein or blocking its binding to competing interaction partners might show promise.

Clearly, SHIP is a complex molecule involved in multiple cellular pathways by way of multiple mechanisms. By thorough examination of these mechanisms, the contexts in which they occur, and their beneficial/detrimental contribution to disease, we paint a clearer picture of the intricate equilibrium of positive and negative signaling pathways that maintain balanced cellular responses. As a consequence, we also identify novel therapeutic approaches to potentially correct the imbalances that occur in diseases such as autoimmunity.



## REFERENCES

1. LeBien, T. W., and T. F. Tedder. 2008. B lymphocytes: how they develop and function. *Blood* 112: 1570-1580.
2. Fagraeus, A. 1947. Plasma cellular reaction and its relation to the formation of antibodies in vitro. *Nature* 159: 499.
3. Jerne, N. K. 1955. The Natural-Selection Theory of Antibody Formation. *Proc Natl Acad Sci U S A* 41: 849-857.
4. Talmage, D. W. 1957. Allergy and immunology. *Annu Rev Immunol*: 239-256.
5. Burnet, F. M. 1957. A modification of Jerne's theory of antibody production using the concept of clonal selection. *Australian Journal of Science*: 67-69.
6. Burnet, F. M. 1959. *The clonal selection theory of acquired immunity*. Vanderbilt University Press, Nashville,.
7. Nossal, G. J. 2007. One cell-one antibody: prelude and aftermath. *Nat Immunol* 8: 1015-1017.
8. Nossal, G. J., and J. Lederberg. 1958. Antibody production by single cells. *Nature* 181: 1419-1420.
9. Cooper, M. D., R. D. Peterson, and R. A. Good. 1965. Delineation of the Thymic and Bursal Lymphoid Systems in the Chicken. *Nature* 205: 143-146.
10. Mitchell, G. F., and J. F. Miller. 1968. Cell to cell interaction in the immune response. II. The source of hemolysin-forming cells in irradiated mice given bone marrow and thymus or thoracic duct lymphocytes. *J Exp Med* 128: 821-837.
11. Coombs, R. R., A. Feinstein, and A. B. Wilson. 1969. Immunoglobulin determinants on the surface of human lymphocytes. *Lancet* 2: 1157-1160.
12. Preud'homme, J. L., and M. Seligmann. 1972. Surface bound immunoglobulins as a cell marker in human lymphoproliferative diseases. *Blood* 40: 777-794.
13. Franco, M. A., and H. B. Greenberg. 1995. Role of B cells and cytotoxic T lymphocytes in clearance of and immunity to rotavirus infection in mice. *J Virol* 69: 7800-7806.
14. Maaser, C., M. P. Housley, M. Iimura, J. R. Smith, B. A. Vallance, B. B. Finlay, J. R. Schreiber, N. M. Varki, M. F. Kagnoff, and L. Eckmann. 2004. Clearance of *Citrobacter rodentium* requires B cells but not secretory immunoglobulin A (IgA) or IgM antibodies. *Infect Immun* 72: 3315-3324.
15. Yang, X., and R. C. Brunham. 1998. Gene knockout B cell-deficient mice demonstrate that B cells play an important role in the initiation of T cell responses to *Chlamydia trachomatis* (mouse pneumonitis) lung infection. *J Immunol* 161: 1439-1446.
16. Magez, S., A. Schwegmann, R. Atkinson, F. Claes, M. Drennan, P. De Baetselier, and F. Brombacher. 2008. The role of B-cells and IgM antibodies in parasitemia, anemia, and VSG switching in *Trypanosoma brucei*-infected mice. *PLoS Pathog* 4: e1000122.
17. Lam, K. P., R. Kuhn, and K. Rajewsky. 1997. In vivo ablation of surface immunoglobulin on mature B cells by inducible gene targeting results in rapid cell death. *Cell* 90: 1073-1083.
18. Reichlin, A., Y. Hu, E. Meffre, H. Nagaoka, S. Gong, M. Kraus, K. Rajewsky, and M. C. Nussenzweig. 2001. B cell development is arrested at the immature B cell stage in mice carrying a mutation in the cytoplasmic domain of immunoglobulin beta. *J Exp Med* 193: 13-23.

19. Antony, P., J. B. Petro, G. Carlesso, N. P. Shinnars, J. Lowe, and W. N. Khan. 2003. B cell receptor directs the activation of NFAT and NF-kappaB via distinct molecular mechanisms. *Exp Cell Res* 291: 11-24.
20. Dintzis, H. M., R. Z. Dintzis, and B. Vogelstein. 1976. Molecular determinants of immunogenicity: the immunon model of immune response. *Proc Natl Acad Sci U S A* 73: 3671-3675.
21. Pecanha, L. M., C. M. Snapper, F. D. Finkelman, and J. J. Mond. 1991. Dextran-conjugated anti-Ig antibodies as a model for T cell-independent type 2 antigen-mediated stimulation of Ig secretion in vitro. I. Lymphokine dependence. *J Immunol* 146: 833-839.
22. Andersson, J., M. H. Schreier, and F. Melchers. 1980. T-cell-dependent B-cell stimulation is H-2 restricted and antigen dependent only at the resting B-cell level. *Proc Natl Acad Sci U S A* 77: 1612-1616.
23. Janeway, C. 2001. *Immunobiology : the immune system in health and disease*. Garland Pub., London ; New York, NY, US.
24. Croft, M., and S. L. Swain. 1991. B cell response to fresh and effector T helper cells. Role of cognate T-B interaction and the cytokines IL-2, IL-4, and IL-6. *J Immunol* 146: 4055-4064.
25. Noelle, R. J., M. Roy, D. M. Shepherd, I. Stamenkovic, J. A. Ledbetter, and A. Aruffo. 1992. A 39-kDa protein on activated helper T cells binds CD40 and transduces the signal for cognate activation of B cells. *Proc Natl Acad Sci U S A* 89: 6550-6554.
26. Dedeoglu, F., B. Horwitz, J. Chaudhuri, F. W. Alt, and R. S. Geha. 2004. Induction of activation-induced cytidine deaminase gene expression by IL-4 and CD40 ligation is dependent on STAT6 and NFKappaB. *Int Immunol* 16: 395-404.
27. Snapper, C. M., K. B. Marcu, and P. Zelazowski. 1997. The immunoglobulin class switch: beyond "accessibility". *Immunity* 6: 217-223.
28. Jacob, J., R. Kassir, and G. Kelsoe. 1991. In situ studies of the primary immune response to (4-hydroxy-3-nitrophenyl)acetyl. I. The architecture and dynamics of responding cell populations. *J Exp Med* 173: 1165-1175.
29. MacLennan, I. C. 1994. Germinal centers. *Annu Rev Immunol* 12: 117-139.
30. Ziegner, M., G. Steinhauser, and C. Berek. 1994. Development of antibody diversity in single germinal centers: selective expansion of high-affinity variants. *Eur J Immunol* 24: 2393-2400.
31. Clark, M. R. 1997. IgG effector mechanisms. *Chem Immunol* 65: 88-110.
32. Ward, E. S., and V. Ghetie. 1995. The effector functions of immunoglobulins: implications for therapy. *Ther Immunol* 2: 77-94.
33. Liu, Y., Y. Wu, L. Ramarathnam, Y. Guo, D. Huszar, M. Trounstein, and M. Zhao. 1995. Gene-targeted B-deficient mice reveal a critical role for B cells in the CD4 T cell response. *Int Immunol* 7: 1353-1362.
34. Ron, Y., P. De Baetselier, J. Gordon, M. Feldman, and S. Segal. 1981. Defective induction of antigen-reactive proliferating T cells in B cell-deprived mice. *Eur J Immunol* 11: 964-968.
35. Bouaziz, J. D., K. Yanaba, G. M. Venturi, Y. Wang, R. M. Tisch, J. C. Poe, and T. F. Tedder. 2007. Therapeutic B cell depletion impairs adaptive and autoreactive CD4+ T cell activation in mice. *Proc Natl Acad Sci U S A* 104: 20878-20883.
36. Ron, Y., and J. Sprent. 1987. T cell priming in vivo: a major role for B cells in presenting antigen to T cells in lymph nodes. *J Immunol* 138: 2848-2856.

37. Baumjohann, D., S. Preite, A. Reboldi, F. Ronchi, K. M. Ansel, A. Lanzavecchia, and F. Sallusto. 2013. Persistent antigen and germinal center B cells sustain T follicular helper cell responses and phenotype. *Immunity* 38: 596-605.
38. Harris, D. P., L. Haynes, P. C. Sayles, D. K. Duso, S. M. Eaton, N. M. Lepak, L. L. Johnson, S. L. Swain, and F. E. Lund. 2000. Reciprocal regulation of polarized cytokine production by effector B and T cells. *Nat Immunol* 1: 475-482.
39. Gagro, A., D. Servis, A. M. Cepika, K. M. Toellner, G. Grafton, D. R. Taylor, S. Branica, and J. Gordon. 2006. Type I cytokine profiles of human naive and memory B lymphocytes: a potential for memory cells to impact polarization. *Immunology* 118: 66-77.
40. Moulin, V., F. Andris, K. Thielemans, C. Maliszewski, J. Urbain, and M. Moser. 2000. B lymphocytes regulate dendritic cell (DC) function in vivo: increased interleukin 12 production by DCs from B cell-deficient mice results in T helper cell type 1 deviation. *J Exp Med* 192: 475-482.
41. Kondratieva, T. K., E. I. Rubakova, I. A. Linge, V. V. Evstifeev, K. B. Majorov, and A. S. Apt. 2010. B cells delay neutrophil migration toward the site of stimulus: tardiness critical for effective bacillus Calmette-Guerin vaccination against tuberculosis infection in mice. *J Immunol* 184: 1227-1234.
42. Iwata, Y., A. Yoshizaki, K. Komura, K. Shimizu, F. Ogawa, T. Hara, E. Muroi, S. Bae, M. Takenaka, T. Yukami, M. Hasegawa, M. Fujimoto, Y. Tomita, T. F. Tedder, and S. Sato. 2009. CD19, a response regulator of B lymphocytes, regulates wound healing through hyaluronan-induced TLR4 signaling. *Am J Pathol* 175: 649-660.
43. Tiegs, S. L., D. M. Russell, and D. Nemazee. 1993. Receptor editing in self-reactive bone marrow B cells. *J Exp Med* 177: 1009-1020.
44. Nemazee, D. A., and K. Burki. 1989. Clonal deletion of B lymphocytes in a transgenic mouse bearing anti-MHC class I antibody genes. *Nature* 337: 562-566.
45. Goodnow, C. C., J. Crosbie, H. Jorgensen, R. A. Brink, and A. Basten. 1989. Induction of self-tolerance in mature peripheral B lymphocytes. *Nature* 342: 385-391.
46. Cambier, J. C., S. B. Gauld, K. T. Merrell, and B. J. Vilen. 2007. B-cell anergy: from transgenic models to naturally occurring anergic B cells? *Nat Rev Immunol* 7: 633-643.
47. Goodnow, C. C., J. Crosbie, S. Adelstein, T. B. Lavoie, S. J. Smith-Gill, R. A. Brink, H. Pritchard-Briscoe, J. S. Wotherspoon, R. H. Loblay, K. Raphael, and et al. 1988. Altered immunoglobulin expression and functional silencing of self-reactive B lymphocytes in transgenic mice. *Nature* 334: 676-682.
48. Hampe, C. S. 2012. B Cell in Autoimmune Diseases. *Scientifica (Cairo)* 2012.
49. Li, R., A. Rezk, Y. Miyazaki, E. Hilgenberg, H. Touil, P. Shen, C. S. Moore, L. Michel, F. Althekair, S. Rajasekharan, J. L. Gommerman, A. Prat, S. Fillatreau, A. Bar-Or, and B. c. i. M. S. T. Canadian. 2015. Proinflammatory GM-CSF-producing B cells in multiple sclerosis and B cell depletion therapy. *Sci Transl Med* 7: 310ra166.
50. Lipsky, P. E. 2001. Systemic lupus erythematosus: an autoimmune disease of B cell hyperactivity. *Nat Immunol* 2: 764-766.
51. Klinman, D. M., A. Shirai, Y. Ishigatsubo, J. Conover, and A. D. Steinberg. 1991. Quantitation of IgM- and IgG-secreting B cells in the peripheral blood of patients with systemic lupus erythematosus. *Arthritis Rheum* 34: 1404-1410.

52. Edwards, J. C., and G. Cambridge. 2001. Sustained improvement in rheumatoid arthritis following a protocol designed to deplete B lymphocytes. *Rheumatology (Oxford)* 40: 205-211.
53. Manzi, S., J. Sanchez-Guerrero, J. T. Merrill, R. Furie, D. Gladman, S. V. Navarra, E. M. Ginzler, D. P. D'Cruz, A. Doria, S. Cooper, Z. J. Zhong, D. Hough, W. Freimuth, M. A. Petri, Bliss, and B.-S. Groups. 2012. Effects of belimumab, a B lymphocyte stimulator-specific inhibitor, on disease activity across multiple organ domains in patients with systemic lupus erythematosus: combined results from two phase III trials. *Ann Rheum Dis* 71: 1833-1838.
54. Pescovitz, M. D., C. J. Greenbaum, H. Krause-Steinrauf, D. J. Becker, S. E. Gitelman, R. Goland, P. A. Gottlieb, J. B. Marks, P. F. McGee, A. M. Moran, P. Raskin, H. Rodriguez, D. A. Schatz, D. Wherrett, D. M. Wilson, J. M. Lachin, J. S. Skyler, and C. D. S. G. Type 1 Diabetes TrialNet Anti. 2009. Rituximab, B-lymphocyte depletion, and preservation of beta-cell function. *N Engl J Med* 361: 2143-2152.
55. Sorensen, P. S., S. Lisby, R. Grove, F. Derosier, S. Shackelford, E. Havrdova, J. Drulovic, and M. Filippi. 2014. Safety and efficacy of ofatumumab in relapsing-remitting multiple sclerosis: a phase 2 study. *Neurology* 82: 573-581.
56. Shlomchik, M. J., M. P. Madaio, D. Ni, M. Trounstein, and D. Huszar. 1994. The role of B cells in lpr/lpr-induced autoimmunity. *J Exp Med* 180: 1295-1306.
57. Svensson, L., J. Jirholt, R. Holmdahl, and L. Jansson. 1998. B cell-deficient mice do not develop type II collagen-induced arthritis (CIA). *Clin Exp Immunol* 111: 521-526.
58. Yanaba, K., Y. Hamaguchi, G. M. Venturi, D. A. Steeber, E. W. St Clair, and T. F. Tedder. 2007. B cell depletion delays collagen-induced arthritis in mice: arthritis induction requires synergy between humoral and cell-mediated immunity. *J Immunol* 179: 1369-1380.
59. Hu, C. Y., D. Rodriguez-Pinto, W. Du, A. Ahuja, O. Henegariu, F. S. Wong, M. J. Shlomchik, and L. Wen. 2007. Treatment with CD20-specific antibody prevents and reverses autoimmune diabetes in mice. *J Clin Invest* 117: 3857-3867.
60. Noorchashm, H., N. Noorchashm, J. Kern, S. Y. Rostami, C. F. Barker, and A. Naji. 1997. B-cells are required for the initiation of insulinitis and sialitis in nonobese diabetic mice. *Diabetes* 46: 941-946.
61. Kumar, K. R., J. Zhu, M. Bhaskarabhatla, M. Yan, and C. Mohan. 2005. Enhanced expression of stem cell antigen-1 (Ly-6A/E) in lymphocytes from lupus prone mice correlates with disease severity. *J Autoimmun* 25: 215-222.
62. Bolland, S., and J. V. Ravetch. 2000. Spontaneous autoimmune disease in Fc(gamma)RIIB-deficient mice results from strain-specific epistasis. *Immunity* 13: 277-285.
63. O'Neill, S. K., A. Getahun, S. B. Gauld, K. T. Merrell, I. Tamir, M. J. Smith, J. M. Dal Porto, Q. Z. Li, and J. C. Cambier. 2011. Monophosphorylation of CD79a and CD79b ITAM motifs initiates a SHIP-1 phosphatase-mediated inhibitory signaling cascade required for B cell anergy. *Immunity* 35: 746-756.
64. Tedder, T. F., J. C. Poe, M. Fujimoto, K. M. Haas, and S. Sato. 2005. The CD19-CD21 signal transduction complex of B lymphocytes regulates the balance between health and autoimmune disease: systemic sclerosis as a model system. *Curr Dir Autoimmun* 8: 55-90.

65. Vlahakos, D. V., M. H. Foster, S. Adams, M. Katz, A. A. Ucci, K. J. Barrett, S. K. Datta, and M. P. Madaio. 1992. Anti-DNA antibodies form immune deposits at distinct glomerular and vascular sites. *Kidney Int* 41: 1690-1700.
66. Stuart, J. M., M. A. Cremer, A. S. Townes, and A. H. Kang. 1982. Type II collagen-induced arthritis in rats. Passive transfer with serum and evidence that IgG anticollagen antibodies can cause arthritis. *J Exp Med* 155: 1-16.
67. Wooley, P. H., H. S. Luthra, S. K. Singh, A. R. Huse, J. M. Stuart, and C. S. David. 1984. Passive transfer of arthritis to mice by injection of human anti-type II collagen antibody. *Mayo Clin Proc* 59: 737-743.
68. Chan, O. T., L. G. Hannum, A. M. Haberman, M. P. Madaio, and M. J. Shlomchik. 1999. A novel mouse with B cells but lacking serum antibody reveals an antibody-independent role for B cells in murine lupus. *J Exp Med* 189: 1639-1648.
69. O'Neill, S. K., M. J. Shlomchik, T. T. Glant, Y. Cao, P. D. Doodles, and A. Finnegan. 2005. Antigen-specific B cells are required as APCs and autoantibody-producing cells for induction of severe autoimmune arthritis. *J Immunol* 174: 3781-3788.
70. Noorchashm, H., Y. K. Lieu, N. Noorchashm, S. Y. Rostami, S. A. Greeley, A. Schlachterman, H. K. Song, L. E. Noto, A. M. Jevnikar, C. F. Barker, and A. Naji. 1999. I-Ag7-mediated antigen presentation by B lymphocytes is critical in overcoming a checkpoint in T cell tolerance to islet beta cells of nonobese diabetic mice. *J Immunol* 163: 743-750.
71. Muller, A. M., A. Medvinsky, J. Strouboulis, F. Grosveld, and E. Dzierzak. 1994. Development of hematopoietic stem cell activity in the mouse embryo. *Immunity* 1: 291-301.
72. Nunez, C., N. Nishimoto, G. L. Gartland, L. G. Billips, P. D. Burrows, H. Kubagawa, and M. D. Cooper. 1996. B cells are generated throughout life in humans. *J Immunol* 156: 866-872.
73. Galy, A., M. Travis, D. Cen, and B. Chen. 1995. Human T, B, natural killer, and dendritic cells arise from a common bone marrow progenitor cell subset. *Immunity* 3: 459-473.
74. Kondo, M., I. L. Weissman, and K. Akashi. 1997. Identification of clonogenic common lymphoid progenitors in mouse bone marrow. *Cell* 91: 661-672.
75. Ryan, D. H., B. L. Nuccie, I. Ritterman, J. L. Liesveld, C. N. Abboud, and R. A. Insel. 1997. Expression of interleukin-7 receptor by lineage-negative human bone marrow progenitors with enhanced lymphoid proliferative potential and B-lineage differentiation capacity. *Blood* 89: 929-940.
76. Pieper, K., B. Grimbacher, and H. Eibel. 2013. B-cell biology and development. *J Allergy Clin Immunol* 131: 959-971.
77. Nutt, S. L., and B. L. Kee. 2007. The transcriptional regulation of B cell lineage commitment. *Immunity* 26: 715-725.
78. Brack, C., M. Hirama, R. Lenhard-Schuller, and S. Tonegawa. 1978. A complete immunoglobulin gene is created by somatic recombination. *Cell* 15: 1-14.
79. Nemazee, D. 2006. Receptor editing in lymphocyte development and central tolerance. *Nat Rev Immunol* 6: 728-740.
80. Hardy, R. R., C. E. Carmack, S. A. Shinton, J. D. Kemp, and K. Hayakawa. 1991. Resolution and characterization of pro-B and pre-pro-B cell stages in normal mouse bone marrow. *J Exp Med* 173: 1213-1225.

81. Loken, M. R., V. O. Shah, K. L. Dattilio, and C. I. Civin. 1987. Flow cytometric analysis of human bone marrow. II. Normal B lymphocyte development. *Blood* 70: 1316-1324.
82. Sakaguchi, N., and F. Melchers. 1986. Lambda 5, a new light-chain-related locus selectively expressed in pre-B lymphocytes. *Nature* 324: 579-582.
83. Melchers, F. 2005. The pre-B-cell receptor: selector of fitting immunoglobulin heavy chains for the B-cell repertoire. *Nat Rev Immunol* 5: 578-584.
84. Rolink, A. G., J. Andersson, and F. Melchers. 1998. Characterization of immature B cells by a novel monoclonal antibody, by turnover and by mitogen reactivity. *Eur J Immunol* 28: 3738-3748.
85. van Zelm, M. C., T. Szczepanski, M. van der Burg, and J. J. van Dongen. 2007. Replication history of B lymphocytes reveals homeostatic proliferation and extensive antigen-induced B cell expansion. *J Exp Med* 204: 645-655.
86. Chung, J. B., M. Silverman, and J. G. Monroe. 2003. Transitional B cells: step by step towards immune competence. *Trends Immunol* 24: 343-349.
87. Melamed, D., and D. Nemazee. 1997. Self-antigen does not accelerate immature B cell apoptosis, but stimulates receptor editing as a consequence of developmental arrest. *Proc Natl Acad Sci U S A* 94: 9267-9272.
88. Kitamura, D., J. Roes, R. Kuhn, and K. Rajewsky. 1991. A B cell-deficient mouse by targeted disruption of the membrane exon of the immunoglobulin mu chain gene. *Nature* 350: 423-426.
89. Zhang, Y., M. Meyer-Hermann, L. A. George, M. T. Figge, M. Khan, M. Goodall, S. P. Young, A. Reynolds, F. Falciani, A. Waisman, C. A. Notley, M. R. Ehrenstein, M. Kosco-Vilbois, and K. M. Toellner. 2013. Germinal center B cells govern their own fate via antibody feedback. *J Exp Med* 210: 457-464.
90. Reth, M. 1989. Antigen receptor tail clue. *Nature* 338: 383-384.
91. Cambier, J. C. 1995. New nomenclature for the Reth motif (or ARH1/TAM/ARAM/YXXL). *Immunol Today* 16: 110.
92. Billadeau, D. D., and P. J. Leibson. 2002. ITAMs versus ITIMs: striking a balance during cell regulation. *J Clin Invest* 109: 161-168.
93. Vivier, E., and M. Daeron. 1997. Immunoreceptor tyrosine-based inhibition motifs. *Immunol Today* 18: 286-291.
94. Ravetch, J. V., and L. L. Lanier. 2000. Immune inhibitory receptors. *Science* 290: 84-89.
95. Osborne, M. A., G. Zenner, M. Lubinus, X. Zhang, Z. Songyang, L. C. Cantley, P. Majerus, P. Burn, and J. P. Kochan. 1996. The inositol 5'-phosphatase SHIP binds to immunoreceptor signaling motifs and responds to high affinity IgE receptor aggregation. *J Biol Chem* 271: 29271-29278.
96. Ganesan, L. P., H. Fang, C. B. Marsh, and S. Tridandapani. 2003. The protein-tyrosine phosphatase SHP-1 associates with the phosphorylated immunoreceptor tyrosine-based activation motif of Fc gamma RIIa to modulate signaling events in myeloid cells. *J Biol Chem* 278: 35710-35717.
97. Barrow, A. D., E. Astoul, A. Floto, G. Brooke, I. A. Relou, N. S. Jennings, K. G. Smith, W. Ouwehand, R. W. Farndale, D. R. Alexander, and J. Trowsdale. 2004. Cutting edge: TREM-like transcript-1, a platelet immunoreceptor tyrosine-based inhibition motif encoding costimulatory immunoreceptor that enhances, rather than inhibits, calcium signaling via SHP-2. *J Immunol* 172: 5838-5842.

98. Barrow, A. D., and J. Trowsdale. 2006. You say ITAM and I say ITIM, let's call the whole thing off: the ambiguity of immunoreceptor signalling. *Eur J Immunol* 36: 1646-1653.
99. Alt, F. W., A. L. Bothwell, M. Knapp, E. Siden, E. Mather, M. Koshland, and D. Baltimore. 1980. Synthesis of secreted and membrane-bound immunoglobulin mu heavy chains is directed by mRNAs that differ at their 3' ends. *Cell* 20: 293-301.
100. Rogers, J., P. Early, C. Carter, K. Calame, M. Bond, L. Hood, and R. Wall. 1980. Two mRNAs with different 3' ends encode membrane-bound and secreted forms of immunoglobulin mu chain. *Cell* 20: 303-312.
101. Venkitaraman, A. R., G. T. Williams, P. Dariavach, and M. S. Neuberger. 1991. The B-cell antigen receptor of the five immunoglobulin classes. *Nature* 352: 777-781.
102. Tolar, P., H. W. Sohn, and S. K. Pierce. 2005. The initiation of antigen-induced B cell antigen receptor signaling viewed in living cells by fluorescence resonance energy transfer. *Nat Immunol* 6: 1168-1176.
103. Mukherjee, S., J. Zhu, J. Zikherman, R. Parameswaran, T. A. Kadlecsek, Q. Wang, B. Au-Yeung, H. Ploegh, J. Kuriyan, J. Das, and A. Weiss. 2013. Monovalent and multivalent ligation of the B cell receptor exhibit differential dependence upon Syk and Src family kinases. *Sci Signal* 6: ra1.
104. Rolli, V., M. Gallwitz, T. Wossning, A. Flemming, W. W. Schamel, C. Zurn, and M. Reth. 2002. Amplification of B cell antigen receptor signaling by a Syk/ITAM positive feedback loop. *Mol Cell* 10: 1057-1069.
105. Dal Porto, J. M., S. B. Gauld, K. T. Merrell, D. Mills, A. E. Pugh-Bernard, and J. Cambier. 2004. B cell antigen receptor signaling 101. *Mol Immunol* 41: 599-613.
106. Klaus, G. G., M. K. Bijsterbosch, A. O'Garra, M. M. Harnett, and K. P. Rigley. 1987. Receptor signalling and crosstalk in B lymphocytes. *Immunol Rev* 99: 19-38.
107. Cheng, P. C., M. L. Dykstra, R. N. Mitchell, and S. K. Pierce. 1999. A role for lipid rafts in B cell antigen receptor signaling and antigen targeting. *J Exp Med* 190: 1549-1560.
108. Woodruff, M. F., B. Reid, and K. James. 1967. Effect of antilymphocytic antibody and antibody fragments on human lymphocytes in vitro. *Nature* 215: 591-594.
109. Vogel, S. S., C. Thaler, and S. V. Koushik. 2006. Fanciful FRET. *Sci STKE* 2006: re2.
110. Tolar, P., J. Hanna, P. D. Krueger, and S. K. Pierce. 2009. The constant region of the membrane immunoglobulin mediates B cell-receptor clustering and signaling in response to membrane antigens. *Immunity* 30: 44-55.
111. Depoil, D., S. Fleire, B. L. Treanor, M. Weber, N. E. Harwood, K. L. Marchbank, V. L. Tybulewicz, and F. D. Batista. 2008. CD19 is essential for B cell activation by promoting B cell receptor-antigen microcluster formation in response to membrane-bound ligand. *Nat Immunol* 9: 63-72.
112. Tolar, P., H. W. Sohn, W. Liu, and S. K. Pierce. 2009. The molecular assembly and organization of signaling active B-cell receptor oligomers. *Immunol Rev* 232: 34-41.
113. Tolar, P., and S. K. Pierce. 2010. A conformation-induced oligomerization model for B cell receptor microclustering and signaling. *Curr Top Microbiol Immunol* 340: 155-169.
114. Yang, J., and M. Reth. 2010. The dissociation activation model of B cell antigen receptor triggering. *FEBS Lett* 584: 4872-4877.
115. Yang, J., and M. Reth. 2010. Oligomeric organization of the B-cell antigen receptor on resting cells. *Nature* 467: 465-469.

116. Klasener, K., P. C. Maity, E. Hobeika, J. Yang, and M. Reth. 2014. B cell activation involves nanoscale receptor reorganizations and inside-out signaling by Syk. *Elife* 3: e02069.
117. Coggeshall, K. M., J. C. McHugh, and A. Altman. 1992. Predominant expression and activation-induced tyrosine phosphorylation of phospholipase C-gamma 2 in B lymphocytes. *Proc Natl Acad Sci U S A* 89: 5660-5664.
118. Engels, N., B. Wollscheid, and J. Wienands. 2001. Association of SLP-65/BLNK with the B cell antigen receptor through a non-ITAM tyrosine of Ig-alpha. *Eur J Immunol* 31: 2126-2134.
119. Kabak, S., B. J. Skaggs, M. R. Gold, M. Affolter, K. L. West, M. S. Foster, K. Siemasko, A. C. Chan, R. Aebersold, and M. R. Clark. 2002. The direct recruitment of BLNK to immunoglobulin alpha couples the B-cell antigen receptor to distal signaling pathways. *Mol Cell Biol* 22: 2524-2535.
120. Fu, C., C. W. Turck, T. Kurosaki, and A. C. Chan. 1998. BLNK: a central linker protein in B cell activation. *Immunity* 9: 93-103.
121. Falasca, M., S. K. Logan, V. P. Lehto, G. Baccante, M. A. Lemmon, and J. Schlessinger. 1998. Activation of phospholipase C gamma by PI 3-kinase-induced PH domain-mediated membrane targeting. *EMBO J* 17: 414-422.
122. Law, C. L., K. A. Chandran, S. P. Sidorenko, and E. A. Clark. 1996. Phospholipase C-gamma1 interacts with conserved phosphotyrosyl residues in the linker region of Syk and is a substrate for Syk. *Mol Cell Biol* 16: 1305-1315.
123. Chiu, C. W., M. Dalton, M. Ishiai, T. Kurosaki, and A. C. Chan. 2002. BLNK: molecular scaffolding through 'cis'-mediated organization of signaling proteins. *EMBO J* 21: 6461-6472.
124. Takata, M., and T. Kurosaki. 1996. A role for Bruton's tyrosine kinase in B cell antigen receptor-mediated activation of phospholipase C-gamma 2. *J Exp Med* 184: 31-40.
125. Ferris, C. D., R. L. Haganir, S. Supattapone, and S. H. Snyder. 1989. Purified inositol 1,4,5-trisphosphate receptor mediates calcium flux in reconstituted lipid vesicles. *Nature* 342: 87-89.
126. Sugawara, H., M. Kurosaki, M. Takata, and T. Kurosaki. 1997. Genetic evidence for involvement of type 1, type 2 and type 3 inositol 1,4,5-trisphosphate receptors in signal transduction through the B-cell antigen receptor. *EMBO J* 16: 3078-3088.
127. Baba, Y., K. Hayashi, Y. Fujii, A. Mizushima, H. Watarai, M. Wakamori, T. Numaga, Y. Mori, M. Iino, M. Hikida, and T. Kurosaki. 2006. Coupling of STIM1 to store-operated Ca<sup>2+</sup> entry through its constitutive and inducible movement in the endoplasmic reticulum. *Proc Natl Acad Sci U S A* 103: 16704-16709.
128. Hoth, M., and R. Penner. 1992. Depletion of intracellular calcium stores activates a calcium current in mast cells. *Nature* 355: 353-356.
129. Clipstone, N. A., and G. R. Crabtree. 1992. Identification of calcineurin as a key signalling enzyme in T-lymphocyte activation. *Nature* 357: 695-697.
130. Winslow, M. M., E. M. Gallo, J. R. Neilson, and G. R. Crabtree. 2006. The calcineurin phosphatase complex modulates immunogenic B cell responses. *Immunity* 24: 141-152.
131. Loh, C., K. T. Shaw, J. Carew, J. P. Viola, C. Luo, B. A. Perrino, and A. Rao. 1996. Calcineurin binds the transcription factor NFAT1 and reversibly regulates its activity. *J Biol Chem* 271: 10884-10891.



132. Saijo, K., I. Mecklenbrauker, A. Santana, M. Leitger, C. Schmedt, and A. Tarakhovsky. 2002. Protein kinase C beta controls nuclear factor kappaB activation in B cells through selective regulation of the IkappaB kinase alpha. *J Exp Med* 195: 1647-1652.
133. Sasaki, Y., and K. Iwai. 2016. Roles of the NF-kappaB Pathway in B-Lymphocyte Biology. *Curr Top Microbiol Immunol* 393: 177-209.
134. Feig, L. A. 1994. Guanine-nucleotide exchange factors: a family of positive regulators of Ras and related GTPases. *Curr Opin Cell Biol* 6: 204-211.
135. D'Ambrosio, D., K. L. Hippen, and J. C. Cambier. 1996. Distinct mechanisms mediate SHC association with the activated and resting B cell antigen receptor. *Eur J Immunol* 26: 1960-1965.
136. Saxton, T. M., I. van Oostveen, D. Bowtell, R. Aebersold, and M. R. Gold. 1994. B cell antigen receptor cross-linking induces phosphorylation of the p21ras oncoprotein activators SHC and mSOS1 as well as assembly of complexes containing SHC, GRB-2, mSOS1, and a 145-kDa tyrosine-phosphorylated protein. *J Immunol* 153: 623-636.
137. Hashimoto, A., H. Okada, A. Jiang, M. Kurosaki, S. Greenberg, E. A. Clark, and T. Kurosaki. 1998. Involvement of guanosine triphosphatases and phospholipase C-gamma2 in extracellular signal-regulated kinase, c-Jun NH2-terminal kinase, and p38 mitogen-activated protein kinase activation by the B cell antigen receptor. *J Exp Med* 188: 1287-1295.
138. Oh-hora, M., S. Johmura, A. Hashimoto, M. Hikida, and T. Kurosaki. 2003. Requirement for Ras guanine nucleotide releasing protein 3 in coupling phospholipase C-gamma2 to Ras in B cell receptor signaling. *J Exp Med* 198: 1841-1851.
139. Teixeira, C., S. L. Stang, Y. Zheng, N. S. Beswick, and J. C. Stone. 2003. Integration of DAG signaling systems mediated by PKC-dependent phosphorylation of RasGRP3. *Blood* 102: 1414-1420.
140. Dong, C., R. J. Davis, and R. A. Flavell. 2002. MAP kinases in the immune response. *Annu Rev Immunol* 20: 55-72.
141. Ishiai, M., M. Kurosaki, R. Pappu, K. Okawa, I. Ronko, C. Fu, M. Shibata, A. Iwamatsu, A. C. Chan, and T. Kurosaki. 1999. BLNK required for coupling Syk to PLC gamma 2 and Rac1-JNK in B cells. *Immunity* 10: 117-125.
142. Aiba, Y., M. Kameyama, T. Yamazaki, T. F. Tedder, and T. Kurosaki. 2008. Regulation of B-cell development by BCAP and CD19 through their binding to phosphoinositide 3-kinase. *Blood* 111: 1497-1503.
143. Tze, L. E., B. R. Schram, K. P. Lam, K. A. Hogquist, K. L. Hippen, J. Liu, S. A. Shinton, K. L. Otipoby, P. R. Rodine, A. L. Vegoe, M. Kraus, R. R. Hardy, M. S. Schlissel, K. Rajewsky, and T. W. Behrens. 2005. Basal immunoglobulin signaling actively maintains developmental stage in immature B cells. *PLoS Biol* 3: e82.
144. Kovesdi, D., S. E. Bell, and M. Turner. 2010. The development of mature B lymphocytes requires the combined function of CD19 and the p110delta subunit of PI3K. *Self Nonself* 1: 144-153.
145. Clayton, E., G. Bardi, S. E. Bell, D. Chantry, C. P. Downes, A. Gray, L. A. Humphries, D. Rawlings, H. Reynolds, E. Vigorito, and M. Turner. 2002. A crucial role for the p110delta subunit of phosphatidylinositol 3-kinase in B cell development and activation. *J Exp Med* 196: 753-763.
146. Okkenhaug, K., A. Bilancio, G. Farjot, H. Priddle, S. Sancho, E. Peskett, W. Pearce, S. E. Meek, A. Salpekar, M. D. Waterfield, A. J. Smith, and B. Vanhaesebroeck. 2002.

- Impaired B and T cell antigen receptor signaling in p110delta PI 3-kinase mutant mice. *Science* 297: 1031-1034.
147. Gold, M. R., and R. Aebersold. 1994. Both phosphatidylinositol 3-kinase and phosphatidylinositol 4-kinase products are increased by antigen receptor signaling in B cells. *J Immunol* 152: 42-50.
  148. Okkenhaug, K. 2013. Signaling by the phosphoinositide 3-kinase family in immune cells. *Annu Rev Immunol* 31: 675-704.
  149. Lemmon, M. A., and K. M. Ferguson. 2000. Signal-dependent membrane targeting by pleckstrin homology (PH) domains. *Biochem J* 350 Pt 1: 1-18.
  150. Brauweiler, A., I. Tamir, J. Dal Porto, R. J. Benschop, C. D. Helgason, R. K. Humphries, J. H. Freed, and J. C. Cambier. 2000. Differential regulation of B cell development, activation, and death by the src homology 2 domain-containing 5' inositol phosphatase (SHIP). *J Exp Med* 191: 1545-1554.
  151. Li, H., and A. J. Marshall. 2015. Phosphatidylinositol (3,4) bisphosphate-specific phosphatases and effector proteins: A distinct branch of PI3K signaling. *Cell Signal* 27: 1789-1798.
  152. Gewinner, C., Z. C. Wang, A. Richardson, J. Teruya-Feldstein, D. Etemadmoghadam, D. Bowtell, J. Barretina, W. M. Lin, L. Rameh, L. Salmena, P. P. Pandolfi, and L. C. Cantley. 2009. Evidence that inositol polyphosphate 4-phosphatase type II is a tumor suppressor that inhibits PI3K signaling. *Cancer Cell* 16: 115-125.
  153. Li, H., X. Wu, S. Hou, M. Malek, A. Kielkowska, E. Noh, K. J. Makondo, Q. Du, J. A. Wilkins, J. B. Johnston, S. B. Gibson, F. Lin, and A. J. Marshall. 2016. Phosphatidylinositol-3,4-Bisphosphate and Its Binding Protein Lamellipodin Regulate Chemotaxis of Malignant B Lymphocytes. *J Immunol* 196: 586-595.
  154. Limon, J. J., and D. A. Fruman. 2010. B cell receptor signaling: picky about PI3Ks. *Sci Signal* 3: pe25.
  155. Fruman, D. A., R. E. Meyers, and L. C. Cantley. 1998. Phosphoinositide kinases. *Annu Rev Biochem* 67: 481-507.
  156. Guillermet-Guibert, J., K. Bjorklof, A. Salpekar, C. Gonella, F. Ramadani, A. Bilancio, S. Meek, A. J. Smith, K. Okkenhaug, and B. Vanhaesebroeck. 2008. The p110beta isoform of phosphoinositide 3-kinase signals downstream of G protein-coupled receptors and is functionally redundant with p110gamma. *Proc Natl Acad Sci U S A* 105: 8292-8297.
  157. Stoyanov, B., S. Volinia, T. Hanck, I. Rubio, M. Loubtchenkov, D. Malek, S. Stoyanova, B. Vanhaesebroeck, R. Dhand, B. Nurnberg, and et al. 1995. Cloning and characterization of a G protein-activated human phosphoinositide-3 kinase. *Science* 269: 690-693.
  158. Pauls, S. D., S. T. Lafarge, I. Landego, T. Zhang, and A. J. Marshall. 2012. The phosphoinositide 3-kinase signaling pathway in normal and malignant B cells: activation mechanisms, regulation and impact on cellular functions. *Front Immunol* 3: 224.
  159. Ramadani, F., D. J. Bolland, F. Garcon, J. L. Emery, B. Vanhaesebroeck, A. E. Corcoran, and K. Okkenhaug. 2010. The PI3K isoforms p110alpha and p110delta are essential for pre-B cell receptor signaling and B cell development. *Sci Signal* 3: ra60.
  160. Beer-Hammer, S., E. Zebedin, M. von Holleben, J. Alferink, B. Reis, P. Dresing, D. Grandi, S. Scheu, E. Hirsch, V. Sexl, K. Pfeffer, B. Nurnberg, and R. P. Piekorz. 2010.

- The catalytic PI3K isoforms p110gamma and p110delta contribute to B cell development and maintenance, transformation, and proliferation. *J Leukoc Biol* 87: 1083-1095.
161. Sasaki, T., J. Irie-Sasaki, R. G. Jones, A. J. Oliveira-dos-Santos, W. L. Stanford, B. Bolon, A. Wakeham, A. Itie, D. Bouchard, I. Kozieradzki, N. Joza, T. W. Mak, P. S. Ohashi, A. Suzuki, and J. M. Penninger. 2000. Function of PI3Kgamma in thymocyte development, T cell activation, and neutrophil migration. *Science* 287: 1040-1046.
  162. Kraus, M., M. B. Alimzhanov, N. Rajewsky, and K. Rajewsky. 2004. Survival of resting mature B lymphocytes depends on BCR signaling via the Igalpha/beta heterodimer. *Cell* 117: 787-800.
  163. Srinivasan, L., Y. Sasaki, D. P. Calado, B. Zhang, J. H. Paik, R. A. DePinho, J. L. Kutok, J. F. Kearney, K. L. Otipoby, and K. Rajewsky. 2009. PI3 kinase signals BCR-dependent mature B cell survival. *Cell* 139: 573-586.
  164. Al-Alwan, M. M., K. Okkenhaug, B. Vanhaesebroeck, J. S. Hayflick, and A. J. Marshall. 2007. Requirement for phosphoinositide 3-kinase p110delta signaling in B cell antigen receptor-mediated antigen presentation. *J Immunol* 178: 2328-2335.
  165. Arana, E., A. Vehlow, N. E. Harwood, E. Vigorito, R. Henderson, M. Turner, V. L. Tybulewicz, and F. D. Batista. 2008. Activation of the small GTPase Rac2 via the B cell receptor regulates B cell adhesion and immunological-synapse formation. *Immunity* 28: 88-99.
  166. Durand, C. A., K. Hartvigsen, L. Fogelstrand, S. Kim, S. Iritani, B. Vanhaesebroeck, J. L. Witztum, K. D. Puri, and M. R. Gold. 2009. Phosphoinositide 3-kinase p110 delta regulates natural antibody production, marginal zone and B-1 B cell function, and autoantibody responses. *J Immunol* 183: 5673-5684.
  167. Zhang, T. T., K. J. Makondo, and A. J. Marshall. 2012. p110delta phosphoinositide 3-kinase represses IgE switch by potentiating BCL6 expression. *J Immunol* 188: 3700-3708.
  168. Zhang, T. T., K. Okkenhaug, B. F. Nashed, K. D. Puri, Z. A. Knight, K. M. Shokat, B. Vanhaesebroeck, and A. J. Marshall. 2008. Genetic or pharmaceutical blockade of p110delta phosphoinositide 3-kinase enhances IgE production. *J Allergy Clin Immunol* 122: 811-819 e812.
  169. Yu, J., C. Wjasow, and J. M. Backer. 1998. Regulation of the p85/p110alpha phosphatidylinositol 3'-kinase. Distinct roles for the n-terminal and c-terminal SH2 domains. *J Biol Chem* 273: 30199-30203.
  170. Burke, J. E., O. Vadas, A. Berndt, T. Finegan, O. Perisic, and R. L. Williams. 2011. Dynamics of the phosphoinositide 3-kinase p110delta interaction with p85alpha and membranes reveals aspects of regulation distinct from p110alpha. *Structure* 19: 1127-1137.
  171. Yu, J., Y. Zhang, J. McIlroy, T. Rordorf-Nikolic, G. A. Orr, and J. M. Backer. 1998. Regulation of the p85/p110 phosphatidylinositol 3'-kinase: stabilization and inhibition of the p110alpha catalytic subunit by the p85 regulatory subunit. *Mol Cell Biol* 18: 1379-1387.
  172. Zhang, X., O. Vadas, O. Perisic, K. E. Anderson, J. Clark, P. T. Hawkins, L. R. Stephens, and R. L. Williams. 2011. Structure of lipid kinase p110beta/p85beta elucidates an unusual SH2-domain-mediated inhibitory mechanism. *Mol Cell* 41: 567-578.

173. Okada, T., A. Maeda, A. Iwamatsu, K. Gotoh, and T. Kurosaki. 2000. BCAP: the tyrosine kinase substrate that connects B cell receptor to phosphoinositide 3-kinase activation. *Immunity* 13: 817-827.
174. Yamazaki, T., K. Takeda, K. Gotoh, H. Takeshima, S. Akira, and T. Kurosaki. 2002. Essential immunoregulatory role for BCAP in B cell development and function. *J Exp Med* 195: 535-545.
175. Delgado, P., B. Cubelos, E. Calleja, N. Martinez-Martin, A. Cipres, I. Merida, C. Bellas, X. R. Bustelo, and B. Alarcon. 2009. Essential function for the GTPase TC21 in homeostatic antigen receptor signaling. In *Nat Immunol*, United States. 880-888.
176. Moon, K. D., C. B. Post, D. L. Durden, Q. Zhou, P. De, M. L. Harrison, and R. L. Geahlen. 2005. Molecular basis for a direct interaction between the Syk protein-tyrosine kinase and phosphoinositide 3-kinase. *J Biol Chem* 280: 1543-1551.
177. Castello, A., M. Gaya, J. Tucholski, T. Oellerich, K. H. Lu, A. Tafuri, T. Pawson, J. Wienands, M. Engelke, and F. D. Batista. 2013. Nck-mediated recruitment of BCAP to the BCR regulates the PI(3)K-Akt pathway in B cells. *Nat Immunol* 14: 966-975.
178. Hon, W. C., A. Berndt, and R. L. Williams. 2011. Regulation of lipid binding underlies the activation mechanism of class IA PI3-kinases. *Oncogene*.
179. Jimenez, C., C. Hernandez, B. Pimentel, and A. C. Carrera. 2002. The p85 regulatory subunit controls sequential activation of phosphoinositide 3-kinase by Tyr kinases and Ras. *J Biol Chem* 277: 41556-41562.
180. Rodriguez-Viciania, P., P. H. Warne, R. Dhand, B. Vanhaesebroeck, I. Gout, M. J. Fry, M. D. Waterfield, and J. Downward. 1994. Phosphatidylinositol-3-OH kinase as a direct target of Ras. *Nature* 370: 527-532.
181. Inabe, K., M. Ishiai, A. M. Scharenberg, N. Freshney, J. Downward, and T. Kurosaki. 2002. Vav3 modulates B cell receptor responses by regulating phosphoinositide 3-kinase activation. *J Exp Med* 195: 189-200.
182. Dbouk, H. A., O. Vadas, A. Shymanets, J. E. Burke, R. S. Salamon, B. D. Khalil, M. O. Barrett, G. L. Waldo, C. Surve, C. Hsueh, O. Perisic, C. Harteneck, P. R. Shepherd, T. K. Harden, A. V. Smrcka, R. Taussig, A. R. Bresnick, B. Nurnberg, R. L. Williams, and J. M. Backer. 2012. G protein-coupled receptor-mediated activation of p110beta by Gbetagamma is required for cellular transformation and invasiveness. *Sci Signal* 5: ra89.
183. Kurosu, H., T. Maehama, T. Okada, T. Yamamoto, S. Hoshino, Y. Fukui, M. Ui, O. Hazeki, and T. Katada. 1997. Heterodimeric phosphoinositide 3-kinase consisting of p85 and p110beta is synergistically activated by the betagamma subunits of G proteins and phosphotyrosyl peptide. *J Biol Chem* 272: 24252-24256.
184. Brock, C., M. Schaefer, H. P. Reusch, C. Czupalla, M. Michalke, K. Spicher, G. Schultz, and B. Nurnberg. 2003. Roles of G beta gamma in membrane recruitment and activation of p110 gamma/p101 phosphoinositide 3-kinase gamma. *J Cell Biol* 160: 89-99.
185. Murga, C., L. Laguinge, R. Wetzker, A. Cuadrado, and J. S. Gutkind. 1998. Activation of Akt/protein kinase B by G protein-coupled receptors. A role for alpha and beta gamma subunits of heterotrimeric G proteins acting through phosphatidylinositol-3-OH kinase gamma. *J Biol Chem* 273: 19080-19085.
186. Kirsch, C., R. Wetzker, and R. Klinger. 2001. Anionic phospholipids are involved in membrane targeting of PI 3-kinase gamma. *Biochem Biophys Res Commun* 282: 691-696.
187. Pacold, M. E., S. Suire, O. Perisic, S. Lara-Gonzalez, C. T. Davis, E. H. Walker, P. T. Hawkins, L. Stephens, J. F. Eccleston, and R. L. Williams. 2000. Crystal structure and

- functional analysis of Ras binding to its effector phosphoinositide 3-kinase gamma. *Cell* 103: 931-943.
188. Kurig, B., A. Shymanets, T. Bohnacker, Prajwal, C. Brock, M. R. Ahmadian, M. Schaefer, A. Gohla, C. Harteneck, M. P. Wymann, E. Jeanclos, and B. Nurnberg. 2009. Ras is an indispensable coregulator of the class IB phosphoinositide 3-kinase p87/p110gamma. *Proc Natl Acad Sci U S A* 106: 20312-20317.
  189. Gold, M. R., M. P. Scheid, L. Santos, M. Dang-Lawson, R. A. Roth, L. Matsuuchi, V. Duronio, and D. L. Krebs. 1999. The B cell antigen receptor activates the Akt (protein kinase B)/glycogen synthase kinase-3 signaling pathway via phosphatidylinositol 3-kinase. *J Immunol* 163: 1894-1905.
  190. Pogue, S. L., T. Kurosaki, J. Bolen, and R. Herbst. 2000. B cell antigen receptor-induced activation of Akt promotes B cell survival and is dependent on Syk kinase. *J Immunol* 165: 1300-1306.
  191. Burgering, B. M., and P. J. Coffey. 1995. Protein kinase B (c-Akt) in phosphatidylinositol-3-OH kinase signal transduction. *Nature* 376: 599-602.
  192. Astoul, E., S. Watton, and D. Cantrell. 1999. The dynamics of protein kinase B regulation during B cell antigen receptor engagement. *J Cell Biol* 145: 1511-1520.
  193. Frech, M., M. Andjelkovic, E. Ingley, K. K. Reddy, J. R. Falck, and B. A. Hemmings. 1997. High affinity binding of inositol phosphates and phosphoinositides to the pleckstrin homology domain of RAC/protein kinase B and their influence on kinase activity. *J Biol Chem* 272: 8474-8481.
  194. Milburn, C. C., M. Deak, S. M. Kelly, N. C. Price, D. R. Alessi, and D. M. Van Aalten. 2003. Binding of phosphatidylinositol 3,4,5-trisphosphate to the pleckstrin homology domain of protein kinase B induces a conformational change. *Biochem J* 375: 531-538.
  195. Bellacosa, A., T. O. Chan, N. N. Ahmed, K. Datta, S. Malstrom, D. Stokoe, F. McCormick, J. Feng, and P. Tsichlis. 1998. Akt activation by growth factors is a multiple-step process: the role of the PH domain. *Oncogene* 17: 313-325.
  196. Limon, J. J., and D. A. Fruman. 2012. Akt and mTOR in B Cell Activation and Differentiation. *Front Immunol* 3: 228.
  197. Meier, R., D. R. Alessi, P. Cron, M. Andjelkovic, and B. A. Hemmings. 1997. Mitogenic activation, phosphorylation, and nuclear translocation of protein kinase Bbeta. *J Biol Chem* 272: 30491-30497.
  198. del Peso, L., M. Gonzalez-Garcia, C. Page, R. Herrera, and G. Nunez. 1997. Interleukin-3-induced phosphorylation of BAD through the protein kinase Akt. *Science* 278: 687-689.
  199. Cross, D. A., D. R. Alessi, P. Cohen, M. Andjelkovich, and B. A. Hemmings. 1995. Inhibition of glycogen synthase kinase-3 by insulin mediated by protein kinase B. *Nature* 378: 785-789.
  200. Bai, D., L. Ueno, and P. K. Vogt. 2009. Akt-mediated regulation of NFkappaB and the essentialness of NFkappaB for the oncogenicity of PI3K and Akt. *Int J Cancer* 125: 2863-2870.
  201. Ozes, O. N., L. D. Mayo, J. A. Gustin, S. R. Pfeffer, L. M. Pfeffer, and D. B. Donner. 1999. NF-kappaB activation by tumour necrosis factor requires the Akt serine-threonine kinase. *Nature* 401: 82-85.
  202. Smith, C. I., B. Baskin, P. Humire-Greiff, J. N. Zhou, P. G. Olsson, H. S. Maniar, P. Kjellen, J. D. Lambris, B. Christensson, L. Hammarstrom, and et al. 1994. Expression of

- Bruton's agammaglobulinemia tyrosine kinase gene, BTK, is selectively down-regulated in T lymphocytes and plasma cells. *J Immunol* 152: 557-565.
203. Murayama, K., M. Kato-Murayama, C. Mishima, R. Akasaka, M. Shirouzu, Y. Fukui, and S. Yokoyama. 2008. Crystal structure of the Bruton's tyrosine kinase PH domain with phosphatidylinositol. *Biochem Biophys Res Commun* 377: 23-28.
  204. Salim, K., M. J. Bottomley, E. Querfurth, M. J. Zvelebil, I. Gout, R. Scaife, R. L. Margolis, R. Gigg, C. I. Smith, P. C. Driscoll, M. D. Waterfield, and G. Panayotou. 1996. Distinct specificity in the recognition of phosphoinositides by the pleckstrin homology domains of dynamin and Bruton's tyrosine kinase. *EMBO J* 15: 6241-6250.
  205. Cheung, S. M., J. C. Kornelson, M. Al-Alwan, and A. J. Marshall. 2007. Regulation of phosphoinositide 3-kinase signaling by oxidants: hydrogen peroxide selectively enhances immunoreceptor-induced recruitment of phosphatidylinositol (3,4) biphosphate-binding PH domain proteins. *Cell Signal* 19: 902-912.
  206. Krahn, A. K., K. Ma, S. Hou, V. Duronio, and A. J. Marshall. 2004. Two distinct waves of membrane-proximal B cell antigen receptor signaling differentially regulated by Src homology 2-containing inositol polyphosphate 5-phosphatase. *J Immunol* 172: 331-339.
  207. Hashimoto, S., A. Iwamatsu, M. Ishiai, K. Okawa, T. Yamadori, M. Matsushita, Y. Baba, T. Kishimoto, T. Kurosaki, and S. Tsukada. 1999. Identification of the SH2 domain binding protein of Bruton's tyrosine kinase as BLNK--functional significance of Btk-SH2 domain in B-cell antigen receptor-coupled calcium signaling. *Blood* 94: 2357-2364.
  208. Fluckiger, A. C., Z. Li, R. M. Kato, M. I. Wahl, H. D. Ochs, R. Longnecker, J. P. Kinet, O. N. Witte, A. M. Scharenberg, and D. J. Rawlings. 1998. Btk/Tec kinases regulate sustained increases in intracellular Ca<sup>2+</sup> following B-cell receptor activation. *EMBO J* 17: 1973-1985.
  209. Kurosaki, T., and S. Tsukada. 2000. BLNK: connecting Syk and Btk to calcium signals. *Immunity* 12: 1-5.
  210. Bajpai, U. D., K. Zhang, M. Teutsch, R. Sen, and H. H. Wortis. 2000. Bruton's tyrosine kinase links the B cell receptor to nuclear factor kappaB activation. *J Exp Med* 191: 1735-1744.
  211. Petro, J. B., S. M. Rahman, D. W. Ballard, and W. N. Khan. 2000. Bruton's tyrosine kinase is required for activation of IkappaB kinase and nuclear factor kappaB in response to B cell receptor engagement. *J Exp Med* 191: 1745-1754.
  212. Spaargaren, M., E. A. Beuling, M. L. Rurup, H. P. Meijer, M. D. Klok, S. Middendorp, R. W. Hendriks, and S. T. Pals. 2003. The B cell antigen receptor controls integrin activity through Btk and PLCgamma2. *J Exp Med* 198: 1539-1550.
  213. Sharma, S., G. Orłowski, and W. Song. 2009. Btk regulates B cell receptor-mediated antigen processing and presentation by controlling actin cytoskeleton dynamics in B cells. *J Immunol* 182: 329-339.
  214. Thomas, J. D., P. Sideras, C. I. Smith, I. Vorechovsky, V. Chapman, and W. E. Paul. 1993. Colocalization of X-linked agammaglobulinemia and X-linked immunodeficiency genes. *Science* 261: 355-358.
  215. Westerberg, L., G. Greicius, S. B. Snapper, P. Aspenstrom, and E. Severinson. 2001. Cdc42, Rac1, and the Wiskott-Aldrich syndrome protein are involved in the cytoskeletal regulation of B lymphocytes. *Blood* 98: 1086-1094.

216. Walmsley, M. J., S. K. Ooi, L. F. Reynolds, S. H. Smith, S. Ruf, A. Mathiot, L. Vanes, D. A. Williams, M. P. Cancro, and V. L. Tybulewicz. 2003. Critical roles for Rac1 and Rac2 GTPases in B cell development and signaling. *Science* 302: 459-462.
217. Al-Alwan, M., S. Hou, T. T. Zhang, K. Makondo, and A. J. Marshall. 2010. Bam32/DAPP1 promotes B cell adhesion and formation of polarized conjugates with T cells. *J Immunol* 184: 6961-6969.
218. Han, J., K. Luby-Phelps, B. Das, X. Shu, Y. Xia, R. D. Mosteller, U. M. Krishna, J. R. Falck, M. A. White, and D. Broek. 1998. Role of substrates and products of PI 3-kinase in regulating activation of Rac-related guanosine triphosphatases by Vav. *Science* 279: 558-560.
219. Heo, J., R. Thapar, and S. L. Campbell. 2005. Recognition and activation of Rho GTPases by Vav1 and Vav2 guanine nucleotide exchange factors. *Biochemistry* 44: 6573-6585.
220. Das, B., X. Shu, G. J. Day, J. Han, U. M. Krishna, J. R. Falck, and D. Broek. 2000. Control of intramolecular interactions between the pleckstrin homology and Dbl homology domains of Vav and Sos1 regulates Rac binding. *J Biol Chem* 275: 15074-15081.
221. Lopez-Lago, M., H. Lee, C. Cruz, N. Movilla, and X. R. Bustelo. 2000. Tyrosine phosphorylation mediates both activation and downmodulation of the biological activity of Vav. *Mol Cell Biol* 20: 1678-1691.
222. McLeod, S. J., A. J. Shum, R. L. Lee, F. Takei, and M. R. Gold. 2004. The Rap GTPases regulate integrin-mediated adhesion, cell spreading, actin polymerization, and Pyk2 tyrosine phosphorylation in B lymphocytes. *J Biol Chem* 279: 12009-12019.
223. Freeman, S. A., V. Lei, M. Dang-Lawson, K. Mizuno, C. D. Roskelley, and M. R. Gold. 2011. Cofilin-mediated F-actin severing is regulated by the Rap GTPase and controls the cytoskeletal dynamics that drive lymphocyte spreading and BCR microcluster formation. *J Immunol* 187: 5887-5900.
224. Carter, R. H., and D. T. Fearon. 1992. CD19: lowering the threshold for antigen receptor stimulation of B lymphocytes. *Science* 256: 105-107.
225. Fearon, D. T., and R. H. Carter. 1995. The CD19/CR2/TAPA-1 complex of B lymphocytes: linking natural to acquired immunity. *Annu Rev Immunol* 13: 127-149.
226. Fujimoto, M., Y. Fujimoto, J. C. Poe, P. J. Jansen, C. A. Lowell, A. L. DeFranco, and T. F. Tedder. 2000. CD19 regulates Src family protein tyrosine kinase activation in B lymphocytes through processive amplification. *Immunity* 13: 47-57.
227. Tuveson, D. A., R. H. Carter, S. P. Soltoff, and D. T. Fearon. 1993. CD19 of B cells as a surrogate kinase insert region to bind phosphatidylinositol 3-kinase. *Science* 260: 986-989.
228. Buhl, A. M., C. M. Pleiman, R. C. Rickert, and J. C. Cambier. 1997. Qualitative regulation of B cell antigen receptor signaling by CD19: selective requirement for PI3-kinase activation, inositol-1,4,5-trisphosphate production and Ca<sup>2+</sup> mobilization. *J Exp Med* 186: 1897-1910.
229. Carter, R. H., G. M. Doody, J. B. Bolen, and D. T. Fearon. 1997. Membrane IgM-induced tyrosine phosphorylation of CD19 requires a CD19 domain that mediates association with components of the B cell antigen receptor complex. *J Immunol* 158: 3062-3069.

230. Sgroi, D., A. Varki, S. Braesch-Andersen, and I. Stamenkovic. 1993. CD22, a B cell-specific immunoglobulin superfamily member, is a sialic acid-binding lectin. *J Biol Chem* 268: 7011-7018.
231. Adachi, T., S. Harumiya, H. Takematsu, Y. Kozutsumi, M. Wabl, M. Fujimoto, and T. F. Tedder. 2012. CD22 serves as a receptor for soluble IgM. *Eur J Immunol* 42: 241-247.
232. Doody, G. M., L. B. Justement, C. C. Delibrias, R. J. Matthews, J. Lin, M. L. Thomas, and D. T. Fearon. 1995. A role in B cell activation for CD22 and the protein tyrosine phosphatase SHP. *Science* 269: 242-244.
233. Pezzutto, A., B. Dorken, G. Moldenhauer, and E. A. Clark. 1987. Amplification of human B cell activation by a monoclonal antibody to the B cell-specific antigen CD22, Bp 130/140. *J Immunol* 138: 98-103.
234. Sato, S., P. J. Jansen, and T. F. Tedder. 1997. CD19 and CD22 expression reciprocally regulates tyrosine phosphorylation of Vav protein during B lymphocyte signaling. *Proc Natl Acad Sci U S A* 94: 13158-13162.
235. Poe, J. C., M. Fujimoto, P. J. Jansen, A. S. Miller, and T. F. Tedder. 2000. CD22 forms a quaternary complex with SHIP, Grb2, and Shc. A pathway for regulation of B lymphocyte antigen receptor-induced calcium flux. *J Biol Chem* 275: 17420-17427.
236. Ravetch, J. V., and S. Bolland. 2001. IgG Fc receptors. *Annu Rev Immunol* 19: 275-290.
237. Chan, V. W., F. Meng, P. Soriano, A. L. DeFranco, and C. A. Lowell. 1997. Characterization of the B lymphocyte populations in Lyn-deficient mice and the role of Lyn in signal initiation and down-regulation. *Immunity* 7: 69-81.
238. Ono, M., S. Bolland, P. Tempst, and J. V. Ravetch. 1996. Role of the inositol phosphatase SHIP in negative regulation of the immune system by the receptor Fc(gamma)RIIB. *Nature* 383: 263-266.
239. Tridandapani, S., G. W. Chacko, J. R. Van Brocklyn, and K. M. Coggeshall. 1997. Negative signaling in B cells causes reduced Ras activity by reducing Shc-Grb2 interactions. *J Immunol* 158: 1125-1132.
240. Isnardi, I., P. Bruhns, G. Bismuth, W. H. Fridman, and M. Daeron. 2006. The SH2 domain-containing inositol 5-phosphatase SHIP1 is recruited to the intracytoplasmic domain of human FcgammaRIIB and is mandatory for negative regulation of B cell activation. *Immunol Lett* 104: 156-165.
241. Ono, M., H. Okada, S. Bolland, S. Yanagi, T. Kurosaki, and J. V. Ravetch. 1997. Deletion of SHIP or SHP-1 reveals two distinct pathways for inhibitory signaling. *Cell* 90: 293-301.
242. Hasler, P., and M. Zouali. 2001. B cell receptor signaling and autoimmunity. *FASEB J* 15: 2085-2098.
243. Burger, J. A., and N. Chiorazzi. 2013. B cell receptor signaling in chronic lymphocytic leukemia. *Trends Immunol* 34: 592-601.
244. O'Keefe, T. L., G. T. Williams, F. D. Batista, and M. S. Neuberger. 1999. Deficiency in CD22, a B cell-specific inhibitory receptor, is sufficient to predispose to development of high affinity autoantibodies. *J Exp Med* 189: 1307-1313.
245. O'Keefe, T. L., G. T. Williams, S. L. Davies, and M. S. Neuberger. 1996. Hyperresponsive B cells in CD22-deficient mice. *Science* 274: 798-801.
246. Browne, C. D., C. J. Del Nagro, M. H. Cato, H. S. Dengler, and R. C. Rickert. 2009. Suppression of phosphatidylinositol 3,4,5-trisphosphate production is a key determinant of B cell energy. *Immunity* 31: 749-760.



247. Shultz, L. D., P. A. Schweitzer, T. V. Rajan, T. Yi, J. N. Ihle, R. J. Matthews, M. L. Thomas, and D. R. Beier. 1993. Mutations at the murine motheaten locus are within the hematopoietic cell protein-tyrosine phosphatase (Hcph) gene. *Cell* 73: 1445-1454.
248. Engel, P., L. J. Zhou, D. C. Ord, S. Sato, B. Koller, and T. F. Tedder. 1995. Abnormal B lymphocyte development, activation, and differentiation in mice that lack or overexpress the CD19 signal transduction molecule. *Immunity* 3: 39-50.
249. Inaoki, M., S. Sato, B. C. Weintraub, C. C. Goodnow, and T. F. Tedder. 1997. CD19-regulated signaling thresholds control peripheral tolerance and autoantibody production in B lymphocytes. *J Exp Med* 186: 1923-1931.
250. Sato, S., M. Hasegawa, M. Fujimoto, T. F. Tedder, and K. Takehara. 2000. Quantitative genetic variation in CD19 expression correlates with autoimmunity. *J Immunol* 165: 6635-6643.
251. Davis, R. E., V. N. Ngo, G. Lenz, P. Tolar, R. M. Young, P. B. Romesser, H. Kohlhammer, L. Lamy, H. Zhao, Y. Yang, W. Xu, A. L. Shaffer, G. Wright, W. Xiao, J. Powell, J. K. Jiang, C. J. Thomas, A. Rosenwald, G. Ott, H. K. Muller-Hermelink, R. D. Gascoyne, J. M. Connors, N. A. Johnson, L. M. Rimsza, E. Campo, E. S. Jaffe, W. H. Wilson, J. Delabie, E. B. Smeland, R. I. Fisher, R. M. Braziel, R. R. Tubbs, J. R. Cook, D. D. Weisenburger, W. C. Chan, S. K. Pierce, and L. M. Staudt. 2010. Chronic active B-cell-receptor signalling in diffuse large B-cell lymphoma. *Nature* 463: 88-92.
252. Herishanu, Y., P. Perez-Galan, D. Liu, A. Biancotto, S. Pittaluga, B. Vire, F. Gibellini, N. Njuguna, E. Lee, L. Stennett, N. Raghavachari, P. Liu, J. P. McCoy, M. Raffeld, M. Stetler-Stevenson, C. Yuan, R. Sherry, D. C. Arthur, I. Maric, T. White, G. E. Marti, P. Munson, W. H. Wilson, and A. Wiestner. 2011. The lymph node microenvironment promotes B-cell receptor signaling, NF-kappaB activation, and tumor proliferation in chronic lymphocytic leukemia. *Blood* 117: 563-574.
253. Ringshausen, I., F. Schneller, C. Bogner, S. Hipp, J. Duyster, C. Peschel, and T. Decker. 2002. Constitutively activated phosphatidylinositol-3 kinase (PI-3K) is involved in the defect of apoptosis in B-CLL: association with protein kinase Cdelta. *Blood* 100: 3741-3748.
254. Shehata, M., S. Schnabl, D. Demirtas, M. Hilgarth, R. Hubmann, E. Ponath, S. Badrnya, C. Lehner, A. Hoelbl, M. Duechler, A. Gaiger, C. Zielinski, J. D. Schwarzmeier, and U. Jaeger. 2010. Reconstitution of PTEN activity by CK2 inhibitors and interference with the PI3-K/Akt cascade counteract the antiapoptotic effect of human stromal cells in chronic lymphocytic leukemia. *Blood* 116: 2513-2521.
255. Lenz, G., G. W. Wright, N. C. Emre, H. Kohlhammer, S. S. Dave, R. E. Davis, S. Carty, L. T. Lam, A. L. Shaffer, W. Xiao, J. Powell, A. Rosenwald, G. Ott, H. K. Muller-Hermelink, R. D. Gascoyne, J. M. Connors, E. Campo, E. S. Jaffe, J. Delabie, E. B. Smeland, L. M. Rimsza, R. I. Fisher, D. D. Weisenburger, W. C. Chan, and L. M. Staudt. 2008. Molecular subtypes of diffuse large B-cell lymphoma arise by distinct genetic pathways. In *Proc Natl Acad Sci U S A*, United States. 13520-13525.
256. Rao, E., C. Jiang, M. Ji, X. Huang, J. Iqbal, G. Lenz, G. Wright, L. M. Staudt, Y. Zhao, T. W. McKeithan, W. C. Chan, and K. Fu. 2012. The miRNA-17 approximately 92 cluster mediates chemoresistance and enhances tumor growth in mantle cell lymphoma via PI3K/AKT pathway activation. *Leukemia* 26: 1064-1072.

257. Pedersen, I. M., D. Otero, E. Kao, A. V. Miletic, C. Hother, E. Ralfkiaer, R. C. Rickert, K. Gronbaek, and M. David. 2009. Onco-miR-155 targets SHIP1 to promote TNFalpha-dependent growth of B cell lymphomas. *EMBO Mol Med* 1: 288-295.
258. Contri, A., A. M. Brunati, L. Trentin, A. Cabrelle, M. Miorin, L. Cesaro, L. A. Pinna, R. Zambello, G. Semenzato, and A. Donella-Deana. 2005. Chronic lymphocytic leukemia B cells contain anomalous Lyn tyrosine kinase, a putative contribution to defective apoptosis. *J Clin Invest* 115: 369-378.
259. Gutierrez, N. C., E. M. Ocio, J. de Las Rivas, P. Maiso, M. Delgado, E. Ferminan, M. J. Arcos, M. L. Sanchez, J. M. Hernandez, and J. F. San Miguel. 2007. Gene expression profiling of B lymphocytes and plasma cells from Waldenstrom's macroglobulinemia: comparison with expression patterns of the same cell counterparts from chronic lymphocytic leukemia, multiple myeloma and normal individuals. *Leukemia* 21: 541-549.
260. Davids, M. S., and J. R. Brown. 2013. Phosphoinositide 3'-kinase inhibition in chronic lymphocytic leukemia. *Hematol Oncol Clin North Am* 27: 329-339.
261. Maffei, R., S. Fiorcari, S. Martinelli, L. Potenza, M. Luppi, and R. Marasca. 2015. Targeting neoplastic B cells and harnessing microenvironment: the "double face" of ibrutinib and idelalisib. *J Hematol Oncol* 8: 60.
262. Smit, L., A. M. de Vries-Smits, J. L. Bos, and J. Borst. 1994. B cell antigen receptor stimulation induces formation of a Shc-Grb2 complex containing multiple tyrosine-phosphorylated proteins. *J Biol Chem* 269: 20209-20212.
263. Liu, L., J. E. Damen, R. L. Cutler, and G. Krystal. 1994. Multiple cytokines stimulate the binding of a common 145-kilodalton protein to Shc at the Grb2 recognition site of Shc. *Mol Cell Biol* 14: 6926-6935.
264. Chacko, G. W., S. Tridandapani, J. E. Damen, L. Liu, G. Krystal, and K. M. Coggeshall. 1996. Negative signaling in B lymphocytes induces tyrosine phosphorylation of the 145-kDa inositol polyphosphate 5-phosphatase, SHIP. *J Immunol* 157: 2234-2238.
265. Damen, J. E., L. Liu, P. Rosten, R. K. Humphries, A. B. Jefferson, P. W. Majerus, and G. Krystal. 1996. The 145-kDa protein induced to associate with Shc by multiple cytokines is an inositol tetrakisphosphate and phosphatidylinositol 3,4,5-triphosphate 5-phosphatase. *Proc Natl Acad Sci U S A* 93: 1689-1693.
266. Ware, M. D., P. Rosten, J. E. Damen, L. Liu, R. K. Humphries, and G. Krystal. 1996. Cloning and characterization of human SHIP, the 145-kD inositol 5-phosphatase that associates with SHC after cytokine stimulation. *Blood* 88: 2833-2840.
267. Okada, H., S. Bolland, A. Hashimoto, M. Kurosaki, Y. Kabuyama, M. Iino, J. V. Ravetch, and T. Kurosaki. 1998. Role of the inositol phosphatase SHIP in B cell receptor-induced Ca<sup>2+</sup> oscillatory response. *J Immunol* 161: 5129-5132.
268. Helgason, C. D., J. E. Damen, P. Rosten, R. Grewal, P. Sorensen, S. M. Chappel, A. Borowski, F. Jirik, G. Krystal, and R. K. Humphries. 1998. Targeted disruption of SHIP leads to hemopoietic perturbations, lung pathology, and a shortened life span. *Genes Dev* 12: 1610-1620.
269. Leung, W. H., T. Tarasenko, Z. Biesova, H. Kole, E. R. Walsh, and S. Bolland. 2013. Aberrant antibody affinity selection in SHIP-deficient B cells. *Eur J Immunol* 43: 371-381.
270. Lioubin, M. N., P. A. Algate, S. Tsai, K. Carlberg, A. Aebersold, and L. R. Rohrschneider. 1996. p150Ship, a signal transduction molecule with inositol polyphosphate-5-phosphatase activity. *Genes Dev* 10: 1084-1095.

271. Scharenberg, A. M., O. El-Hillal, D. A. Fruman, L. O. Beitz, Z. Li, S. Lin, I. Gout, L. C. Cantley, D. J. Rawlings, and J. P. Kinet. 1998. Phosphatidylinositol-3,4,5-trisphosphate (PtdIns-3,4,5-P3)/Tec kinase-dependent calcium signaling pathway: a target for SHIP-mediated inhibitory signals. *EMBO J* 17: 1961-1972.
272. Rohrschneider, L. R., J. F. Fuller, I. Wolf, Y. Liu, and D. M. Lucas. 2000. Structure, function, and biology of SHIP proteins. *Genes Dev* 14: 505-520.
273. Bolland, S., R. N. Pearse, T. Kurosaki, and J. V. Ravetch. 1998. SHIP modulates immune receptor responses by regulating membrane association of Btk. *Immunity* 8: 509-516.
274. Landego, I., N. Jayachandran, S. Wullschleger, T. T. Zhang, I. W. Gibson, A. Miller, D. R. Alessi, and A. J. Marshall. 2012. Interaction of TAPP adapter proteins with phosphatidylinositol (3,4)-bisphosphate regulates B-cell activation and autoantibody production. *Eur J Immunol* 42: 2760-2770.
275. Li, H., S. Hou, X. Wu, S. Nandagopal, F. Lin, S. Kung, and A. J. Marshall. 2013. The tandem PH domain-containing protein 2 (TAPP2) regulates chemokine-induced cytoskeletal reorganization and malignant B cell migration. *PLoS One* 8: e57809.
276. Insall, R. H., and O. D. Weiner. 2001. PIP3, PIP2, and cell movement--similar messages, different meanings? *Dev Cell* 1: 743-747.
277. An, H., H. Xu, M. Zhang, J. Zhou, T. Feng, C. Qian, R. Qi, and X. Cao. 2005. Src homology 2 domain-containing inositol-5-phosphatase 1 (SHIP1) negatively regulates TLR4-mediated LPS response primarily through a phosphatase activity- and PI-3K-independent mechanism. *Blood* 105: 4685-4692.
278. Damen, J. E., M. D. Ware, J. Kalesnikoff, M. R. Hughes, and G. Krystal. 2001. SHIP's C-terminus is essential for its hydrolysis of PIP3 and inhibition of mast cell degranulation. *Blood* 97: 1343-1351.
279. Ong, C. J., A. Ming-Lum, M. Nodwell, A. Ghanipour, L. Yang, D. E. Williams, J. Kim, L. Demirjian, P. Qasimi, J. Ruschmann, L. P. Cao, K. Ma, S. W. Chung, V. Duronio, R. J. Andersen, G. Krystal, and A. L. Mui. 2007. Small-molecule agonists of SHIP1 inhibit the phosphoinositide 3-kinase pathway in hematopoietic cells. *Blood* 110: 1942-1949.
280. Stenton, G. R., L. F. Mackenzie, P. Tam, J. L. Cross, C. Harwig, J. Raymond, J. Toews, D. Chernoff, T. Macrury, and C. Szabo. Characterization of AQX-1125, a small molecule SHIP1 activator Part 2. Efficacy studies in allergic and pulmonary inflammation models in vivo. *Br J Pharmacol*.
281. Stenton, G. R., L. F. Mackenzie, P. Tam, J. L. Cross, C. Harwig, J. Raymond, J. Toews, J. Wu, N. Ogden, T. Macrury, and C. Szabo. Characterization of AQX-1125, a small molecule SHIP1 activator Part 1. Effects on inflammatory cell activation and chemotaxis in vitro and pharmacokinetic characterization in vivo. *Br J Pharmacol*.
282. Nickel, J. C., B. Egerdie, E. Davis, R. Evans, L. Mackenzie, and S. B. Shrewsbury. 2016. A Phase II Study of Efficacy and Safety of a Novel, Oral SHIP1 Activator, AQX-1125, in Subjects with Moderate to Severe Interstitial Cystitis/Bladder Pain Syndrome (IC/BPS). *J Urol*.
283. Zhang, J., S. F. Walk, K. S. Ravichandran, and J. C. Garrison. 2009. Regulation of the Src homology 2 domain-containing inositol 5'-phosphatase (SHIP1) by the cyclic AMP-dependent protein kinase. *J Biol Chem* 284: 20070-20078.
284. Zhang, J., K. S. Ravichandran, and J. C. Garrison. 2010. A key role for the phosphorylation of Ser440 by the cyclic AMP-dependent protein kinase in regulating the

- activity of the Src homology 2 domain-containing Inositol 5'-phosphatase (SHIP1). *J Biol Chem* 285: 34839-34849.
285. Unkeless, J. C., and J. Jin. 1997. Inhibitory receptors, ITIM sequences and phosphatases. *Curr Opin Immunol* 9: 338-343.
286. Tridandapani, S., T. Kelley, M. Pradhan, D. Cooney, L. B. Justement, and K. M. Coggeshall. 1997. Recruitment and phosphorylation of SH2-containing inositol phosphatase and Shc to the B-cell Fc gamma immunoreceptor tyrosine-based inhibition motif peptide motif. *Mol Cell Biol* 17: 4305-4311.
287. Nakamura, K., A. Brauweiler, and J. C. Cambier. 2000. Effects of Src homology domain 2 (SH2)-containing inositol phosphatase (SHIP), SH2-containing phosphotyrosine phosphatase (SHP)-1, and SHP-2 SH2 decoy proteins on Fc gamma RIIB1-effector interactions and inhibitory functions. *J Immunol* 164: 631-638.
288. Maresco, D. L., J. M. Osborne, D. Cooney, K. M. Coggeshall, and C. L. Anderson. 1999. The SH2-containing 5'-inositol phosphatase (SHIP) is tyrosine phosphorylated after Fc gamma receptor clustering in monocytes. *J Immunol* 162: 6458-6465.
289. Peng, Q., S. Malhotra, J. A. Torchia, W. G. Kerr, K. M. Coggeshall, and M. B. Humphrey. 2010. TREM2- and DAP12-dependent activation of PI3K requires DAP10 and is inhibited by SHIP1. *Sci Signal* 3: ra38.
290. Harris, S. J., R. V. Parry, J. G. Foster, M. D. Blunt, A. Wang, F. Marelli-Berg, J. Westwick, and S. G. Ward. 2011. Evidence that the lipid phosphatase SHIP-1 regulates T lymphocyte morphology and motility. *J Immunol* 186: 4936-4945.
291. Huber, M., C. D. Helgason, J. E. Damen, L. Liu, R. K. Humphries, and G. Krystal. 1998. The src homology 2-containing inositol phosphatase (SHIP) is the gatekeeper of mast cell degranulation. *Proc Natl Acad Sci U S A* 95: 11330-11335.
292. Pradhan, M., and K. M. Coggeshall. 1997. Activation-induced bi-dentate interaction of SHIP and Shc in B lymphocytes. *J Cell Biochem* 67: 32-42.
293. Liu, L., J. E. Damen, M. R. Hughes, I. Babic, F. R. Jirik, and G. Krystal. 1997. The Src homology 2 (SH2) domain of SH2-containing inositol phosphatase (SHIP) is essential for tyrosine phosphorylation of SHIP, its association with Shc, and its induction of apoptosis. *J Biol Chem* 272: 8983-8988.
294. Robson, J. D., D. Davidson, and A. Veillette. 2004. Inhibition of the Jun N-terminal protein kinase pathway by SHIP-1, a lipid phosphatase that interacts with the adaptor molecule Dok-3. *Mol Cell Biol* 24: 2332-2343.
295. Tridandapani, S., M. Pradhan, J. R. LaDine, S. Garber, C. L. Anderson, and K. M. Coggeshall. 1999. Protein interactions of Src homology 2 (SH2) domain-containing inositol phosphatase (SHIP): association with Shc displaces SHIP from Fc gamma RIIB in B cells. *J Immunol* 162: 1408-1414.
296. Ming-Lum, A., S. Shojania, E. So, E. McCarrell, E. Shaw, D. Vu, I. Wang, L. P. McIntosh, and A. L. Mui. 2012. A pleckstrin homology-related domain in SHIP1 mediates membrane localization during Fc gamma receptor-induced phagocytosis. *FASEB J* 26: 3163-3177.
297. Aman, M. J., S. F. Walk, M. E. March, H. P. Su, D. J. Carver, and K. S. Ravichandran. 2000. Essential role for the C-terminal noncatalytic region of SHIP in Fc gamma RIIB1-mediated inhibitory signaling. *Mol Cell Biol* 20: 3576-3589.
298. Isnardi, I., R. Lesourne, P. Bruhns, W. H. Fridman, J. C. Cambier, and M. Daeron. 2004. Two distinct tyrosine-based motifs enable the inhibitory receptor Fc gamma RIIB to

- cooperatively recruit the inositol phosphatases SHIP1/2 and the adapters Grb2/Grap. *J Biol Chem* 279: 51931-51938.
299. Hibbs, M. L., K. W. Harder, J. Armes, N. Kountouri, C. Quilici, F. Casagrande, A. R. Dunn, and D. M. Tarlinton. 2002. Sustained activation of Lyn tyrosine kinase in vivo leads to autoimmunity. *J Exp Med* 196: 1593-1604.
300. Phee, H., A. Jacob, and K. M. Coggeshall. 2000. Enzymatic activity of the Src homology 2 domain-containing inositol phosphatase is regulated by a plasma membrane location. *J Biol Chem* 275: 19090-19097.
301. Lamkin, T. D., S. F. Walk, L. Liu, J. E. Damen, G. Krystal, and K. S. Ravichandran. 1997. Shc interaction with Src homology 2 domain containing inositol phosphatase (SHIP) in vivo requires the Shc-phosphotyrosine binding domain and two specific phosphotyrosines on SHIP. *J Biol Chem* 272: 10396-10401.
302. Kiener, P. A., M. N. Lioubin, L. R. Rohrschneider, J. A. Ledbetter, S. G. Nadler, and M. L. Diegel. 1997. Co-ligation of the antigen and Fc receptors gives rise to the selective modulation of intracellular signaling in B cells. Regulation of the association of phosphatidylinositol 3-kinase and inositol 5'-phosphatase with the antigen receptor complex. *J Biol Chem* 272: 3838-3844.
303. Tridandapani, S., T. Kelley, D. Cooney, M. Pradhan, and K. M. Coggeshall. 1997. Negative signaling in B cells: SHIP Grbs Shc. *Immunol Today* 18: 424-427.
304. Tamir, I., J. C. Stolpa, C. D. Helgason, K. Nakamura, P. Bruhns, M. Daeron, and J. C. Cambier. 2000. The RasGAP-binding protein p62dok is a mediator of inhibitory FcγRIIB signals in B cells. *Immunity* 12: 347-358.
305. Sattler, M., S. Verma, Y. B. Pride, R. Salgia, L. R. Rohrschneider, and J. D. Griffin. 2001. SHIP1, an SH2 domain containing polyinositol-5-phosphatase, regulates migration through two critical tyrosine residues and forms a novel signaling complex with DOK1 and CRKL. *J Biol Chem* 276: 2451-2458.
306. Noguchi, T., T. Matozaki, K. Inagaki, M. Tsuda, K. Fukunaga, Y. Kitamura, T. Kitamura, K. Shii, Y. Yamanashi, and M. Kasuga. 1999. Tyrosine phosphorylation of p62(Dok) induced by cell adhesion and insulin: possible role in cell migration. *EMBO J* 18: 1748-1760.
307. Cao, L., K. Yu, C. Banh, V. Nguyen, A. Ritz, B. J. Raphael, Y. Kawakami, T. Kawakami, and A. R. Salomon. 2007. Quantitative time-resolved phosphoproteomic analysis of mast cell signaling. *J Immunol* 179: 5864-5876.
308. Harmer, S. L., and A. L. DeFranco. 1999. The src homology domain 2-containing inositol phosphatase SHIP forms a ternary complex with Shc and Grb2 in antigen receptor-stimulated B lymphocytes. *J Biol Chem* 274: 12183-12191.
309. Eis, P. S., W. Tam, L. Sun, A. Chadburn, Z. Li, M. F. Gomez, E. Lund, and J. E. Dahlberg. 2005. Accumulation of miR-155 and BIC RNA in human B cell lymphomas. *Proc Natl Acad Sci U S A* 102: 3627-3632.
310. Kluiver, J., S. Poppema, D. de Jong, T. Blokzijl, G. Harms, S. Jacobs, B. J. Kroesen, and A. van den Berg. 2005. BIC and miR-155 are highly expressed in Hodgkin, primary mediastinal and diffuse large B cell lymphomas. *J Pathol* 207: 243-249.
311. Costinean, S., N. Zanesi, Y. Pekarsky, E. Tili, S. Volinia, N. Heerema, and C. M. Croce. 2006. Pre-B cell proliferation and lymphoblastic leukemia/high-grade lymphoma in E(mu)-miR155 transgenic mice. *Proc Natl Acad Sci U S A* 103: 7024-7029.

312. Costinean, S., S. K. Sandhu, I. M. Pedersen, E. Tili, R. Trotta, D. Perrotti, D. Ciarlariello, P. Neviani, J. Harb, L. R. Kauffman, A. Shidham, and C. M. Croce. 2009. Src homology 2 domain-containing inositol-5-phosphatase and CCAAT enhancer-binding protein beta are targeted by miR-155 in B cells of Emicro-MiR-155 transgenic mice. *Blood* 114: 1374-1382.
313. O'Connell, R. M., A. A. Chaudhuri, D. S. Rao, and D. Baltimore. 2009. Inositol phosphatase SHIP1 is a primary target of miR-155. *Proc Natl Acad Sci U S A* 106: 7113-7118.
314. Ruschmann, J., V. Ho, F. Antignano, E. Kuroda, V. Lam, M. Ibaraki, K. Snyder, C. Kim, R. A. Flavell, T. Kawakami, L. Sly, A. G. Turhan, and G. Krystal. 2010. Tyrosine phosphorylation of SHIP promotes its proteasomal degradation. *Exp Hematol* 38: 392-402, 402 e391.
315. Su, K., J. Wu, J. C. Edberg, X. Li, P. Ferguson, G. S. Cooper, C. D. Langefeld, and R. P. Kimberly. 2004. A promoter haplotype of the immunoreceptor tyrosine-based inhibitory motif-bearing FcgammaRIIb alters receptor expression and associates with autoimmunity. I. Regulatory FCGR2B polymorphisms and their association with systemic lupus erythematosus. *J Immunol* 172: 7186-7191.
316. Kono, H., C. Kyogoku, T. Suzuki, N. Tsuchiya, H. Honda, K. Yamamoto, K. Tokunaga, and Z. Honda. 2005. FcgammaRIIB Ile232Thr transmembrane polymorphism associated with human systemic lupus erythematosus decreases affinity to lipid rafts and attenuates inhibitory effects on B cell receptor signaling. *Hum Mol Genet* 14: 2881-2892.
317. Jiang, Y., S. Hirose, M. Abe, R. Sanokawa-Akakura, M. Ohtsuji, X. Mi, N. Li, Y. Xiu, D. Zhang, J. Shirai, Y. Hamano, H. Fujii, and T. Shirai. 2000. Polymorphisms in IgG Fc receptor IIB regulatory regions associated with autoimmune susceptibility. *Immunogenetics* 51: 429-435.
318. Jiang, H. R., L. Lumsden, and J. V. Forrester. 1999. Macrophages and dendritic cells in IRBP-induced experimental autoimmune uveoretinitis in B10RIII mice. *Invest Ophthalmol Vis Sci* 40: 3177-3185.
319. McGaha, T. L., B. Sorrentino, and J. V. Ravetch. 2005. Restoration of tolerance in lupus by targeted inhibitory receptor expression. *Science* 307: 590-593.
320. Yuasa, T., S. Kubo, T. Yoshino, A. Ujike, K. Matsumura, M. Ono, J. V. Ravetch, and T. Takai. 1999. Deletion of fcgamma receptor IIB renders H-2(b) mice susceptible to collagen-induced arthritis. *J Exp Med* 189: 187-194.
321. Yajima, K., A. Nakamura, A. Sugahara, and T. Takai. 2003. FcgammaRIIB deficiency with Fas mutation is sufficient for the development of systemic autoimmune disease. *Eur J Immunol* 33: 1020-1029.
322. Boross, P., V. L. Arandhara, J. Martin-Ramirez, M. L. Santiago-Raber, F. Carlucci, R. Flierman, J. van der Kaa, C. Breukel, J. W. Claassens, M. Camps, E. Lubberts, D. Salvatori, M. P. Rastaldi, F. Ossendorp, M. R. Daha, H. T. Cook, S. Izui, M. Botto, and J. S. Verbeek. 2011. The inhibiting Fc receptor for IgG, FcgammaRIIB, is a modifier of autoimmune susceptibility. *J Immunol* 187: 1304-1313.
323. Brownlie, R. J., K. E. Lawlor, H. A. Niederer, A. J. Cutler, Z. Xiang, M. R. Clatworthy, R. A. Floto, D. R. Greaves, P. A. Lyons, and K. G. Smith. 2008. Distinct cell-specific control of autoimmunity and infection by FcgammaRIIb. *J Exp Med* 205: 883-895.
324. Taher, T. E., K. Parikh, F. Flores-Borja, S. Mletzko, D. A. Isenberg, M. P. Peppelenbosch, and R. A. Mageed. 2010. Protein phosphorylation and kinome profiling

- reveal altered regulation of multiple signaling pathways in B lymphocytes from patients with systemic lupus erythematosus. *Arthritis Rheum* 62: 2412-2423.
325. Li, C., D. Schibli, and S. S. Li. 2009. The XLP syndrome protein SAP interacts with SH3 proteins to regulate T cell signaling and proliferation. *Cell Signal* 21: 111-119.
  326. Horton, H. M., S. Y. Chu, E. C. Ortiz, E. Pong, S. Cemerski, I. W. Leung, N. Jacob, J. Zalevsky, J. R. Desjarlais, W. Stohl, and D. E. Szymkowski. 2011. Antibody-mediated coengagement of FcγRIIb and B cell receptor complex suppresses humoral immunity in systemic lupus erythematosus. *J Immunol* 186: 4223-4233.
  327. Akerlund, J., A. Getahun, and J. C. Cambier. 2015. B cell expression of the SH2-containing inositol 5-phosphatase (SHIP-1) is required to establish anergy to high affinity, proteinacious autoantigens. *J Autoimmun* 62: 45-54.
  328. Dharajiya, N., S. V. Vaidya, H. Murai, V. Cardenas, A. Kurosky, I. Boldogh, and S. A. Sur. 2010. FcγRIIb inhibits allergic lung inflammation in a murine model of allergic asthma. *PLoS One* 5: e9337.
  329. Haddon, D. J., F. Antignano, M. R. Hughes, M. R. Blanchet, L. Zbytniuk, G. Krystal, and K. M. McNagny. 2009. SHIP1 is a repressor of mast cell hyperplasia, cytokine production, and allergic inflammation in vivo. *J Immunol* 183: 228-236.
  330. Maxwell, M. J., M. Duan, J. E. Armes, G. P. Anderson, D. M. Tarlinton, and M. L. Hibbs. 2011. Genetic segregation of inflammatory lung disease and autoimmune disease severity in SHIP-1<sup>-/-</sup> mice. *J Immunol* 186: 7164-7175.
  331. Stenton, G. R., L. F. Mackenzie, P. Tam, J. L. Cross, C. Harwig, J. Raymond, J. Toews, D. Chernoff, T. MacRury, and C. Szabo. 2013. Characterization of AQX-1125, a small-molecule SHIP1 activator: part 2. Efficacy studies in allergic and pulmonary inflammation models in vivo. *Br J Pharmacol* 168: 1519-1529.
  332. Stenton, G. R., L. F. Mackenzie, P. Tam, J. L. Cross, C. Harwig, J. Raymond, J. Toews, J. Wu, N. Ogden, T. MacRury, and C. Szabo. 2013. Characterization of AQX-1125, a small-molecule SHIP1 activator: part 1. Effects on inflammatory cell activation and chemotaxis in vitro and pharmacokinetic characterization in vivo. *Br J Pharmacol* 168: 1506-1518.
  333. Mogilner, A., and G. Oster. 1996. Cell motility driven by actin polymerization. *Biophys J* 71: 3030-3045.
  334. Kunkel, E. J., and E. C. Butcher. 2003. Plasma-cell homing. *Nat Rev Immunol* 3: 822-829.
  335. Fleire, S. J., J. P. Goldman, Y. R. Carrasco, M. Weber, D. Bray, and F. D. Batista. 2006. B cell ligand discrimination through a spreading and contraction response. *Science* 312: 738-741.
  336. Bretscher, A. 1999. Regulation of cortical structure by the ezrin-radixin-moesin protein family. *Curr Opin Cell Biol* 11: 109-116.
  337. Treanor, B., D. Depoil, A. Gonzalez-Granja, P. Barral, M. Weber, O. Dushek, A. Bruckbauer, and F. D. Batista. 2010. The membrane skeleton controls diffusion dynamics and signaling through the B cell receptor. *Immunity* 32: 187-199.
  338. Liu, C., H. Miller, G. Orłowski, H. Hang, A. Upadhyaya, and W. Song. 2012. Actin reorganization is required for the formation of polarized B cell receptor signalosomes in response to both soluble and membrane-associated antigens. *J Immunol* 188: 3237-3246.

339. Gupta, N., B. Wollscheid, J. D. Watts, B. Scheer, R. Aebersold, and A. L. DeFranco. 2006. Quantitative proteomic analysis of B cell lipid rafts reveals that ezrin regulates antigen receptor-mediated lipid raft dynamics. *Nat Immunol* 7: 625-633.
340. Treanor, B., D. Depoil, A. Bruckbauer, and F. D. Batista. 2011. Dynamic cortical actin remodeling by ERM proteins controls BCR microcluster organization and integrity. *J Exp Med* 208: 1055-1068.
341. Song, W., C. Liu, and A. Upadhyaya. 2014. The pivotal position of the actin cytoskeleton in the initiation and regulation of B cell receptor activation. *Biochim Biophys Acta* 1838: 569-578.
342. Mullins, R. D., J. A. Heuser, and T. D. Pollard. 1998. The interaction of Arp2/3 complex with actin: nucleation, high affinity pointed end capping, and formation of branching networks of filaments. *Proc Natl Acad Sci U S A* 95: 6181-6186.
343. Amann, K. J., and T. D. Pollard. 2001. The Arp2/3 complex nucleates actin filament branches from the sides of pre-existing filaments. *Nat Cell Biol* 3: 306-310.
344. Pollitt, A. Y., and R. H. Insall. 2009. WASP and SCAR/WAVE proteins: the drivers of actin assembly. *J Cell Sci* 122: 2575-2578.
345. Padrick, S. B., and M. K. Rosen. 2010. Physical mechanisms of signal integration by WASP family proteins. *Annu Rev Biochem* 79: 707-735.
346. Rohatgi, R., L. Ma, H. Miki, M. Lopez, T. Kirchhausen, T. Takenawa, and M. W. Kirschner. 1999. The interaction between N-WASP and the Arp2/3 complex links Cdc42-dependent signals to actin assembly. *Cell* 97: 221-231.
347. Tomasevic, N., Z. Jia, A. Russell, T. Fujii, J. J. Hartman, S. Clancy, M. Wang, C. Beraud, K. W. Wood, and R. Sakowicz. 2007. Differential regulation of WASP and N-WASP by Cdc42, Rac1, Nck, and PI(4,5)P2. *Biochemistry* 46: 3494-3502.
348. Zeng, R., J. L. Cannon, R. T. Abraham, M. Way, D. D. Billadeau, J. Bubeck-Wardenberg, and J. K. Burkhardt. 2003. SLP-76 coordinates Nck-dependent Wiskott-Aldrich syndrome protein recruitment with Vav-1/Cdc42-dependent Wiskott-Aldrich syndrome protein activation at the T cell-APC contact site. *J Immunol* 171: 1360-1368.
349. Mizuno, K., Y. Tagawa, K. Mitomo, N. Watanabe, T. Katagiri, M. Ogimoto, and H. Yakura. 2002. Src homology region 2 domain-containing phosphatase 1 positively regulates B cell receptor-induced apoptosis by modulating association of B cell linker protein with Nck and activation of c-Jun NH2-terminal kinase. *J Immunol* 169: 778-786.
350. Liu, C., X. Bai, J. Wu, S. Sharma, A. Upadhyaya, C. I. Dahlberg, L. S. Westerberg, S. B. Snapper, X. Zhao, and W. Song. 2013. N-wasp is essential for the negative regulation of B cell receptor signaling. *PLoS Biol* 11: e1001704.
351. Liu, C., H. Miller, K. L. Hui, B. Grooman, S. Bolland, A. Upadhyaya, and W. Song. 2011. A balance of Bruton's tyrosine kinase and SHIP activation regulates B cell receptor cluster formation by controlling actin remodeling. *J Immunol* 187: 230-239.
352. Weber, M., B. Treanor, D. Depoil, H. Shinohara, N. E. Harwood, M. Hikida, T. Kurosaki, and F. D. Batista. 2008. Phospholipase C-gamma2 and Vav cooperate within signaling microclusters to propagate B cell spreading in response to membrane-bound antigen. *J Exp Med* 205: 853-868.
353. Welch, H. C., W. J. Coadwell, L. R. Stephens, and P. T. Hawkins. 2003. Phosphoinositide 3-kinase-dependent activation of Rac. *FEBS Lett* 546: 93-97.



354. Vedham, V., H. Phee, and K. M. Coggeshall. 2005. Vav activation and function as a rac guanine nucleotide exchange factor in macrophage colony-stimulating factor-induced macrophage chemotaxis. *Mol Cell Biol* 25: 4211-4220.
355. Nishio, M., K. Watanabe, J. Sasaki, C. Taya, S. Takasuga, R. Iizuka, T. Balla, M. Yamazaki, H. Watanabe, R. Itoh, S. Kuroda, Y. Horie, I. Forster, T. W. Mak, H. Yonekawa, J. M. Penninger, Y. Kanaho, A. Suzuki, and T. Sasaki. 2007. Control of cell polarity and motility by the PtdIns(3,4,5)P3 phosphatase SHIP1. *Nat Cell Biol* 9: 36-44.
356. Rey-Ladino, J. A., M. Huber, L. Liu, J. E. Damen, G. Krystal, and F. Takei. 1999. The SH2-containing inositol-5'-phosphatase enhances LFA-1-mediated cell adhesion and defines two signaling pathways for LFA-1 activation. *J Immunol* 162: 5792-5799.
357. Brown, M. J., R. Nijhara, J. A. Hallam, M. Gignac, K. M. Yamada, S. L. Erlandsen, J. Delon, M. Kruhlak, and S. Shaw. 2003. Chemokine stimulation of human peripheral blood T lymphocytes induces rapid dephosphorylation of ERM proteins, which facilitates loss of microvilli and polarization. *Blood* 102: 3890-3899.
358. Nijhara, R., P. B. van Hennik, M. L. Gignac, M. J. Kruhlak, P. L. Hordijk, J. Delon, and S. Shaw. 2004. Rac1 mediates collapse of microvilli on chemokine-activated T lymphocytes. *J Immunol* 173: 4985-4993.
359. Krause, M., J. D. Leslie, M. Stewart, E. M. Lafuente, F. Valderrama, R. Jagannathan, G. A. Strasser, D. A. Rubinson, H. Liu, M. Way, M. B. Yaffe, V. A. Boussiotis, and F. B. Gertler. 2004. Lamellipodin, an Ena/VASP ligand, is implicated in the regulation of lamellipodial dynamics. *Dev Cell* 7: 571-583.
360. Mehta, P., A. S. Wavreille, S. E. Justiniano, R. L. Marsh, J. Yu, R. W. Burry, D. Jarjoura, T. Eubank, M. A. Caligiuri, J. P. Butchar, and S. Tridandapani. 2011. LyGDI, a novel SHIP-interacting protein, is a negative regulator of FcγR-mediated phagocytosis. *PLoS One* 6: e21175.
361. Zinzalla, G., and D. E. Thurston. 2009. Targeting protein-protein interactions for therapeutic intervention: a challenge for the future. *Future Med Chem* 1: 65-93.
362. Hou, S., S. D. Pauls, P. Liu, and A. J. Marshall. 2010. The PH domain adaptor protein Bam32/DAPP1 functions in mast cells to restrain FcεRI-induced calcium flux and granule release. *Mol Immunol* 48: 89-97.
363. Menezes, J., W. Leibold, G. Klein, and G. Clements. 1975. Establishment and characterization of an Epstein-Barr virus (EBV)-negative lymphoblastoid B cell line (BJA-B) from an exceptional, EBV-genome-negative African Burkitt's lymphoma. *Biomedicine* 22: 276-284.
364. Allam, A., H. Niuro, E. A. Clark, and A. J. Marshall. 2004. The adaptor protein Bam32 regulates Rac1 activation and actin remodeling through a phosphorylation-dependent mechanism. *J Biol Chem* 279: 39775-39782.
365. Wienands, J., O. Larbolette, and M. Reth. 1996. Evidence for a preformed transducer complex organized by the B cell antigen receptor. *Proc Natl Acad Sci U S A* 93: 7865-7870.
366. Dwivedi, R. C., O. V. Krokhin, H. S. El-Gabalawy, and J. A. Wilkins. 2016. Development of an SRM method for absolute quantitation of MYDGF/C19orf10 protein. *Proteomics Clin Appl* 10: 663-670.
367. Obenauer, J. C., L. C. Cantley, and M. B. Yaffe. 2003. Scansite 2.0: Proteome-wide prediction of cell signaling interactions using short sequence motifs. *Nucleic Acids Res* 31: 3635-3641.

368. Yaffe, M. B., G. G. Leparc, J. Lai, T. Obata, S. Volinia, and L. C. Cantley. 2001. A motif-based profile scanning approach for genome-wide prediction of signaling pathways. *Nat Biotechnol* 19: 348-353.
369. Li, L., C. Wu, H. Huang, K. Zhang, J. Gan, and S. S. Li. 2008. Prediction of phosphotyrosine signaling networks using a scoring matrix-assisted ligand identification approach. *Nucleic Acids Res* 36: 3263-3273.
370. Huang, H., L. Li, C. Wu, D. Schibli, K. Colwill, S. Ma, C. Li, P. Roy, K. Ho, Z. Songyang, T. Pawson, Y. Gao, and S. S. Li. 2008. Defining the specificity space of the human SRC homology 2 domain. *Mol Cell Proteomics* 7: 768-784.
371. de Castro, R. O., J. Zhang, J. R. Groves, E. A. Barbu, and R. P. Siraganian. 2012. Once phosphorylated, tyrosines in carboxyl terminus of protein-tyrosine kinase Syk interact with signaling proteins, including TULA-2, a negative regulator of mast cell degranulation. *J Biol Chem* 287: 8194-8204.
372. Lettau, M., J. Pieper, and O. Janssen. 2009. Nck adapter proteins: functional versatility in T cells. *Cell Commun Signal* 7: 1.
373. Frese, S., W. D. Schubert, A. C. Findeis, T. Marquardt, Y. S. Roske, T. E. Stradal, and D. W. Heinz. 2006. The phosphotyrosine peptide binding specificity of Nck1 and Nck2 Src homology 2 domains. *J Biol Chem* 281: 18236-18245.
374. Kim, A. S., L. T. Kakalis, N. Abdul-Manan, G. A. Liu, and M. K. Rosen. 2000. Autoinhibition and activation mechanisms of the Wiskott-Aldrich syndrome protein. *Nature* 404: 151-158.
375. Rohatgi, R., H. Y. Ho, and M. W. Kirschner. 2000. Mechanism of N-WASP activation by CDC42 and phosphatidylinositol 4, 5-bisphosphate. *J Cell Biol* 150: 1299-1310.
376. Blundell, M. P., G. Bouma, J. Metelo, A. Worth, Y. Calle, L. A. Cowell, L. S. Westerberg, D. A. Moulding, S. Mirando, C. Kinnon, G. O. Cory, G. E. Jones, S. B. Snapper, S. O. Burns, and A. J. Thrasher. 2009. Phosphorylation of WASp is a key regulator of activity and stability in vivo. *Proc Natl Acad Sci U S A* 106: 15738-15743.
377. Cory, G. O., R. Garg, R. Cramer, and A. J. Ridley. 2002. Phosphorylation of tyrosine 291 enhances the ability of WASp to stimulate actin polymerization and filopodium formation. Wiskott-Aldrich Syndrome protein. *J Biol Chem* 277: 45115-45121.
378. Suetsugu, S., M. Hattori, H. Miki, T. Tezuka, T. Yamamoto, K. Mikoshiba, and T. Takenawa. 2002. Sustained activation of N-WASP through phosphorylation is essential for neurite extension. *Dev Cell* 3: 645-658.
379. Ichetovkin, I., W. Grant, and J. Condeelis. 2002. Cofilin produces newly polymerized actin filaments that are preferred for dendritic nucleation by the Arp2/3 complex. *Curr Biol* 12: 79-84.
380. Chaki, S. P., and G. M. Rivera. 2013. Integration of signaling and cytoskeletal remodeling by Nck in directional cell migration. *Bioarchitecture* 3: 57-63.
381. Rivera, G. M., D. Vasilescu, V. Papayannopoulos, W. A. Lim, and B. J. Mayer. 2009. A reciprocal interdependence between Nck and PI(4,5)P(2) promotes localized N-WASP-mediated actin polymerization in living cells. *Mol Cell* 36: 525-535.
382. Rivero-Lezcano, O. M., A. Marcilla, J. H. Sameshima, and K. C. Robbins. 1995. Wiskott-Aldrich syndrome protein physically associates with Nck through Src homology 3 domains. *Mol Cell Biol* 15: 5725-5731.

383. Donnelly, S. K., I. Weisswange, M. Zettl, and M. Way. 2013. WIP provides an essential link between Nck and N-WASP during Arp2/3-dependent actin polymerization. *Curr Biol* 23: 999-1006.
384. Rohatgi, R., P. Nollau, H. Y. Ho, M. W. Kirschner, and B. J. Mayer. 2001. Nck and phosphatidylinositol 4,5-bisphosphate synergistically activate actin polymerization through the N-WASP-Arp2/3 pathway. *J Biol Chem* 276: 26448-26452.
385. Dart, A. E., S. K. Donnelly, D. W. Holden, M. Way, and E. Caron. 2012. Nck and Cdc42 co-operate to recruit N-WASP to promote Fcγ<sub>3</sub>R-mediated phagocytosis. *J Cell Sci* 125: 2825-2830.
386. Frischknecht, F., V. Moreau, S. Rottger, S. Gonfloni, I. Reckmann, G. Superti-Furga, and M. Way. 1999. Actin-based motility of vaccinia virus mimics receptor tyrosine kinase signalling. *Nature* 401: 926-929.
387. Klein, G., B. Giovanella, A. Westman, J. S. Stehlin, and D. Mumford. 1975. An EBV-genome-negative cell line established from an American Burkitt lymphoma; receptor characteristics. EBV infectibility and permanent conversion into EBV-positive sublines by in vitro infection. *Intervirology* 5: 319-334.
388. Vaughan, A. T., C. Iriyama, S. A. Beers, C. H. Chan, S. H. Lim, E. L. Williams, V. Shah, A. Roghanian, B. Frendeus, M. J. Glennie, and M. S. Cragg. 2014. Inhibitory Fcγ<sub>3</sub>RIIb (CD32b) becomes activated by therapeutic mAb in both cis and trans and drives internalization according to antibody specificity. *Blood* 123: 669-677.
389. Kim, E. W., Z. N. Zakov, D. M. Albert, T. R. Smith, and J. L. Craft. 1979. Intraocular reticulum cell sarcoma: a case report and literature review. *Albrecht Von Graefes Arch Klin Exp Ophthalmol* 209: 167-178.
390. Nalaskowski, M. M., A. Metzner, M. A. Brehm, S. Labiadh, H. Brauer, N. Grabinski, G. W. Mayr, and M. Jucker. 2012. The inositol 5-phosphatase SHIP1 is a nucleocytoplasmic shuttling protein and enzymatically active in cell nuclei. *Cell Signal* 24: 621-628.
391. Hancock, J. F., K. Cadwallader, and C. J. Marshall. 1991. Methylation and proteolysis are essential for efficient membrane binding of prenylated p21K-ras(B). *EMBO J* 10: 641-646.
392. Jefferson, A. B., and P. W. Majerus. 1996. Mutation of the conserved domains of two inositol polyphosphate 5-phosphatases. *Biochemistry* 35: 7890-7894.
393. Brauweiler, A., I. Tamir, S. Marschner, C. D. Helgason, and J. C. Cambier. 2001. Partially distinct molecular mechanisms mediate inhibitory Fcγ<sub>3</sub>RIIb signaling in resting and activated B cells. *J Immunol* 167: 204-211.
394. Heyman, B. 2003. Feedback regulation by IgG antibodies. *Immunol Lett* 88: 157-161.
395. Mackay, M., A. Stanevsky, T. Wang, C. Aranow, M. Li, S. Koenig, J. V. Ravetch, and B. Diamond. 2006. Selective dysregulation of the Fcγ<sub>3</sub>RIIb receptor on memory B cells in SLE. *J Exp Med* 203: 2157-2164.
396. Getahun, A., and J. C. Cambier. 2015. Of ITIMs, ITAMs, and ITAMis: revisiting immunoglobulin Fc receptor signaling. *Immunol Rev* 268: 66-73.
397. Kimura, T., H. Sakamoto, E. Appella, and R. P. Siraganian. 1997. The negative signaling molecule SH2 domain-containing inositol-polyphosphate 5-phosphatase (SHIP) binds to the tyrosine-phosphorylated beta subunit of the high affinity IgE receptor. *J Biol Chem* 272: 13991-13996.

398. Sarmay, G., G. Koncz, and J. Gergely. 1996. Integration of activatory and inhibitory signals in human B-cells. *Immunol Lett* 54: 93-100.
399. Wang, J., T. Koizumi, and T. Watanabe. 1996. Altered antigen receptor signaling and impaired Fas-mediated apoptosis of B cells in Lyn-deficient mice. *J Exp Med* 184: 831-838.
400. Crowley, M. T., S. L. Harmer, and A. L. DeFranco. 1996. Activation-induced association of a 145-kDa tyrosine-phosphorylated protein with Shc and Syk in B lymphocytes and macrophages. *J Biol Chem* 271: 1145-1152.
401. Nagai, K., M. Takata, H. Yamamura, and T. Kurosaki. 1995. Tyrosine phosphorylation of Shc is mediated through Lyn and Syk in B cell receptor signaling. *J Biol Chem* 270: 6824-6829.
402. Jabril-Cuenod, B., C. Zhang, A. M. Scharenberg, R. Paolini, R. Numerof, M. A. Beaven, and J. P. Kinet. 1996. Syk-dependent phosphorylation of Shc. A potential link between FcepsilonRI and the Ras/mitogen-activated protein kinase signaling pathway through SOS and Grb2. *J Biol Chem* 271: 16268-16272.
403. Mukherjee, O., L. Weingarten, I. Padberg, C. Pracht, R. Sinha, T. Hochdorfer, S. Kuppig, R. Backofen, M. Reth, and M. Huber. 2012. The SH2-domain of SHIP1 interacts with the SHIP1 C-terminus: Impact on SHIP1/Ig-alpha interaction. *Biochim Biophys Acta* 1823: 206-214.
404. Fuhler, G. M., R. Brooks, B. Toms, S. Iyer, E. A. Gengo, M. Y. Park, M. Gumbleton, D. R. Viernes, J. D. Chisholm, and W. G. Kerr. 2012. Therapeutic Potential of SH2 Domain-Containing Inositol-5'-Phosphatase 1 (SHIP1) and SHIP2 Inhibition in Cancer. *Mol Med* 18: 65-75.
405. Cady, C. T., J. S. Rice, V. L. Ott, and J. C. Cambier. 2008. Regulation of hematopoietic cell function by inhibitory immunoglobulin G receptors and their inositol lipid phosphatase effectors. *Immunol Rev* 224: 44-57.
406. Park, M. J., R. Sheng, A. Silkov, D. J. Jung, Z. G. Wang, Y. Xin, H. Kim, P. Thiagarajan-Rosenkranz, S. Song, Y. Yoon, W. Nam, I. Kim, E. Kim, D. G. Lee, Y. Chen, I. Singaram, L. Wang, M. H. Jang, C. S. Hwang, B. Honig, S. Ryu, J. Lorieu, Y. M. Kim, and W. Cho. 2016. SH2 Domains Serve as Lipid-Binding Modules for pTyr-Signaling Proteins. *Mol Cell* 62: 7-20.
407. Brooks, R., G. M. Fuhler, S. Iyer, M. J. Smith, M. Y. Park, K. H. Paraiso, R. W. Engelman, and W. G. Kerr. 2010. SHIP1 inhibition increases immunoregulatory capacity and triggers apoptosis of hematopoietic cancer cells. *J Immunol* 184: 3582-3589.
408. Kaneko, T., H. Huang, X. Cao, X. Li, C. Li, C. Voss, S. S. Sidhu, and S. S. Li. 2012. Superbinder SH2 domains act as antagonists of cell signaling. *Sci Signal* 5: ra68.